Climate4you update June 2023

Climate4you.com

Summary of observations until June 2023:

1: Observed average global air temperature change last 40 years is about +0.157°C per decade.
If unchanged, additional average global air temperature increase by year 2100 will be about +1.2°C.
However, part of the apparent temperature increase reported is due to administrative changes, and
the real future increase may therefore be smaller.

2: Tide gauges along coasts indicate a typical global sea level increase of about 1-2 mm/yr.
Coastal sea level change rate last 100 year has essential been stable, without recent acceleration.
If unchanged, global sea level at coasts will typically increase 8-16 cm by year 2100, although many
locations in regions affected by glaciation 20,000 years ago, will experience a relative sea level drop.

3: Since 2004 the global oceans above 1900 m depth on average have warmed about 0.07°C.
The maximum warming (about 0.2°C, 0-100 m depth) mainly affects oceans near Equator,
where the incoming solar radiation is at maximum.

4: Changes in atmospheric CO_2 follow changes in global air temperature.
Changes in global air temperature follow changes in ocean surface temperature.

5: There was no perceptible effect on atmospheric CO_2 due to the 2020-21 COVID-related drop in GHG
emissions. Thus, natural sinks and sources for atmospheric CO_2 far outweigh human contributions.

Contents:

June 2023 global surface air temperature overview

General: This newsletter contains graphs and diagrams showing a selection of key meteorological variables, updated to the most recent past month, if possible. All temperatures are given in degrees Celsius.

Traditionally, a 30 -year reference period is often used by various meteorological institutions for comparison purposes and are supposed to be updated through the end of each decade ending in zero (e.g., 1951-1980, 1961-1990, 1971-2000, etc.). The concept of a normal climate goes back to the first part of the 20th century. At that time, lasting to about 1960, it was generally believed that for all practical purpose's climate could be considered constant, no matter how obvious year-to-year fluctuations might have been. On this basis meteorologist decided to operate with an average or normal climate, defined by a 30-year period, called the normal period, assuming that it was of sufficient length to iron out all intervening variations. In fact, using a 30-yr 'normal' period is genuinely unfortunate, as observations clearly demonstrate that various global climate parameters (see, e.g., page 20) are influenced by periodic changes of 50-70 years. The often used 30-yr reference period is roughly half this time interval and is therefore extremely unsuited as a good reference time interval. In the maps on page 4, showing the geographical pattern of surface air temperature anomalies, the last previous 10 years are therefore used as reference period. This decadal approach corresponds well to the typical memory horizon for many people and is also adopted as reference period by other institutions, e.g., the Danish Meteorological Institute (DMI).

In many diagrams shown in this newsletter the thin line represents the monthly global average value, and the thick line indicate a simple running average, in most cases a simple moving 37-month average, nearly corresponding to a three-year average. The 37-month average is calculated from values covering a range from 18 months before to 18 months after, with equal weight given to all individual months.

The year 1979 has been chosen as starting point in many diagrams, as this approximately corresponds to both the beginning of satellite observations and the onset of the late 20th century warming period. However, several of the data series have a longer record length, which may be inspected in greater detail on www.climate4you.com.

June 2023 surface air temperature

General: For June 2023, the GISS data portal (https://data.giss.nasa.gov/gistemp/) provided 16200 AIRS interpolated surface air data points, based on satellite observations. According to the GISS and NCDC surface air temperature records, the June 2023 global temperature anomaly was higher than in the previous month. The UAH and RSS lower troposphere satellite records show the June 2023 temperature anomaly to be almost like in the previous month. According to AIRS v6 the June 2023 global average surface air temperature anomaly was marginally higher (+0.05°C) than the global June average for the last 10 years.

The Northern Hemisphere surface temperature anomality pattern (p.4) was characterised by regional contrasts, controlled by the dominant jet stream position. Canada and NW Europe were warm relative to the average for the last 10 years, as was easternmost Siberia. Greenland, Russia, central Siberia, SE Europe, and Alaska were relatively cold. Ocean wise, the Greenland Sea, the Norwegian Sea and The North Atlantic shortly east of USA were relatively cold, while the remaining part of the North Atlantic was warm. In the northern Pacific, most of the ocean was cold. Arctic Ocean surface air temperatures were near the 10-yr average.

Near the Equator temperatures were generally near or above the 10-year average. Especially the part of the Pacific Ocean affected by the last cold La Niña episode display above average surface temperatures, as was large parts of the Atlantic Ocean.

Southern Hemisphere temperatures were near the 10-yr average. Western Australia and South Africa were relatively cold, while parts of eastern Australia were warm. Also, most of the Antarctic continent was relatively warm, as were large parts of the surrounding ocean. Apparently, the much-published June 2023 global heat wave was mainly an Antarctic winter phenomenon.

June 2023 global surface air temperature overview versus average June last 10 years
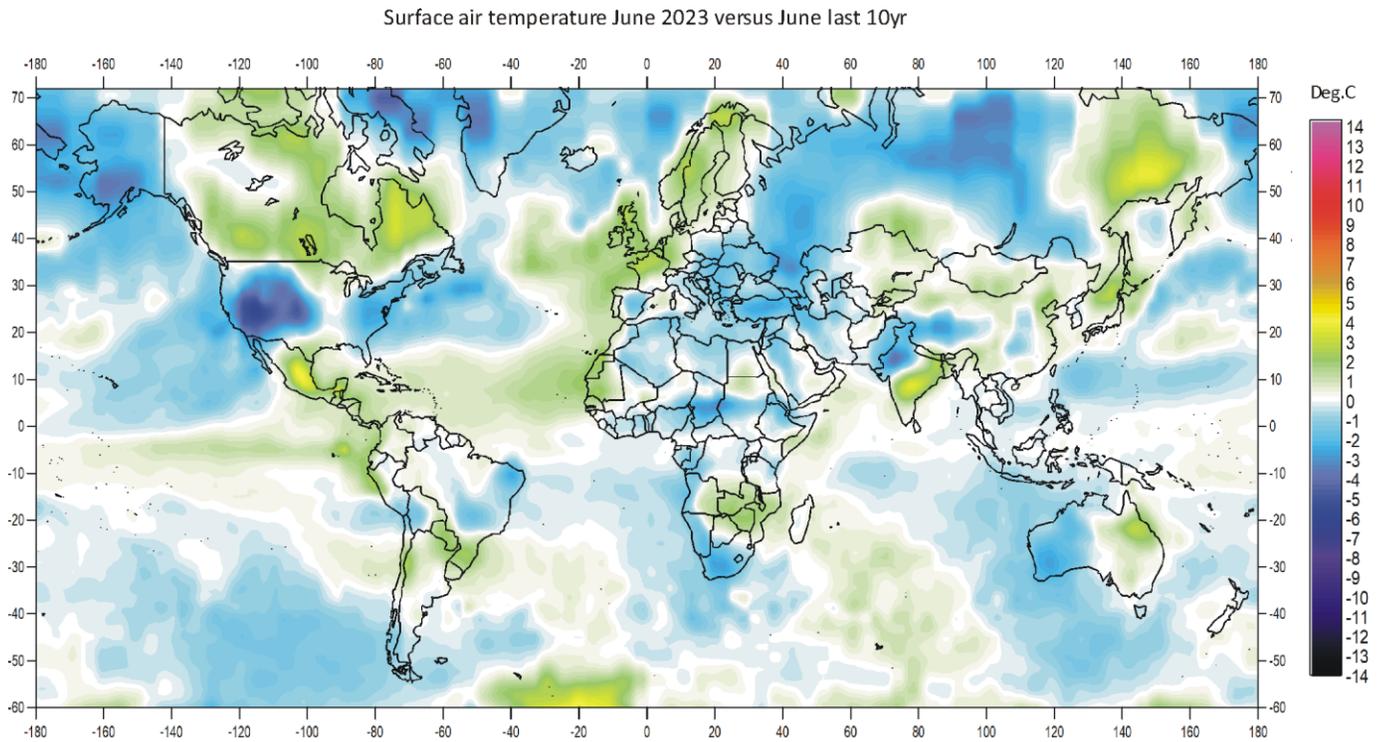
Surface air temperature June 2023 versus June last 10yr
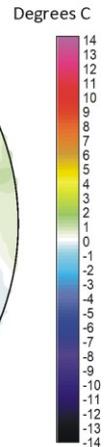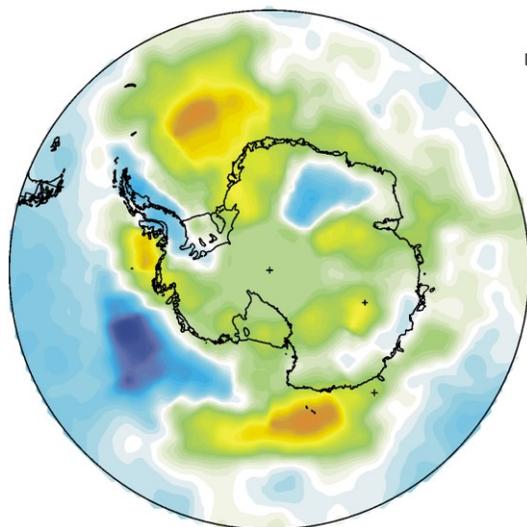
June 2023 surface air temperature compared to the average of June over the last 10 years. Green-yellow-red colours indicate areas with higher temperature than the 10-year average, while blue colours indicate lower than average temperatures. Data source: Remote Sensed Surface Temperature Anomaly, AIRS/Aqua L3 Monthly Standard Physical Retrieval 1-degree x 1-degree V006 (https://airs.jpl.nasa.gov/), obtained from the GISS data portal (https://data.giss.nasa.gov/gistemp/maps/index_v4.html).

4

June 2023 global surface air temperature compared to June 2022

Surface air temperature June 2023 versus June 2022

Surface air temperature June 2023 versus June 2022

Surface air temperature June 2023 versus June 2022
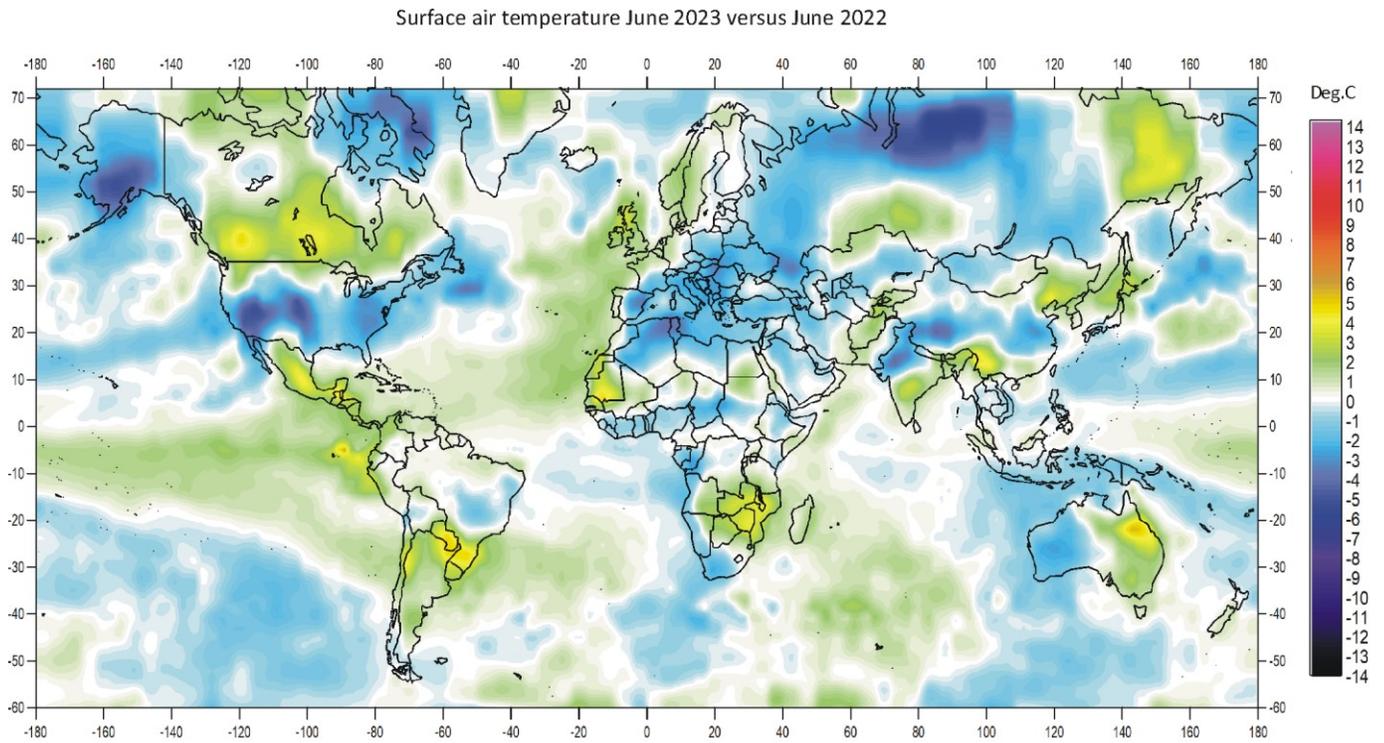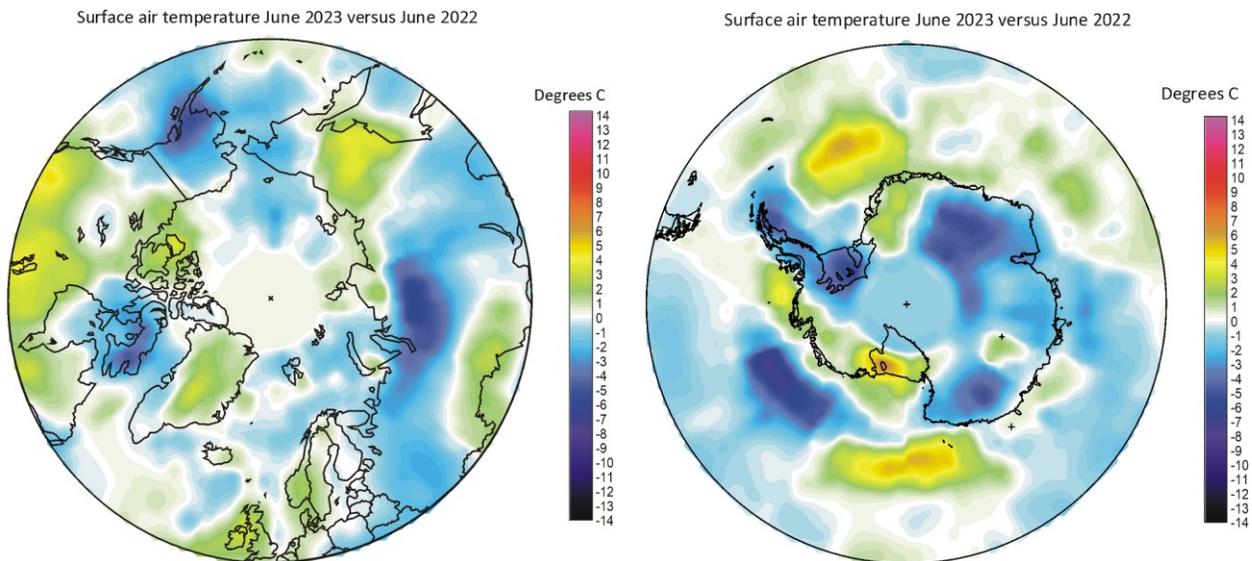
June 2023 surface air temperature compared to June 2022. Green-yellow-red colours indicate regions where the present month was warmer than last year, while blue colours indicate regions where the present month was cooler than last year. Variations in monthly temperature from one year to the next has no tangible climatic importance but may nevertheless be interesting to study. Data source: Remote Sensed Surface Temperature Anomaly, AIRS/Aqua L3 Monthly Standard Physical Retrieval 1-degree x 1-degree V006 (https://airs.jpl.nasa.gov/), obtained from the GISS data portal (https://data.giss.nasa.gov/gistemp/maps/index_v4.html).

Global monthly average lower troposphere temperature (thin line) since 1979 according to University of Alabama at Huntsville, USA. The thick line is the simple running 37-month average. Reference period 1991-2020.

6
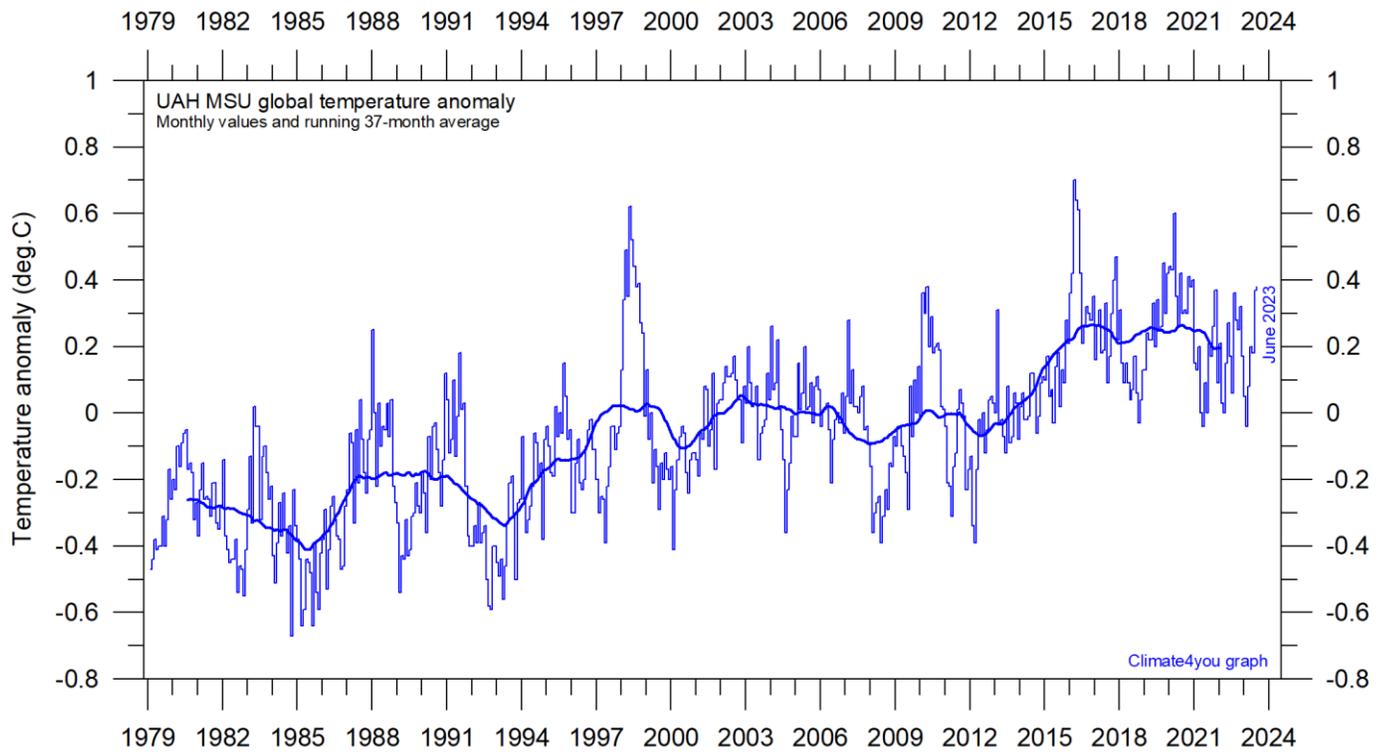
Global monthly average lower troposphere temperature (thin line) since 1979 according to according to Remote Sensing Systems (RSS), USA. The thick line is the simple running 37-month average.

Temperature quality class 2: HadCRUT global surface air temperature, updated to May 2023

HadCRUT5 non-infilled global temperature anomaly
Monthly values and running 37-month average
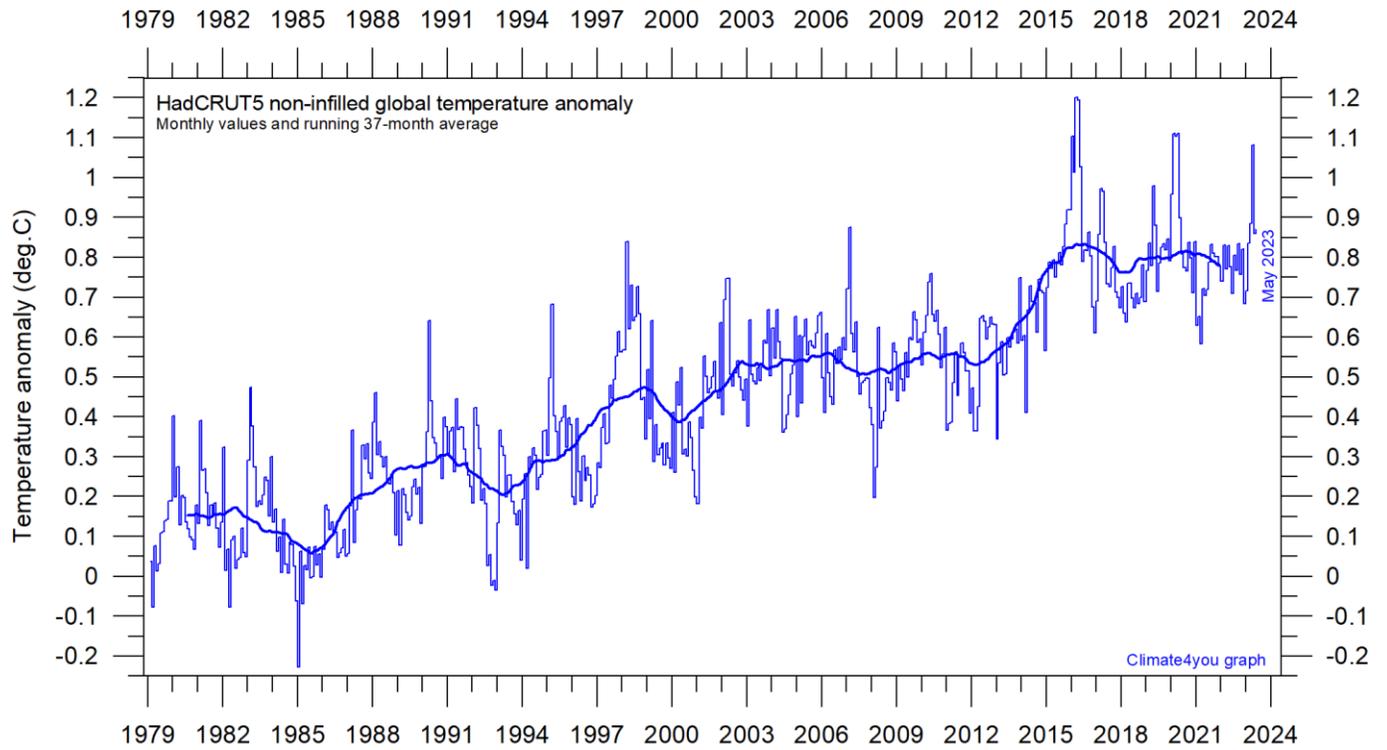
7   *Global monthly average surface air temperature (thin line) since 1979 according to the Hadley Centre for Climate Prediction and Research and the University of East Anglia's Climatic Research Unit (CRU), UK. The thick line is the simple running 37-month average. Please note that HadCRUT5 is not yet updated beyond May 2022.*

Temperature quality class 3: GISS and NCDC global surface air temperature, updated to June 2023
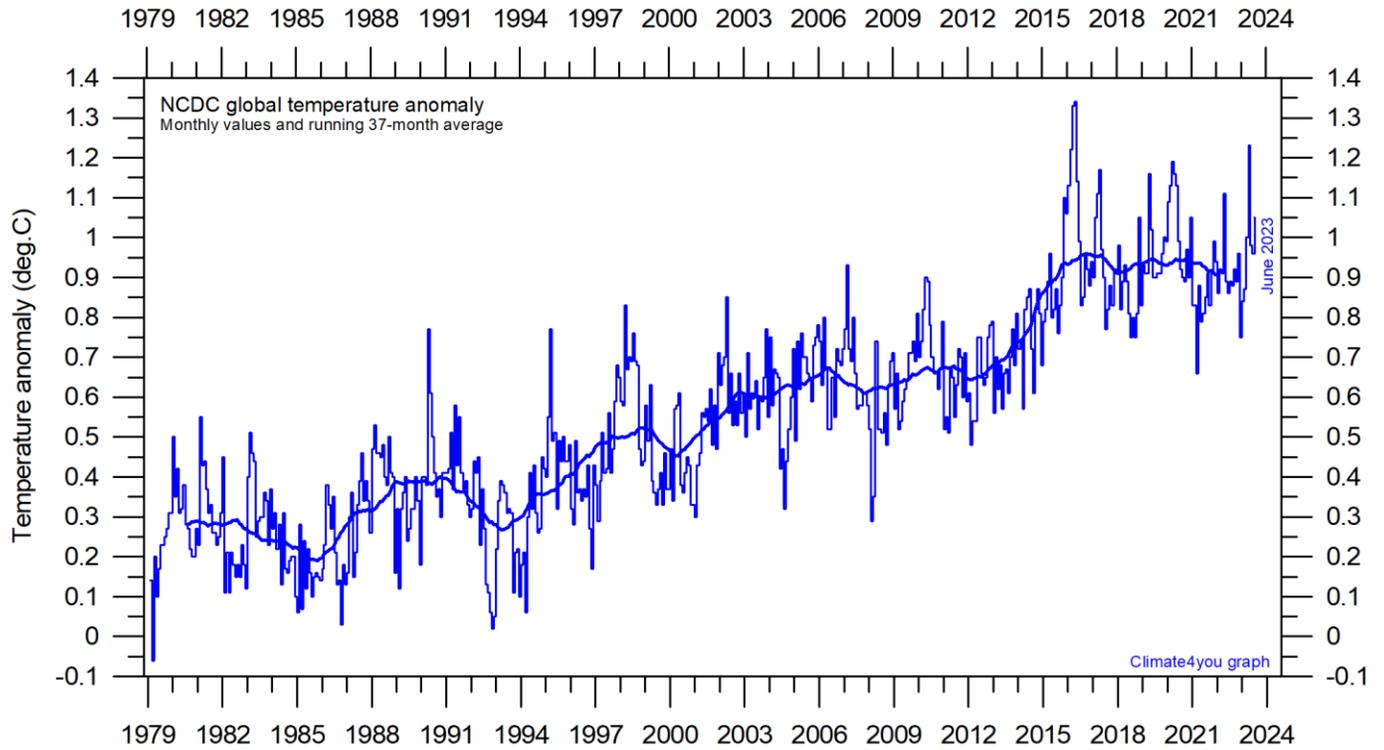
Global monthly average surface air temperature since 1979 according to according to the National Climatic Data Center (NCDC), USA. The thick line is the simple running 37-month average.
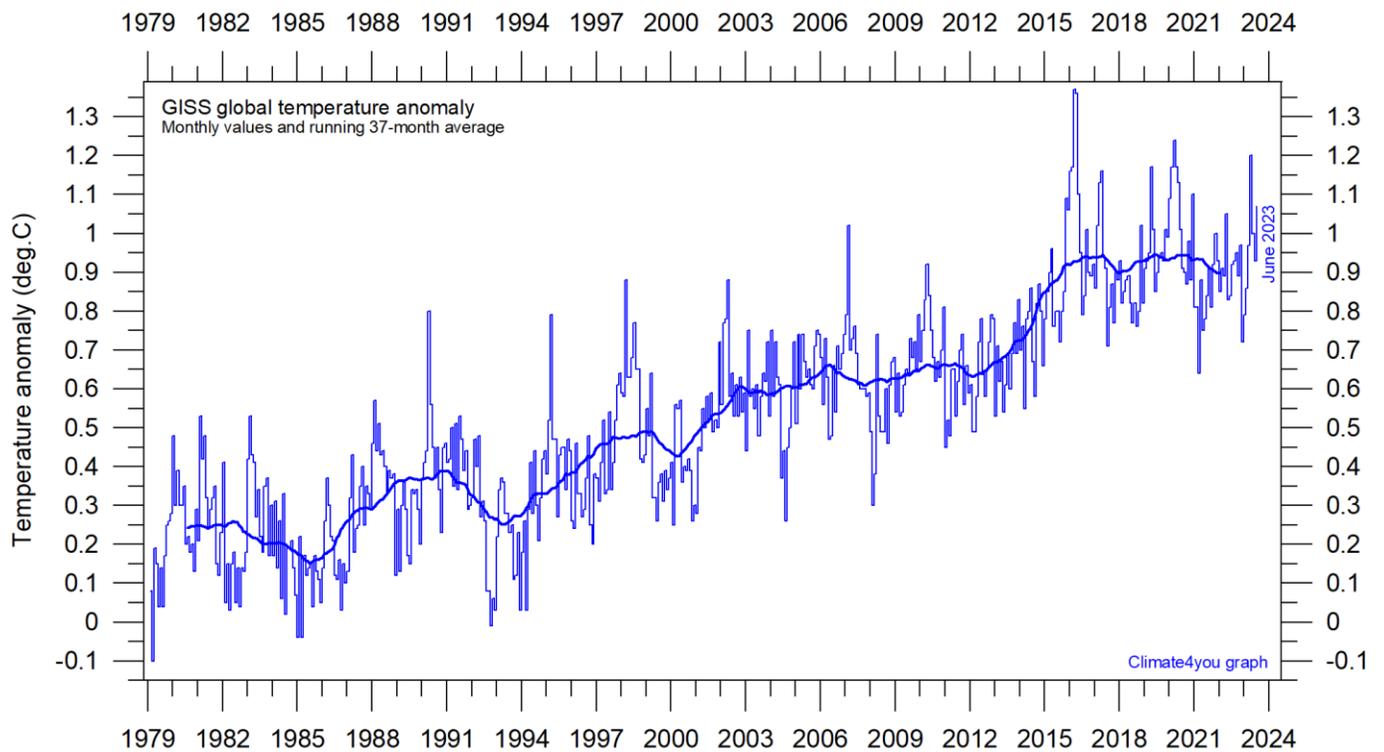
Global monthly average surface air temperature (thin line) since 1979 according to according to the Goddard Institute for Space Studies (GISS), at Columbia University, New York City, USA, using ERSST_v4 ocean surface temperatures. The thick line is the simple running 37-month average.

A note on data record stability and -quality:

The temperature diagrams shown above all have 1979 as starting year. This roughly marks the beginning of the recent episode of global warming, after termination of the previous episode of global cooling from about 1940. In addition, the year 1979 also represents the starting date for the satellite-based global temperature estimates (UAH and RSS). For the three surface air temperature records (HadCRUT, NCDC and GISS), they begin much earlier (in 1850 and 1880, respectively), as can be inspected on www.climate4you.com.

For all three surface air temperature records, but especially NCDC and GISS, administrative changes to anomaly values are quite often introduced, even affecting observations many years back in time. Some changes from the recent past may be due to the delayed addition of new station data or change of station location, while others probably have their origin in changes of the technique implemented to calculate average values from the raw data. It is clearly impossible to evaluate the validity of such administrative changes for the outside user of these records; it is only possible to note that such changes quite often are introduced (se example diagram next page).

In addition, the three surface records represent a blend of sea surface data collected by moving ships or by other means, plus data from land stations of partly unknown quality and unknown degree of representativeness for their region. Many of the land stations also has been moved geographically during their period of operation, instrumentation have been changed, and they are influenced by changes in their near surroundings (vegetation, buildings, etc.). The surface network is inherently heterogeneous (dense over continents but sparse over oceans) and probably contaminated by urbanization surrounding many measurement sites.

The satellite temperature records also have their problems, but these are generally of a more technical nature and probably therefore better correctable. In addition, the temperature sampling by satellites is more regular and complete on a global basis than that represented by the surface records. It is also important that the sensors on satellites measure temperature directly by microwave radiance (thereby unobstructed by clouds), while most modern surface temperature measurements are indirect, using electronic resistance.

Everybody interested in climate science should gratefully acknowledge the big efforts put into maintaining the different temperature databases referred to in the present newsletter. At the same time, however, it is also important to realise that all temperature records cannot be of equal scientific quality. The simple fact that they to some degree differ shows that they cannot all be correct.

On this background, and for practical reasons, Climate4you therefore operates with three quality classes (1-3) for global temperature records, with 1 representing the highest quality level:

Quality class 1: The satellite records (UAH and RSS).
Quality class 2: The HadCRUT surface record.
Quality class 3: The NCDC and GISS surface records.

The main reason for discriminating between the three surface records is the following:

While both NCDC and GISS often experience quite large administrative changes (see example on p.10), and therefore essentially must be considered as unstable records, the changes introduced to HadCRUT are fewer and smaller. For obvious reasons, as the past does not change, any record undergoing continuing changes cannot describe the past correctly all the time. Frequent and large corrections in a database unavoidably signal a fundamental uncertainty about what is likely to represent the correct values.

You can find more on the issue of lack of temporal stability on www.climate4you.com (go to: *Global Temperature*, and then proceed to *Temporal Stability*).
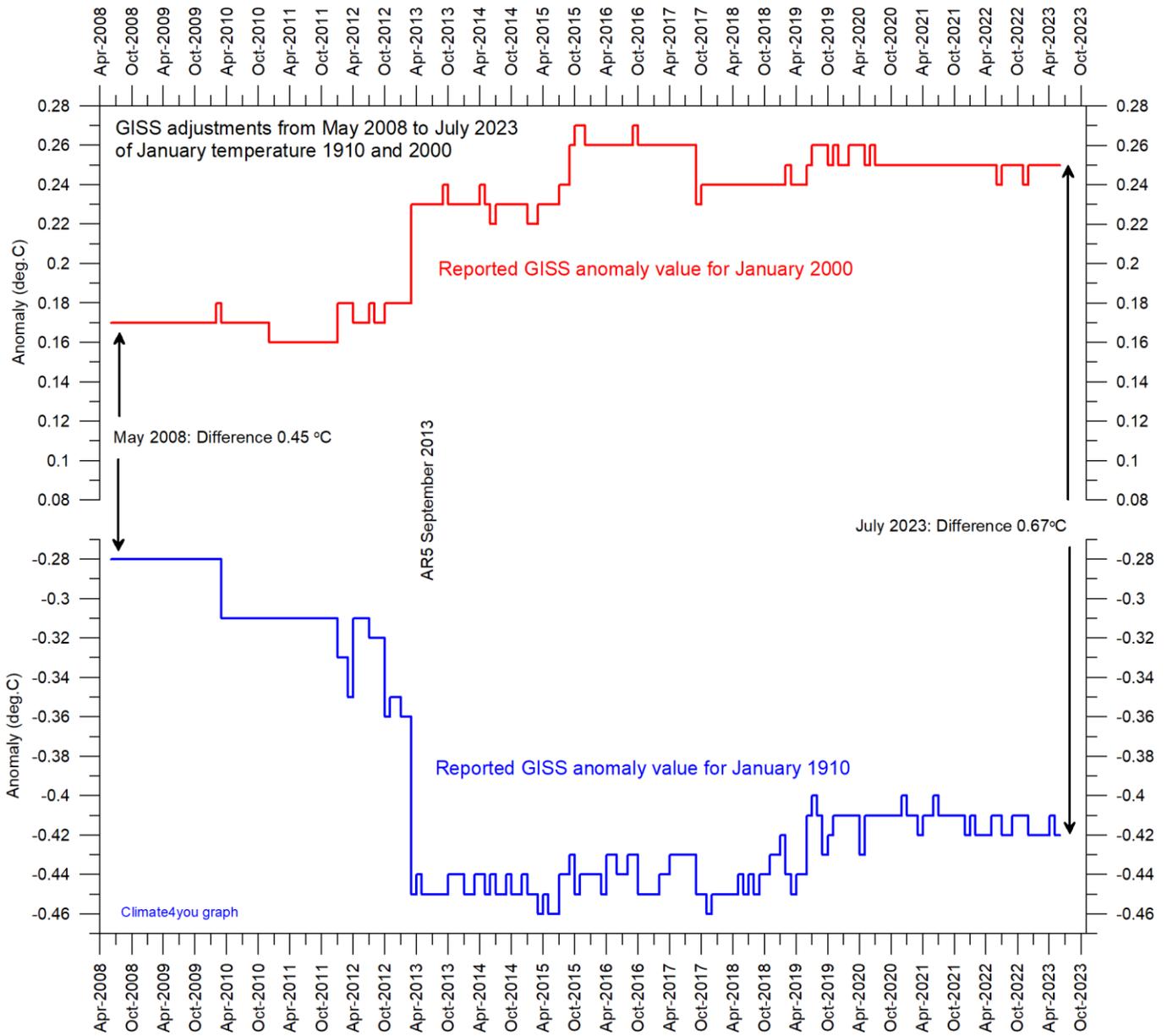
Diagram showing the monthly adjustments made since May 2008 by the [Goddard Institute for Space Studies](#) (GISS), USA, as recorded by published anomaly values for the two months January 1910 and January 2000. AR5 indicates timing of publication of IPCC report AR5 Climate Change 2013: The Physical Science Basis.

The administrative upsurge of the temperature increase from January 1915 to January 2000 has grown from 0.45 (reported May 2008) to 0.67°C (reported July 2023). This represents an about 49% administrative temperature increase over this period, meaning that a significant part (nearly half) of the apparent global temperature increase from January 1910 to January 2000 (as reported by GISS) is caused by administrative changes of the original data since May 2008.
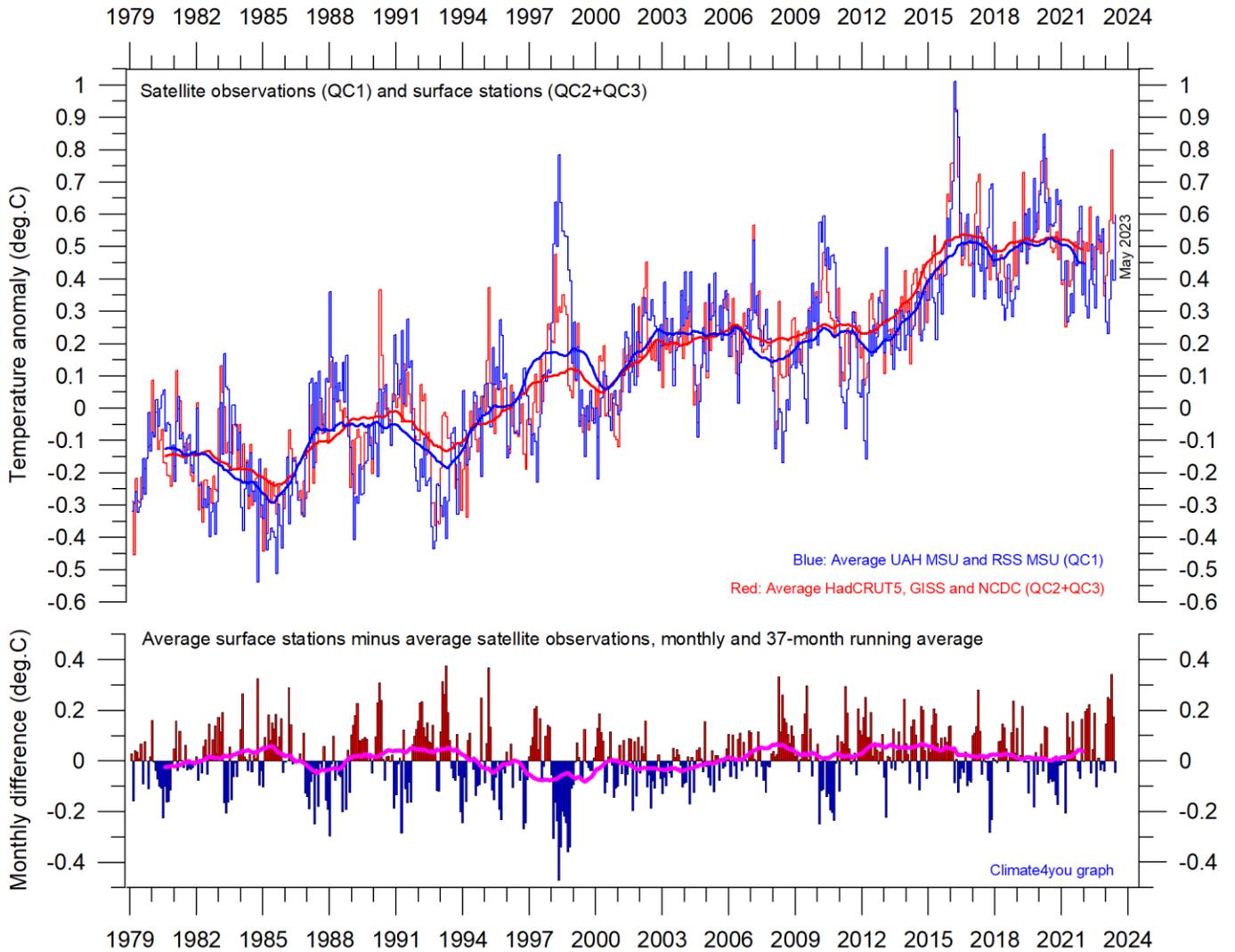
Plot showing the average of monthly global surface air temperature estimates (HadCRUT5, GISS and NCDC) and satellite-based temperature estimates (RSS MSU and UAH MSU). The thin lines indicate the monthly value, while the thick lines represent the simple running 37-month average, nearly corresponding to a running 3-yr average. The lower panel shows the monthly difference between average surface air temperature and satellite temperatures. As the base period differs for the different temperature estimates, they have all been normalised by comparing to the average value of 30 years from January 1979 to December 2008.

Global air temperature linear trends updated to May 2023
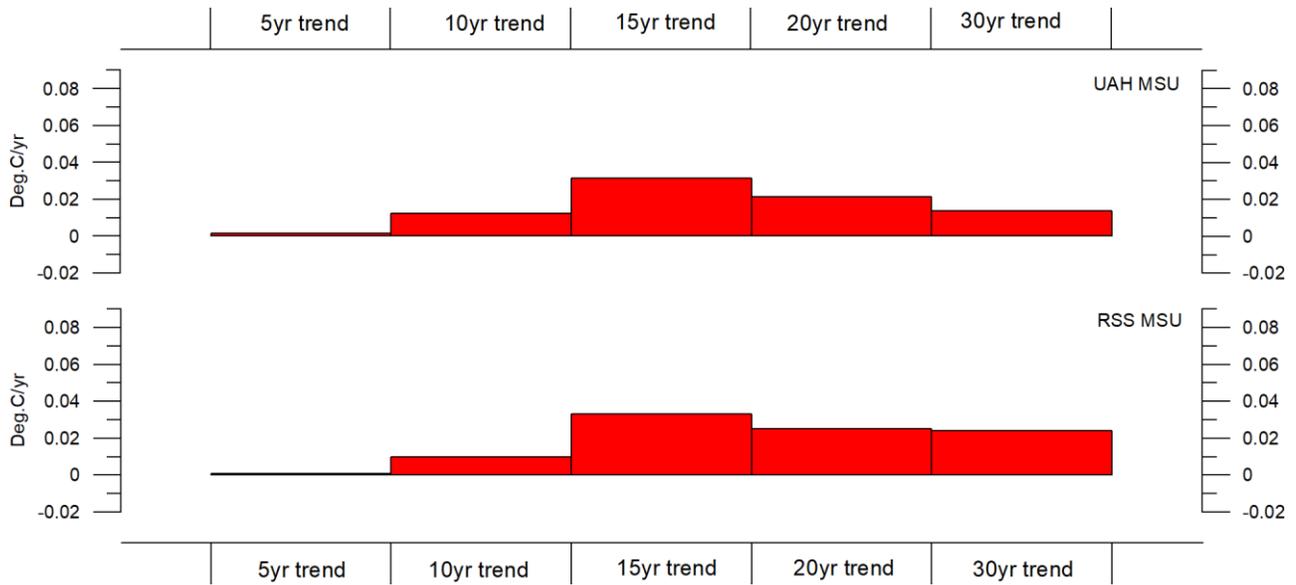
Diagram showing the latest 5, 10, 20 and 30-yr linear annual global temperature trend, calculated as the slope of the linear regression line through the data points, for two satellite-based temperature estimates (UAH MSU and RSS MSU).
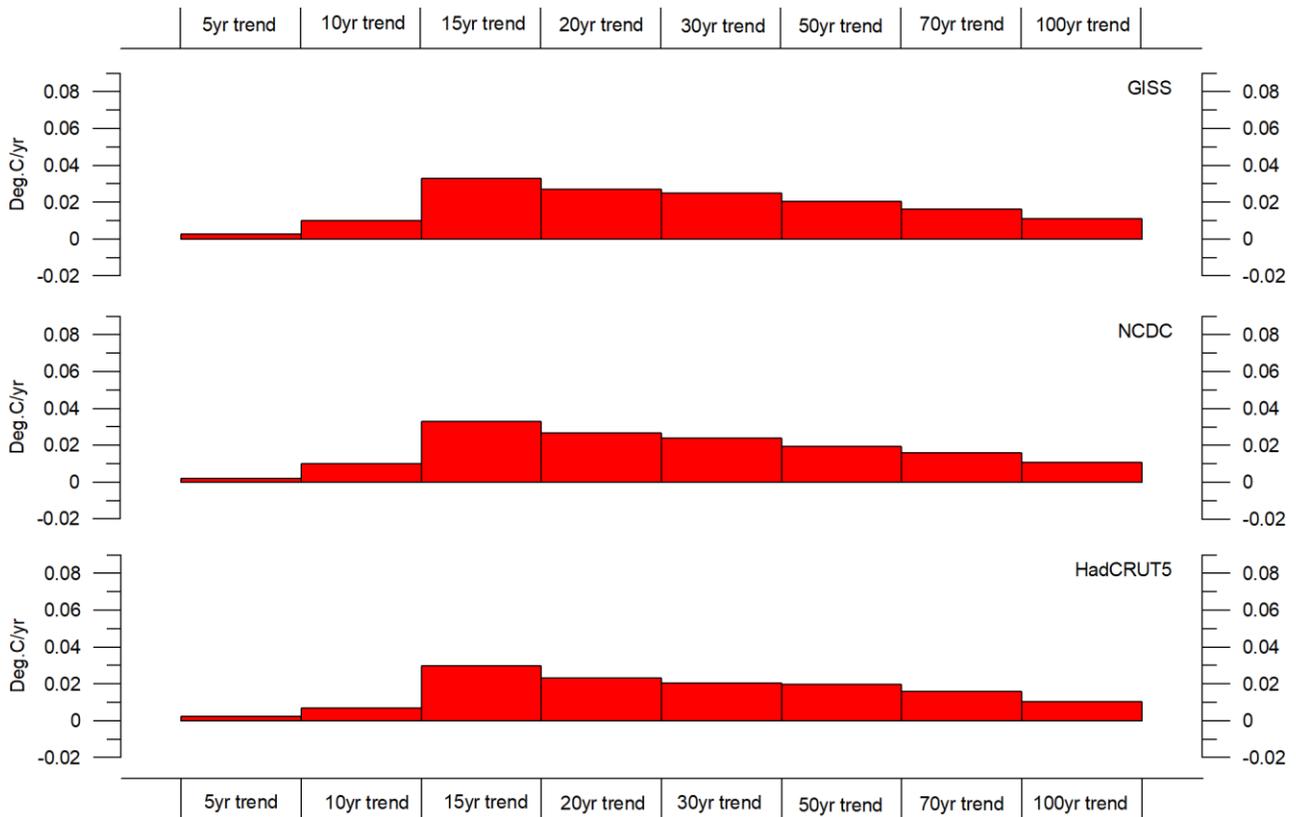
Diagram showing the latest 5, 10, 20, 30, 50, 70 and 100-year linear annual global temperature trend, calculated as the slope of the linear regression line through the data points, for three surface-based temperature estimates (GISS, NCDC and HadCRUT5).
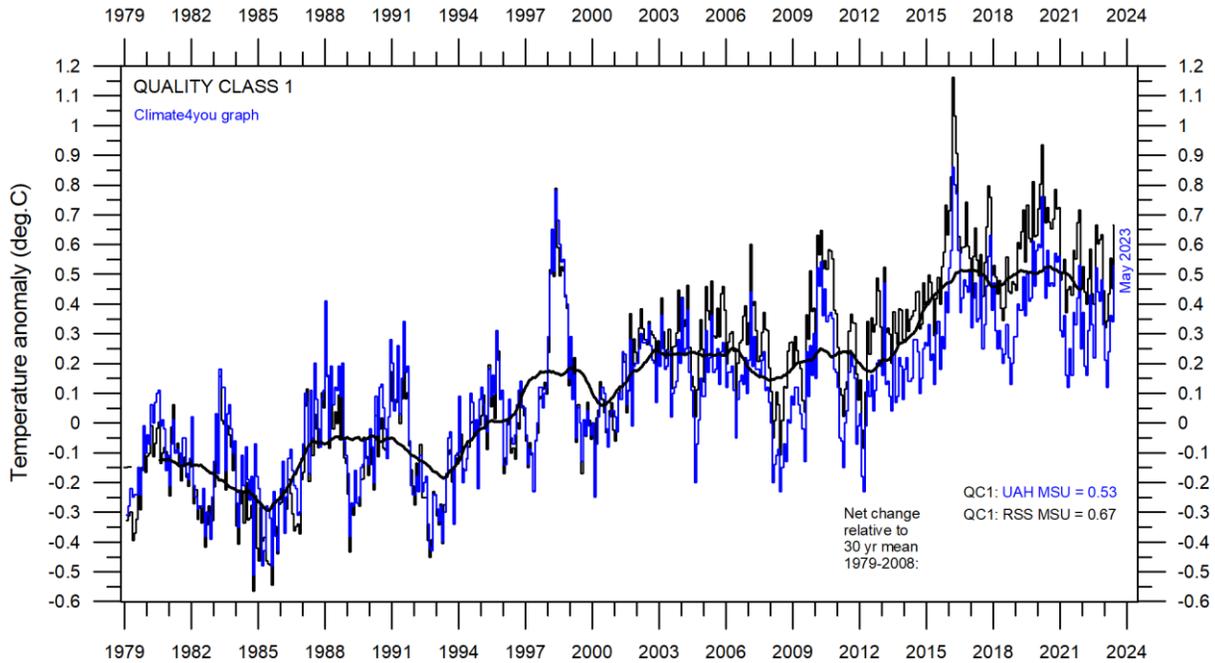
Superimposed plot of Quality Class 1 (UAH and RSS) global monthly temperature estimates. As the base period differs for the individual temperature estimates, they have all been normalised by comparing with the average value of the initial 120 months (30 years) from January 1979 to December 2008. The heavy black line represents the simple running 37 month (c. 3 year) mean of the average of both temperature records. The numbers shown in the lower right corner represent the temperature anomaly relative to the individual 1979-2008 averages.

13
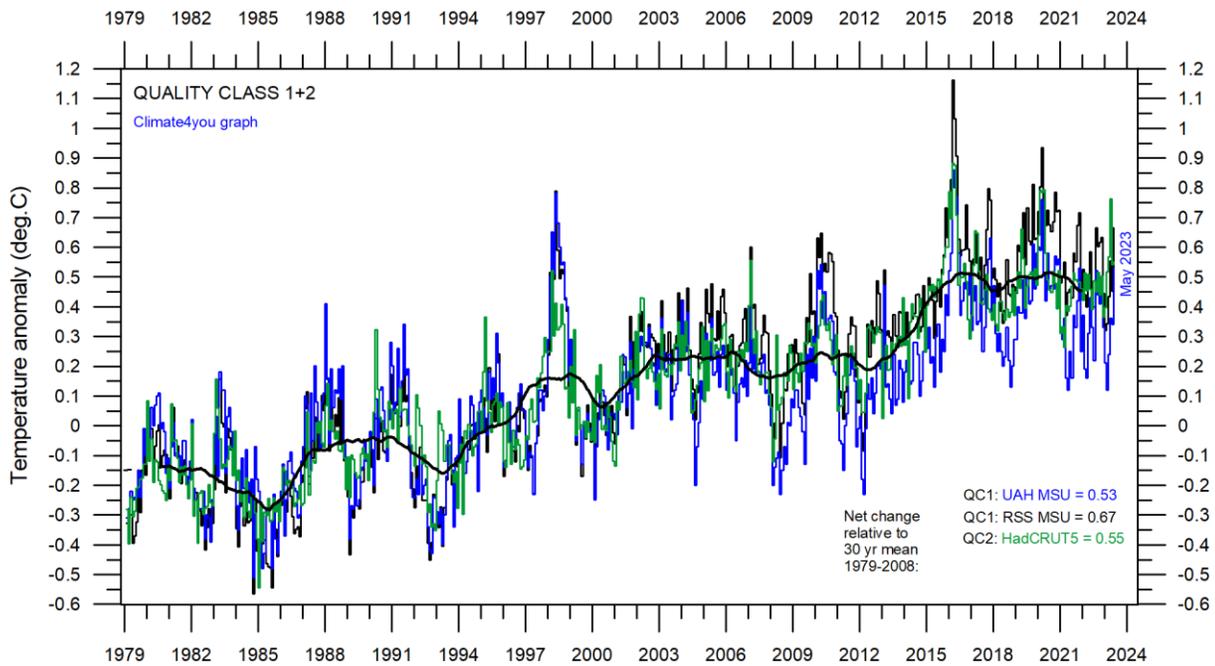
Superimposed plot of Quality Class 1 and 2 (UAH, RSS and HadCRUT) global monthly temperature estimates. As the base period differs for the individual temperature estimates, they have all been normalised by comparing with the average value of the initial 120 months (30 years) from January 1979 to December 2008. The heavy black line represents the simple running 37 month (c. 3 year) mean of the average of all three temperature records. The numbers shown in the lower right corner represent the temperature anomaly relative to the individual 1979-2008 averages.
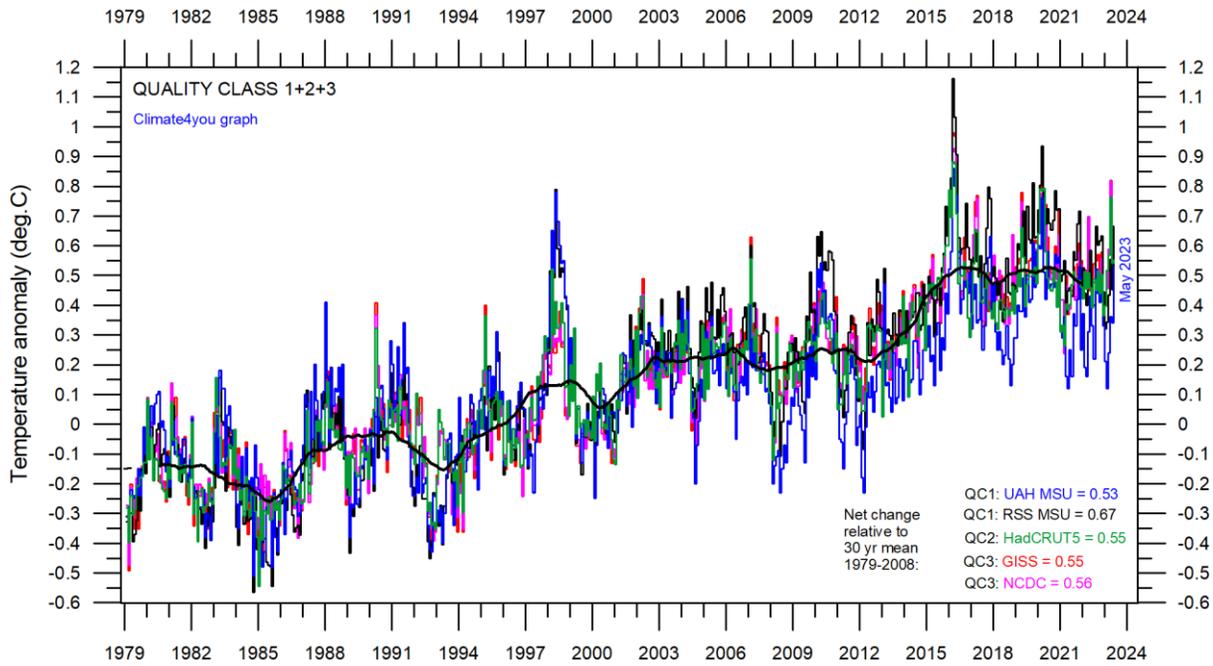
Superimposed plot of Quality Class 1, 2 and 3 global monthly temperature estimates (UAH, RSS, HadCRUT, GISS and NCDC). As the base period differs for the individual temperature estimates, they have all been normalised by comparing with the average value of the initial 120 months (30 years) from January 1979 to December 2008. The heavy black line represents the simple running 37 month (c. 3 year) mean of the average of all five temperature records. The numbers shown in the lower right corner represent the temperature anomaly relative to the individual 1979-2008 averages.

Please see reflections on page 9 relating to the above three quality classes.

14

Satellite- and surface-based temperature estimates are derived from different types of measurements and comparing them directly as in the above diagrams therefore may be somewhat ambiguous.

However, as both types of estimates often are discussed together in various news media, the above composite diagrams may nevertheless be of some interest.

In fact, the different types of temperature estimates appear to agree as to the overall temperature variations on a 2-3-year scale, although on a shorter time scale there are often considerable differences between the individual records. However, since about 2003 the surface records used to be drifting towards higher temperatures than the combined satellite record, but this overall tendency was much removed by the major adjustment of the RSS satellite series in 2015 (see lower diagram on page 6).

The combined records (diagram above) suggest a modest global air temperature increase over the last 30 years, about 0.17°C per decade. It should be noted that the apparent temperature increases since about 2003 at least partly is the result of ongoing administrative adjustments (page 9-10). At the same time, none of the temperature records considered here indicates any overall temperature decrease during the last 20 years.

The present temperature development does not exclude the possibility that global temperatures may begin to increase significantly later. On the other hand, it also remains a possibility that Earth just now is passing an overall temperature peak, and that global temperatures may begin to decrease during the coming 5-10 years.

As always, time will show which of these possibilities is correct.

## Global sea surface temperature, updated to June 2023
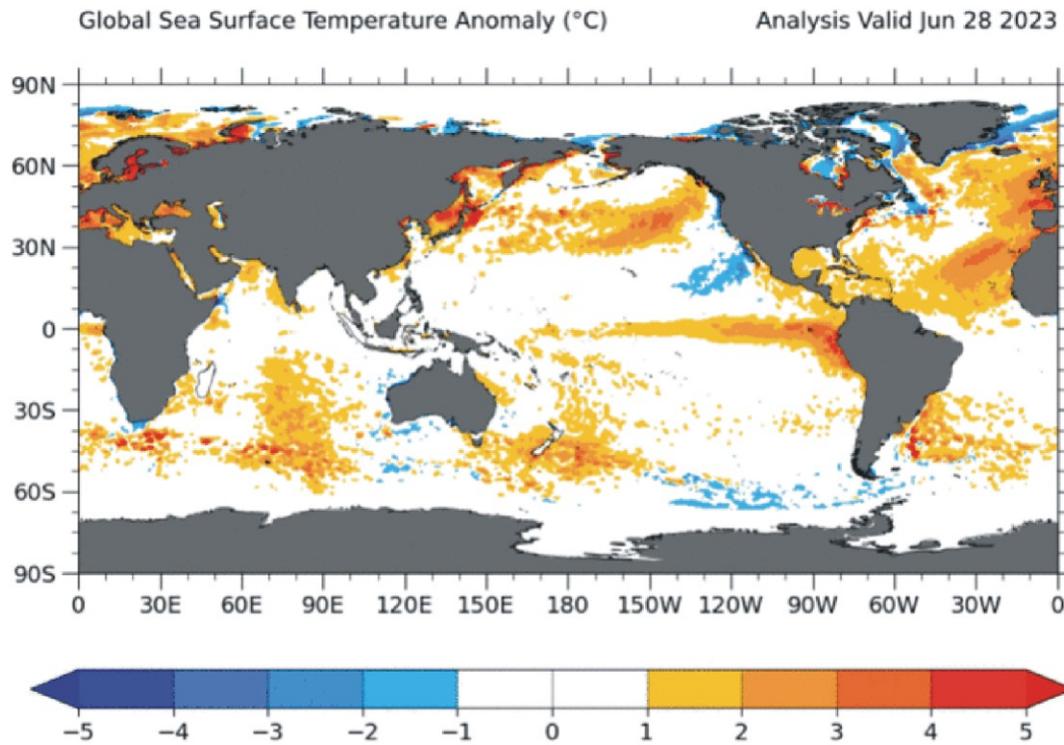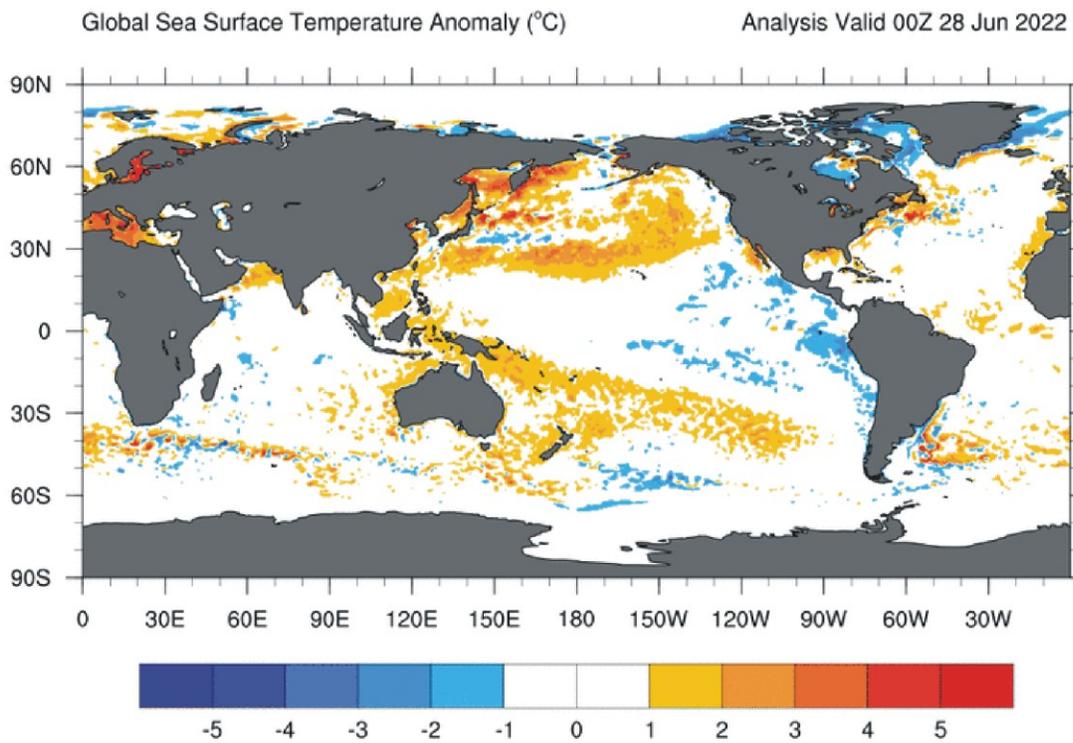
Sea surface temperature anomaly on 28 June 2023 (upper map) and 2022 (lower map). Map source: Plymouth State Weather Center. Reference period: 1977-1991.

Because of the large surface areas near Equator, the temperature of the surface water in these regions is especially important for the global atmospheric temperature (p. 6-8). In fact, no less than 50% of planet Earth's surface area is located within 30°N and 30°S.

A mixture of relatively warm and cold water presently dominates much of the global ocean surface, but with notable variations from month to month. All such ocean surface temperature changes will be influencing global air temperatures in the months to come. A cold La Niña episode (Pacific Ocean) has recently ended and will probably be followed by a warm El Niño episode (see also p. 25).

The significance of short-term cooling or warming reflected in air temperatures should never be overstated. Whenever Earth experiences cold La Niña or warm El Niño episodes major heat exchanges take place between the Pacific Ocean and the atmosphere above, sooner or later showing up in estimates of the global air temperature.

However, this does not necessarily reflect similar changes in the total heat content of the atmosphere-ocean system. In fact, global net changes can be small and such heat exchanges may mainly reflect redistribution of energy between ocean and atmosphere. What matters is the overall temperature development when seen over several years.
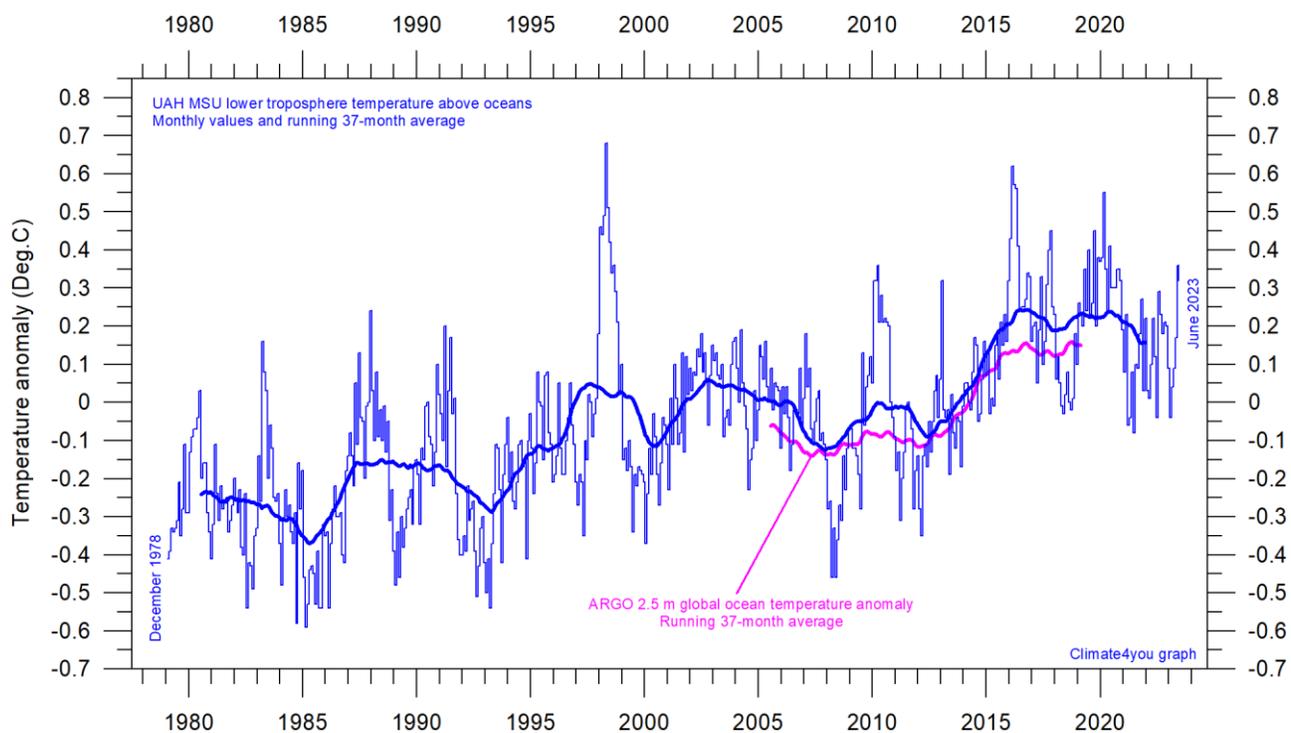
Global monthly average lower troposphere temperature over oceans (thin line) since 1979 according to University of Alabama at Huntsville, USA. The thick line is the simple running 37-month average. Insert: Argo global ocean temperature anomaly from floats, displaced vertically to make visual comparison easier. UAH reference period: 1991-2020.
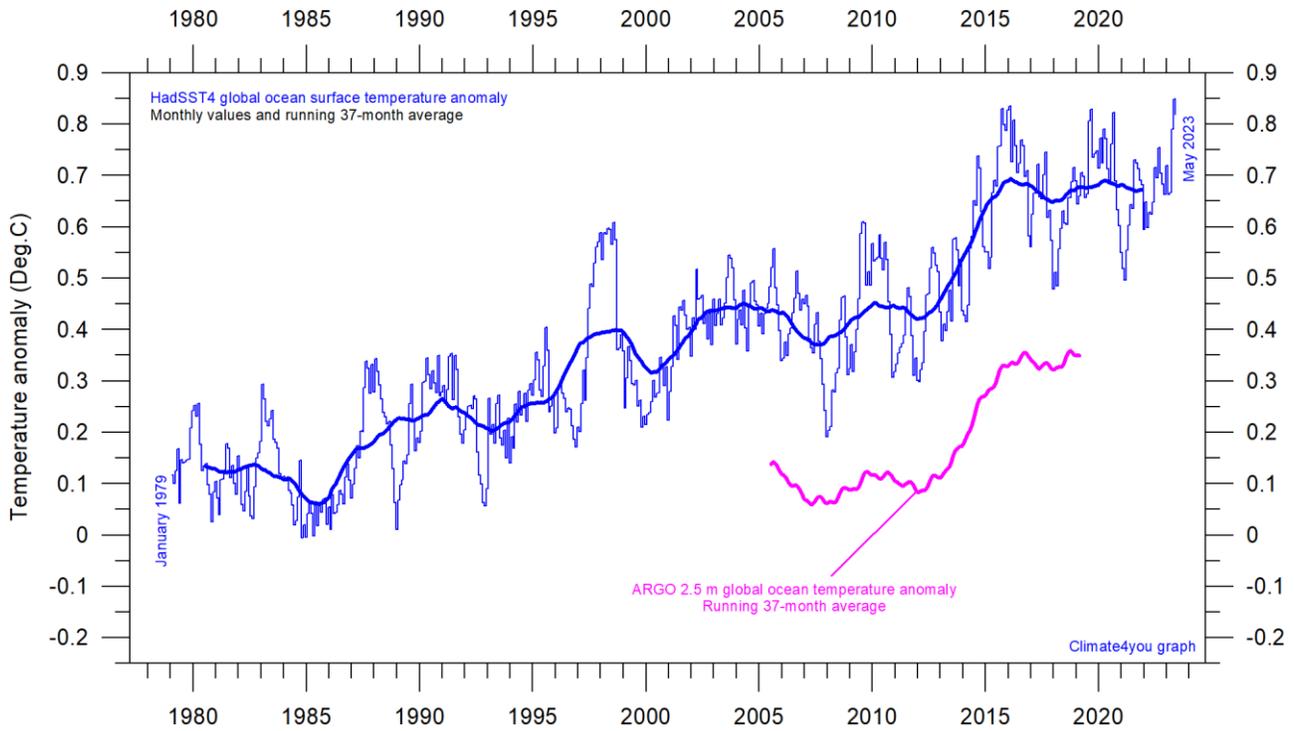
Global monthly average sea surface temperature since 1979 according to University of East Anglia's Climatic Research Unit (CRU), UK. Base period: 1961-1990. The thick line is the simple running 37-month average. Insert: Argo global ocean temperature anomaly from floats, displaced vertically to make visual comparison easier.
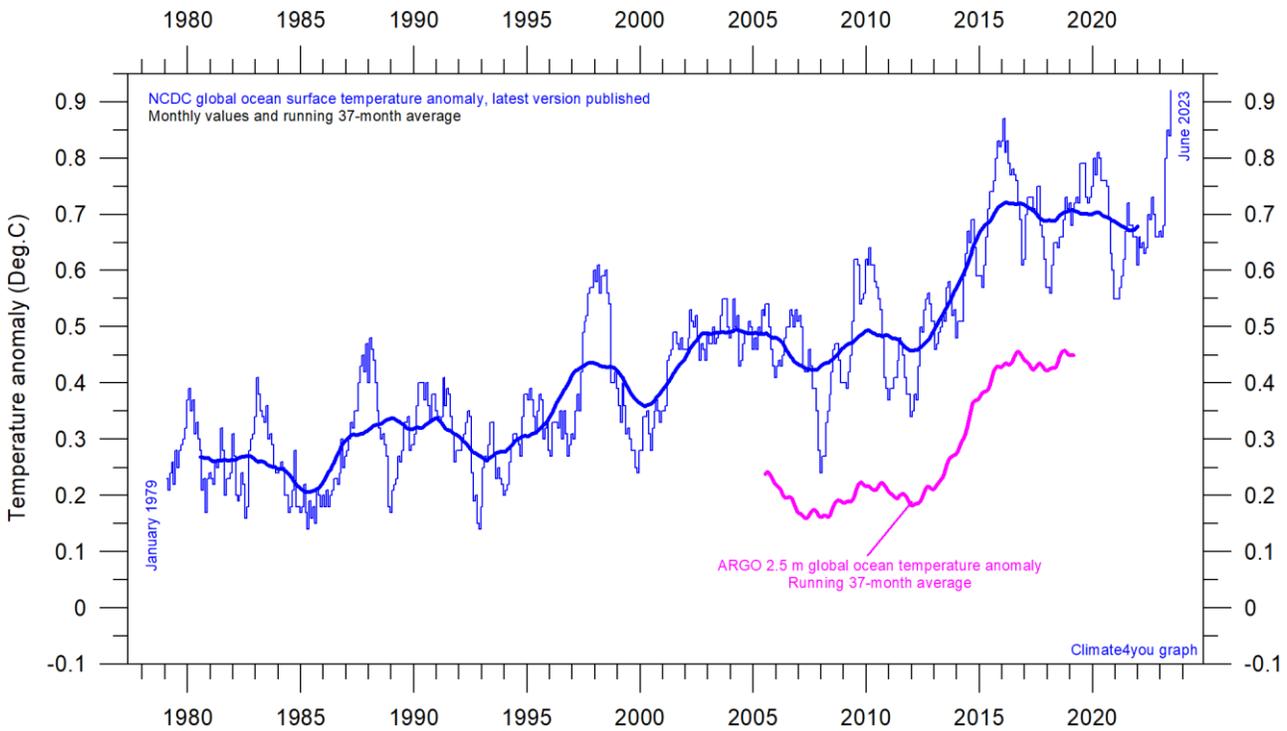
Global monthly average sea surface temperature since 1979 according to the National Climatic Data Center (NCDC), USA. Base period: 1901-2000. The thick line is the simple running 37-month average. Insert: Argo global ocean temperature anomaly from floats, displaced vertically to make visual comparison easier.

Ocean temperature in uppermost 100 m, updated to March 2023
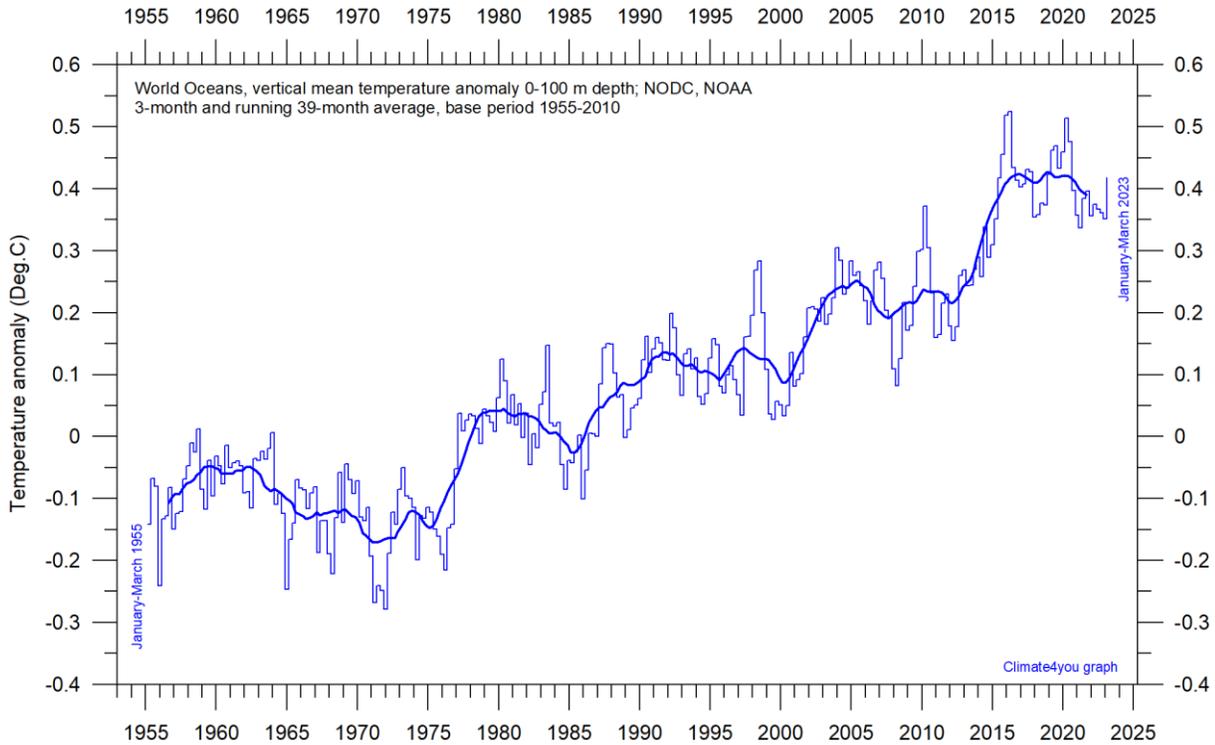
World Oceans vertical average temperature 0-100 m depth since 1955. The thin line indicates 3-month values, and the thick line represents the simple running 39-month (c. 3 year) average. Data source: NOAA National Oceanographic Data Center (NODC). Base period 1955-2010.
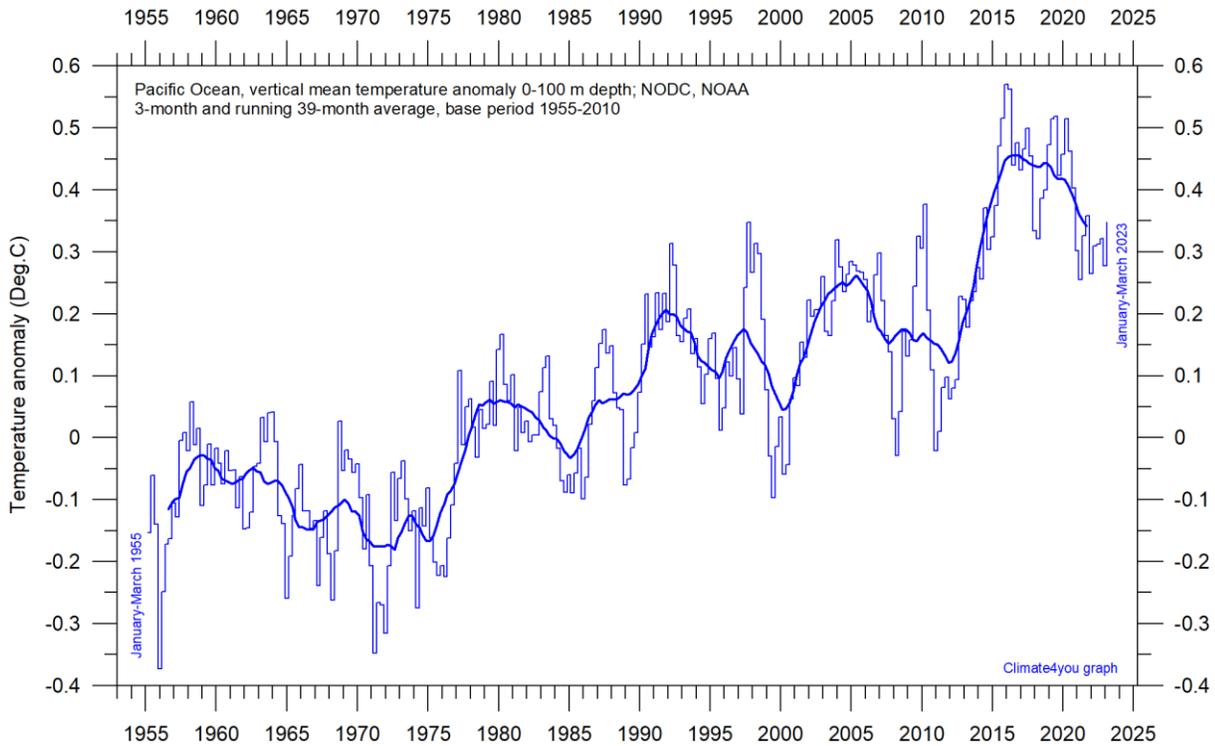
Pacific Ocean vertical average temperature 0-100 m depth since 1955. The thin line indicates 3-month values, and the thick line represents the simple running 39-month (c. 3 year) average. Data source: NOAA National Oceanographic Data Center (NODC). Base period 1955-2010.
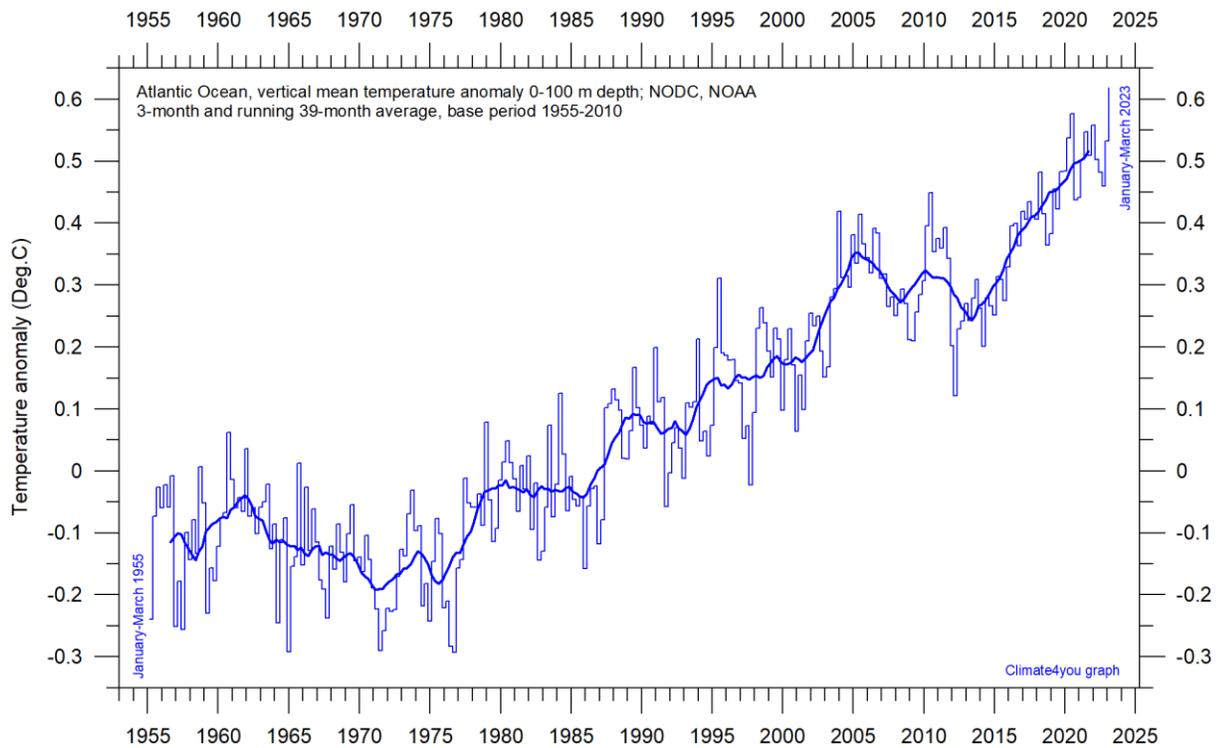
Atlantic Ocean vertical average temperature 0-100 m depth since 1955. The thin line indicates 3-month values, and the thick line represents the simple running 39-month (c. 3 year) average. Data source: NOAA National Oceanographic Data Center (NODC). Base period 1955-2010.
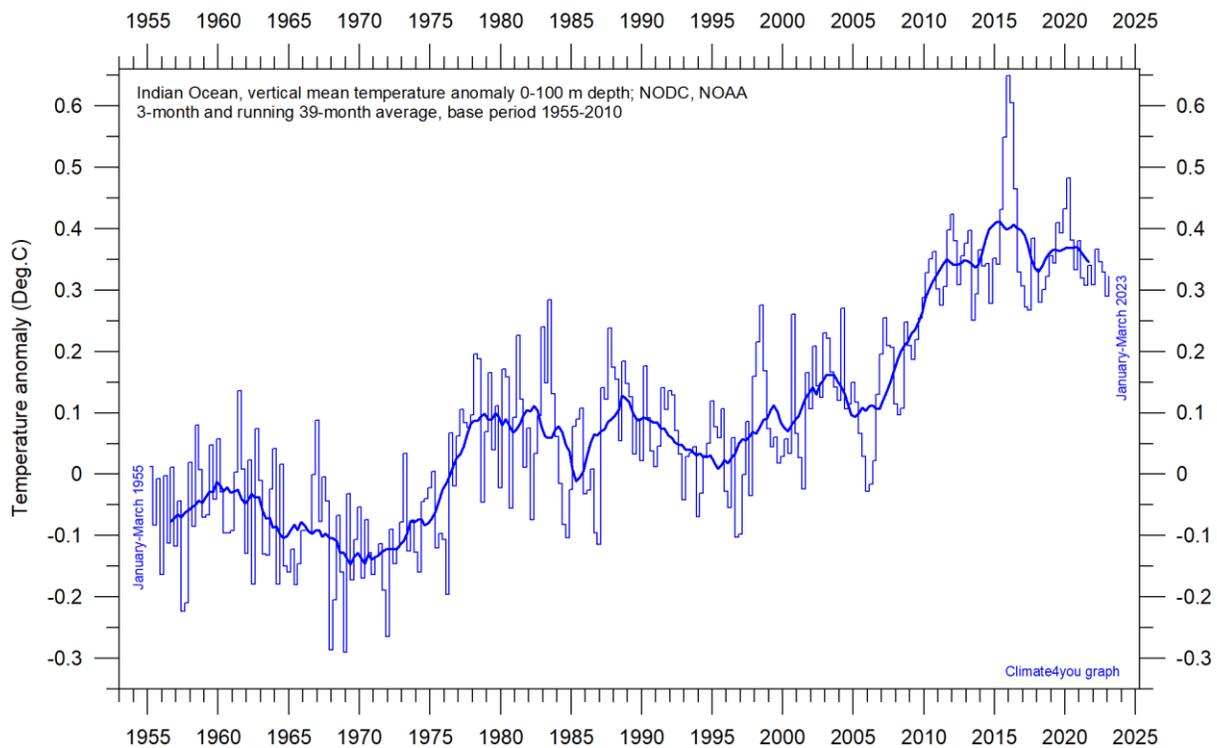
Indian Ocean vertical average temperature 0-100 m depth since 1955. The thin line indicates 3-month values, and the thick line represents the simple running 39-month (c. 3 year) average. Data source: NOAA National Oceanographic Data Center (NODC). Base period 1955-2010.

## Pacific Decadal Oscillation (PDO), updated to June 2023
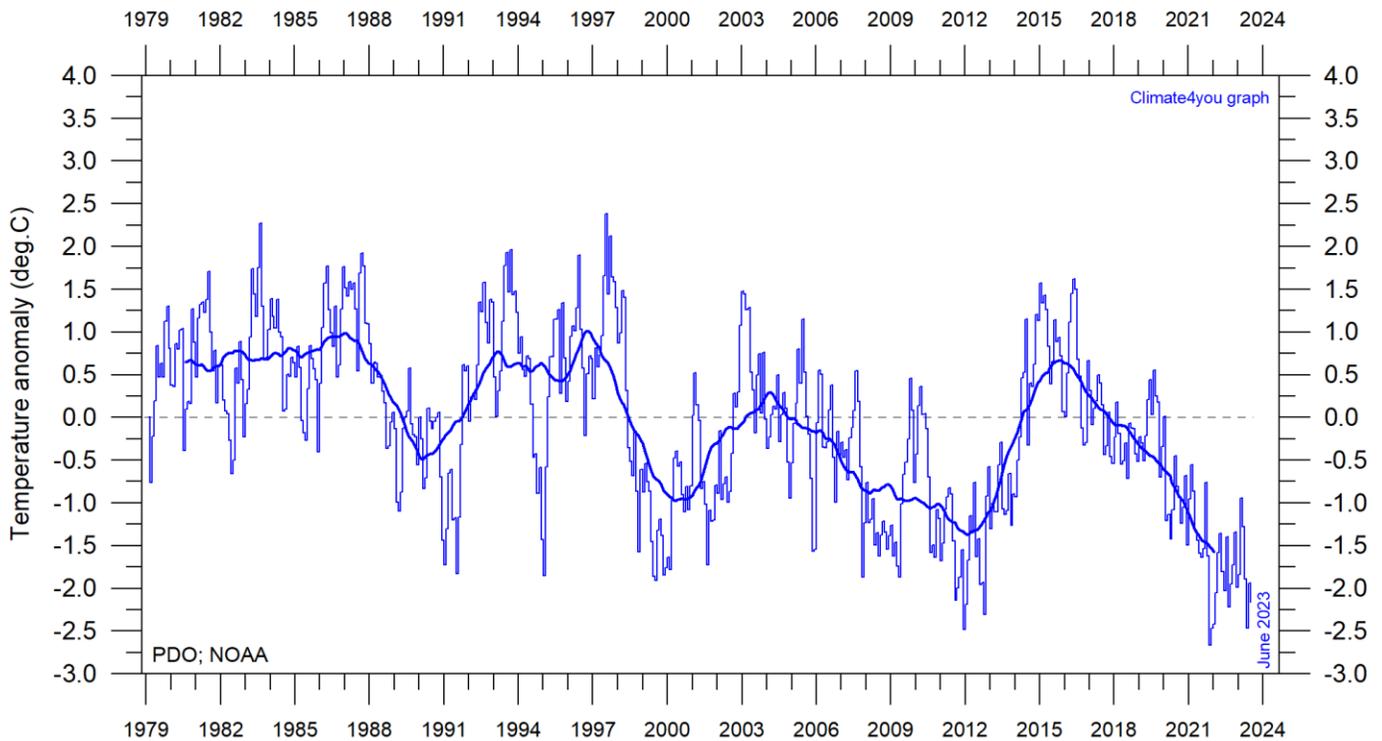
Monthly values of the Pacific Decadal Oscillation *(PDO) since January 1979. The PDO is a long-lived El Niño-like pattern of Pacific climate variability, and the data series goes back to January 1854. Base period: 1982-2002. The thin line indicates monthly PDO values, and the thick line is the simple running 37-month average. Data source: NOAA Physical Science Laboratory (version PDO ERSST V5 plotted above).*

The PDO is a long-lived El Niño-like pattern of Pacific climate variability, with data extending back to January 1854. Causes for PDO are not currently known, but even in the absence of a theoretical understanding, PDO climate information improves season-to-season and year-to-year climate forecasts for North America because of its strong tendency for multi-season and multi-year persistence. The PDO also appears to be roughly in phase with global temperature changes. Thus, from a societal impact's perspective, recognition of PDO is important because it shows that "normal" climate conditions can vary over time periods comparable to the length of a human's lifetime.

The PDO illustrates how global temperatures are tied to sea surface temperatures in the Pacific Ocean, the largest ocean on Earth. When sea surface temperatures are relatively low (negative phase PDO), as it was from 1945 to 1977, global air temperature decreases. When Pacific Ocean surface temperatures are high (positive phase PDO), as from 1977 to 1998, global surface air temperature increases.

A Fourier frequency analysis (not shown here) shows the entire PDO record since 1854 to be influenced by a 5.7-year cycle, and possibly also by a longer about 53-year long cycle.

North Atlantic heat content uppermost 700 m, updated to June 2021
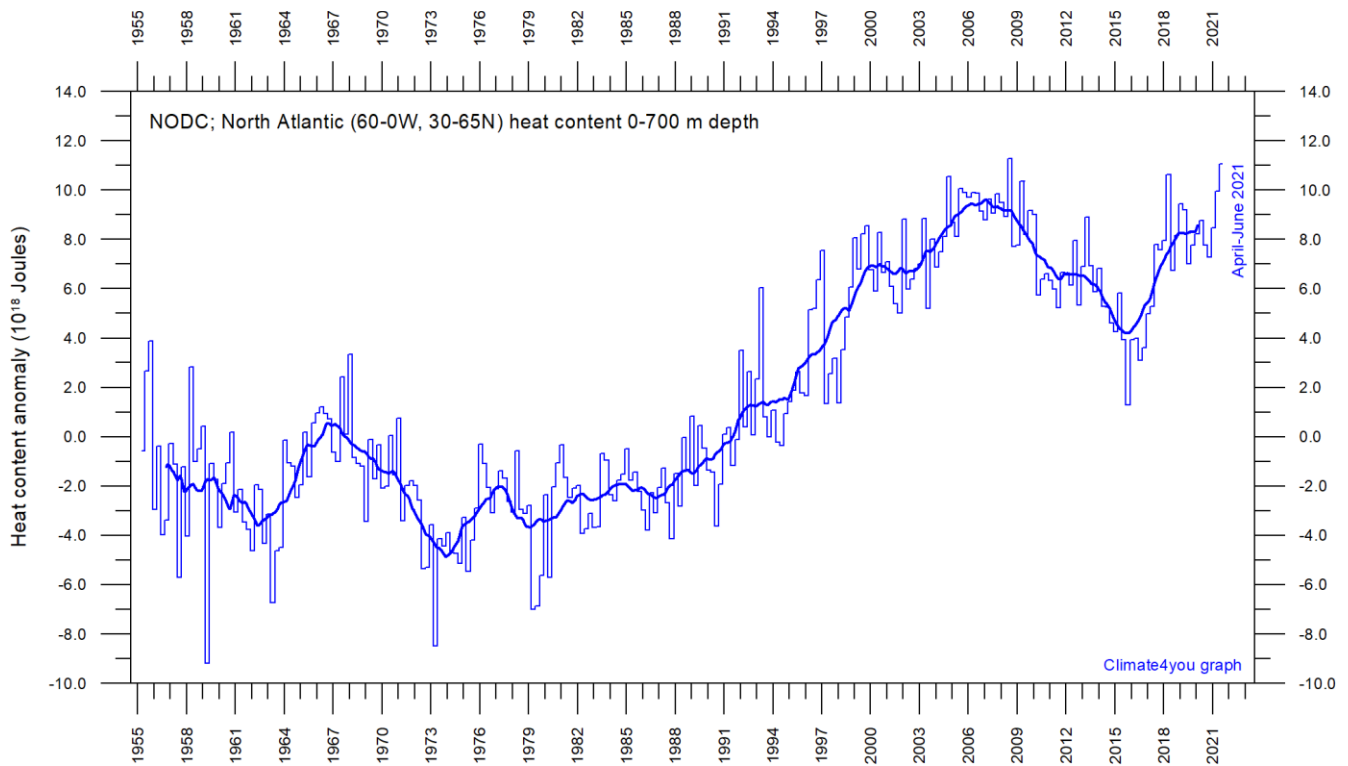
Global monthly heat content anomaly (10^18 Joules) in the uppermost 700 m of the North Atlantic (60-0W, 30-65N; see map above) *ocean since January 1955. The thin line indicates monthly values, and the thick line represents the simple running 37-month (c. 3 year) average. Data source: National Oceanographic Data Center (NODC).*

North Atlantic temperatures 0-800 m depth along 59°N, 30-0W, updated to August 2020

Time series of Argo Temperature (°C)
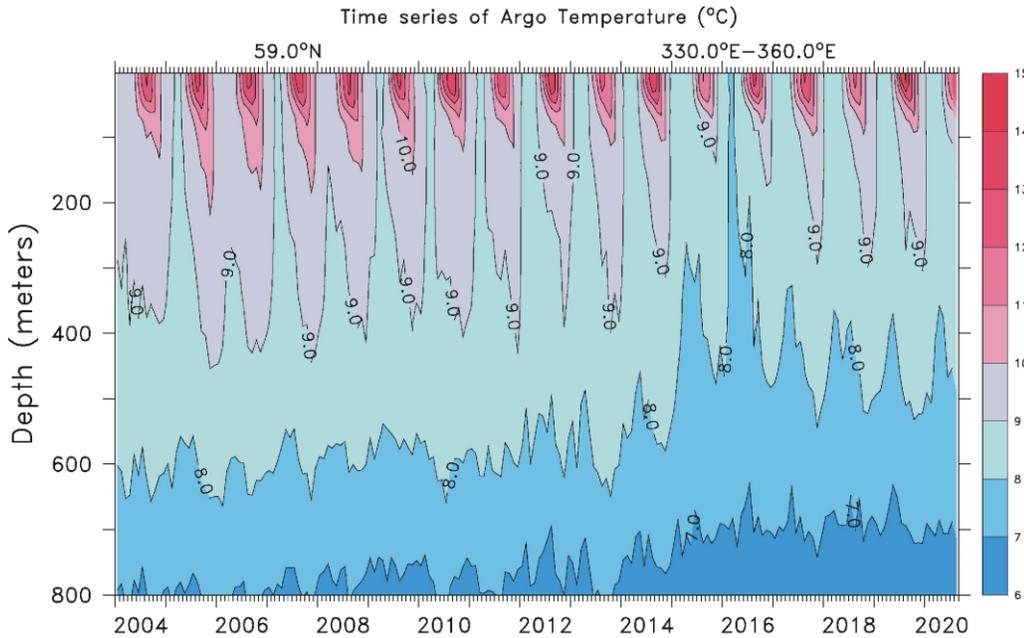
Time series depth-temperature diagram along 59 N across the North Atlantic Current from 30°W to 0°W, from surface to 800 m depth. Source: Global Marine Argo Atlas. See also the diagram below.
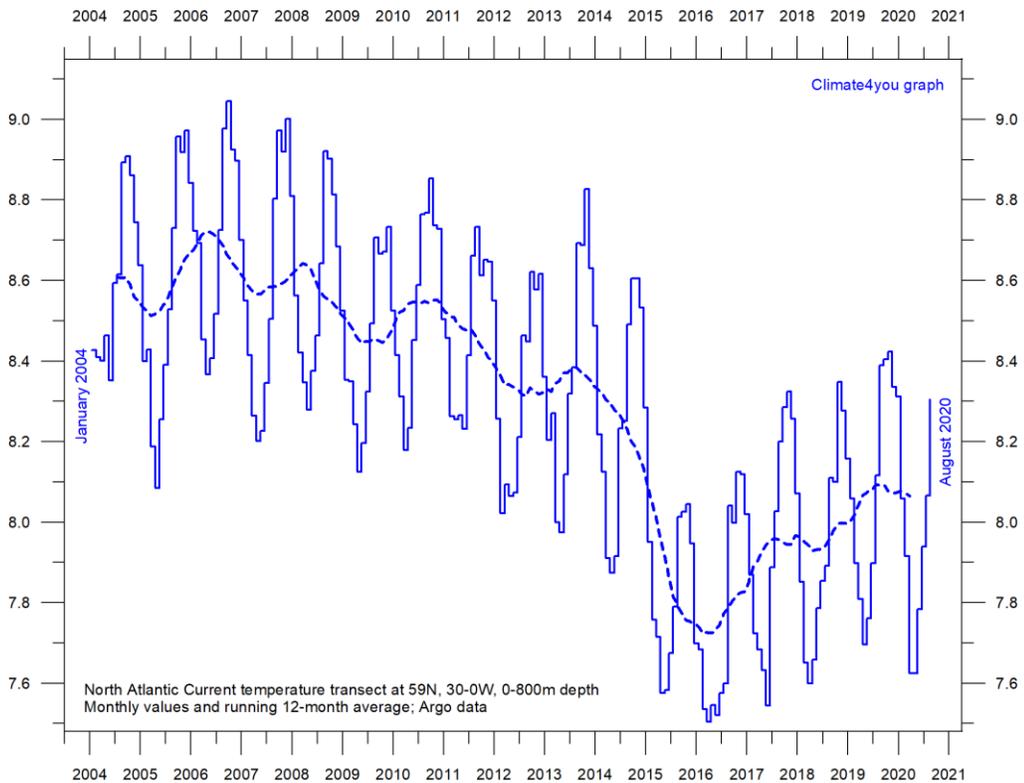
Average temperature along 59 N, 30-0W, 0-800m depth, corresponding to the main part of the North Atlantic Current, using Argo-data. Source: Global Marine Argo Atlas. Additional information can be found in: Roemmich, D. and J. Gilson, 2009. The 2004-2008 mean and annual cycle of temperature, salinity, and steric height in the global ocean from the Argo Program. Progress in Oceanography, 82, 81-100.

Global ocean temperature 0-1900 m depth summary, updated to August 2020
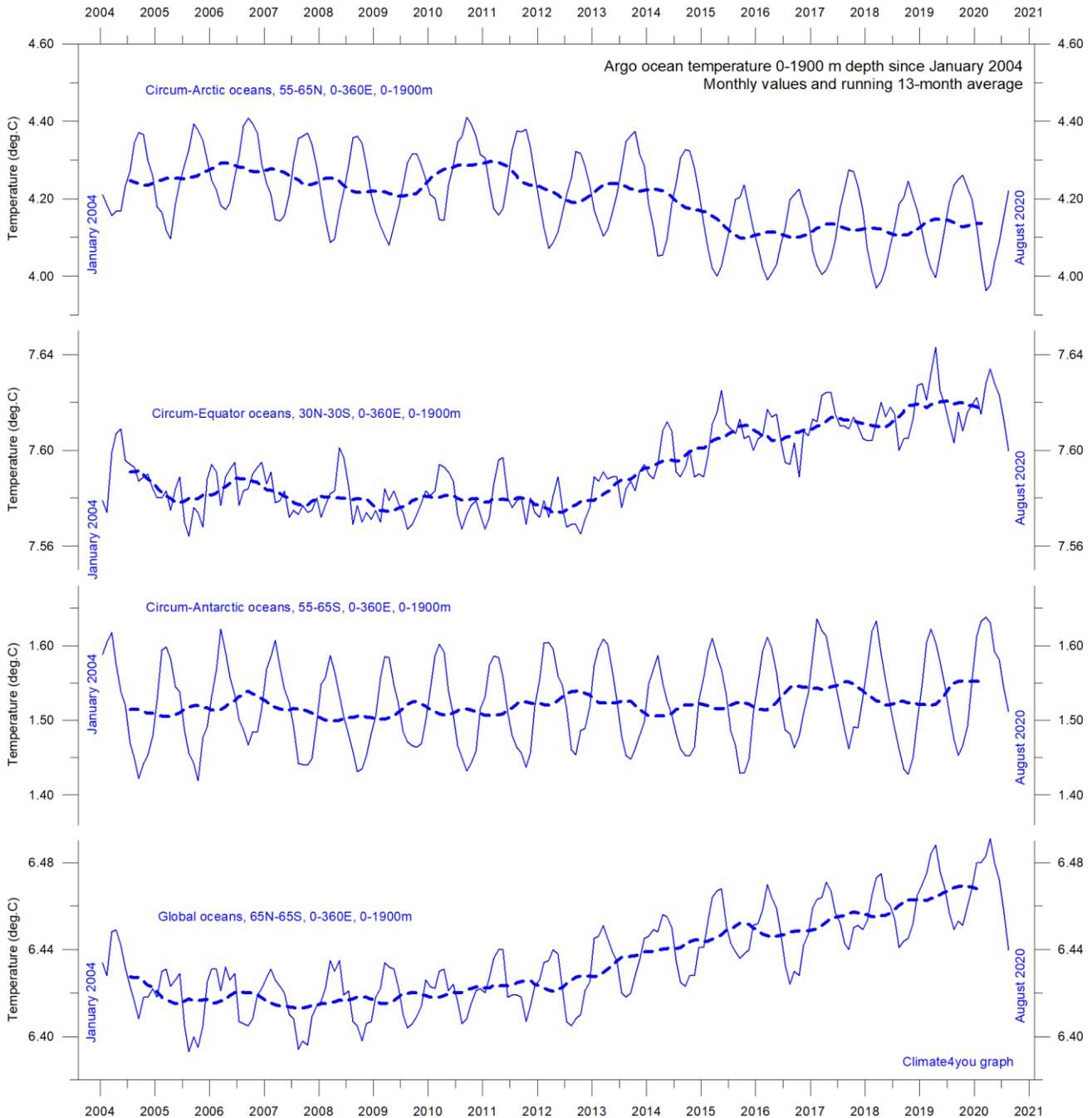
Summary of average temperature in uppermost 1900 m in different parts of the global oceans, using [Argo](#)-data. Source: [Global Marine Argo Atlas](#). Additional information can be found in: Roemmich, D. and J. Gilson, 2009. The 2004-2008 mean and annual cycle of temperature, salinity, and steric height in the global ocean from the Argo Program. [Progress in Oceanography](#), 82, 81-100.

The global summary diagram above shows that, on average, the temperature of the global oceans down to 1900 m depth has been increasing since about 2011. It is also seen that this increase since 2013 dominantly is due to oceanic changes occurring near the Equator, between 30°N and 30°S. In contrast, for the circum-Arctic oceans north of 55°N, depth-integrated ocean temperatures have been decreasing since 2011. Near the Antarctic, south of 55°S, temperatures have essentially been stable. At most latitudes, a clear annual rhythm is evident.

Global ocean net temperature change since 2004 at different depths, updated to August 2020
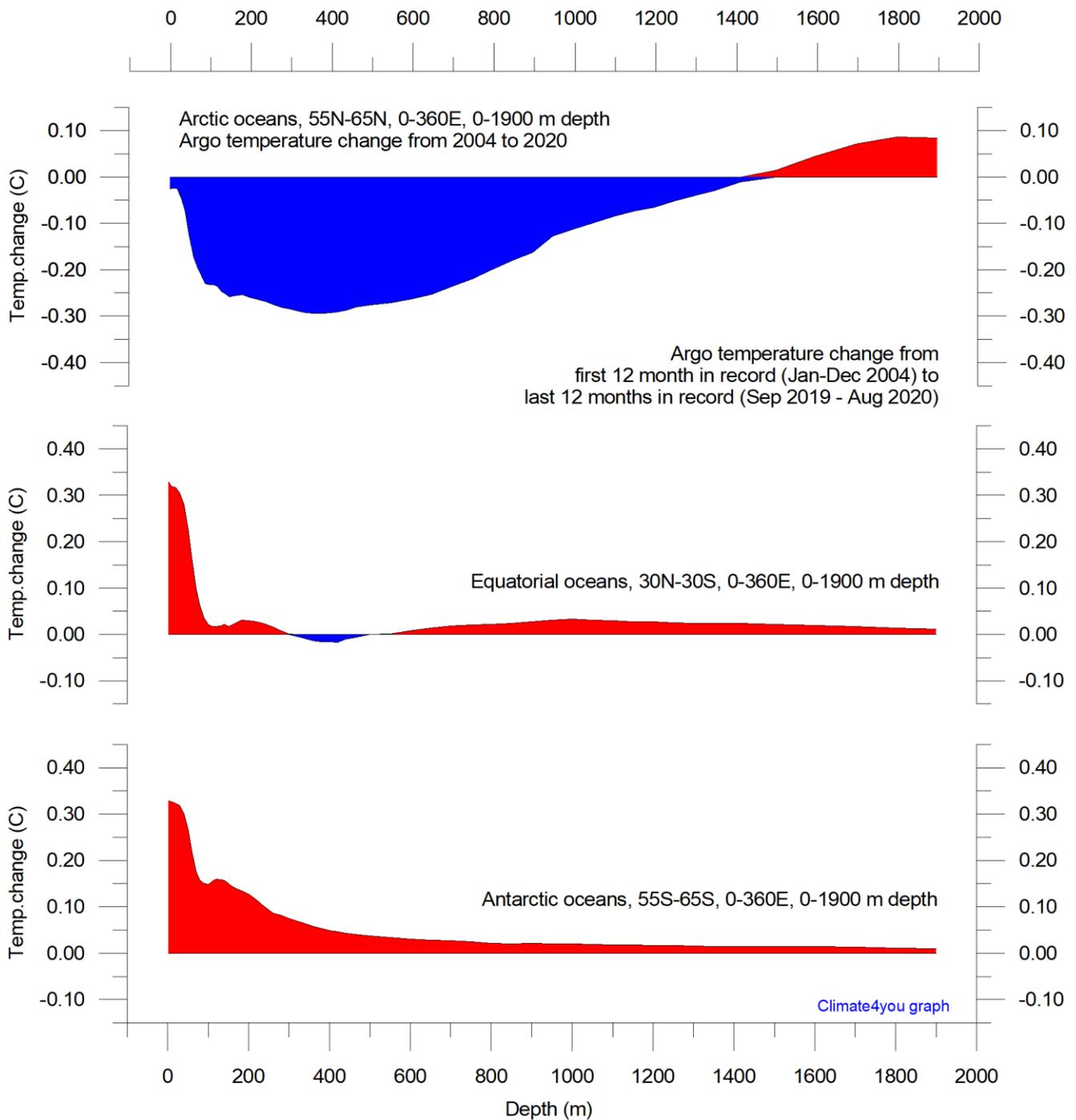
Net temperature change since 2004 from surface to 1900 m depth in different parts of the global oceans, using Argo-data. Source: Global Marine Argo Atlas. Additional information can be found in: Roemmich, D. and J. Gilson, 2009. The 2004-2008 mean and annual cycle of temperature, salinity, and steric height in the global ocean from the Argo Program. Progress in Oceanography, 82, 81-100. Please note that due to the spherical form of Earth, northern and southern latitudes represent only small ocean volumes, compared to latitudes near the Equator.

La Niña and El Niño episodes, Oceanic Niño Index (ONI), updated to June 2023
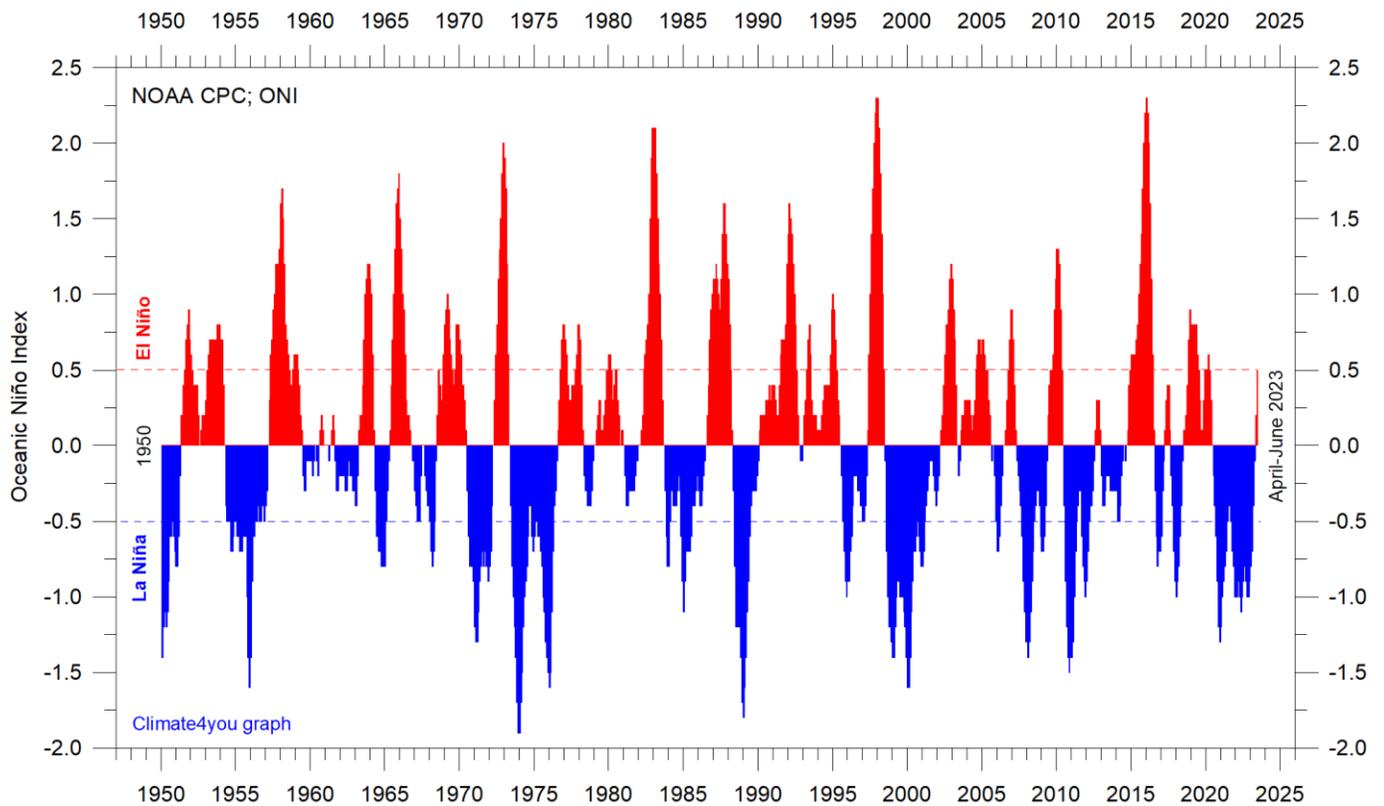
Warm (>+0.5ᵒC) and cold (<0.5ᵒC) episodes for the Oceanic Niño Index (ONI), defined as 3 month running mean of ERSSTv4 SST anomalies in the Niño 3.4 region (5ᵒN-5ᵒS, 120ᵒ-170ᵒW)]. For historical purposes cold and warm episodes are defined when the threshold is met for a minimum of 5 consecutive over-lapping seasons. Anomalies are centred on 30-yr base periods updated every 5 years.

The 2015-16 El Niño episode is among the strongest since the beginning of the record in 1950. Considering the entire record, however, recent variations between El Niño and La Niña episodes do not appear abnormal in any way. See also diagrams on pages 44 and 53.

Zonal lower troposphere temperatures from satellites, updated to June 2023
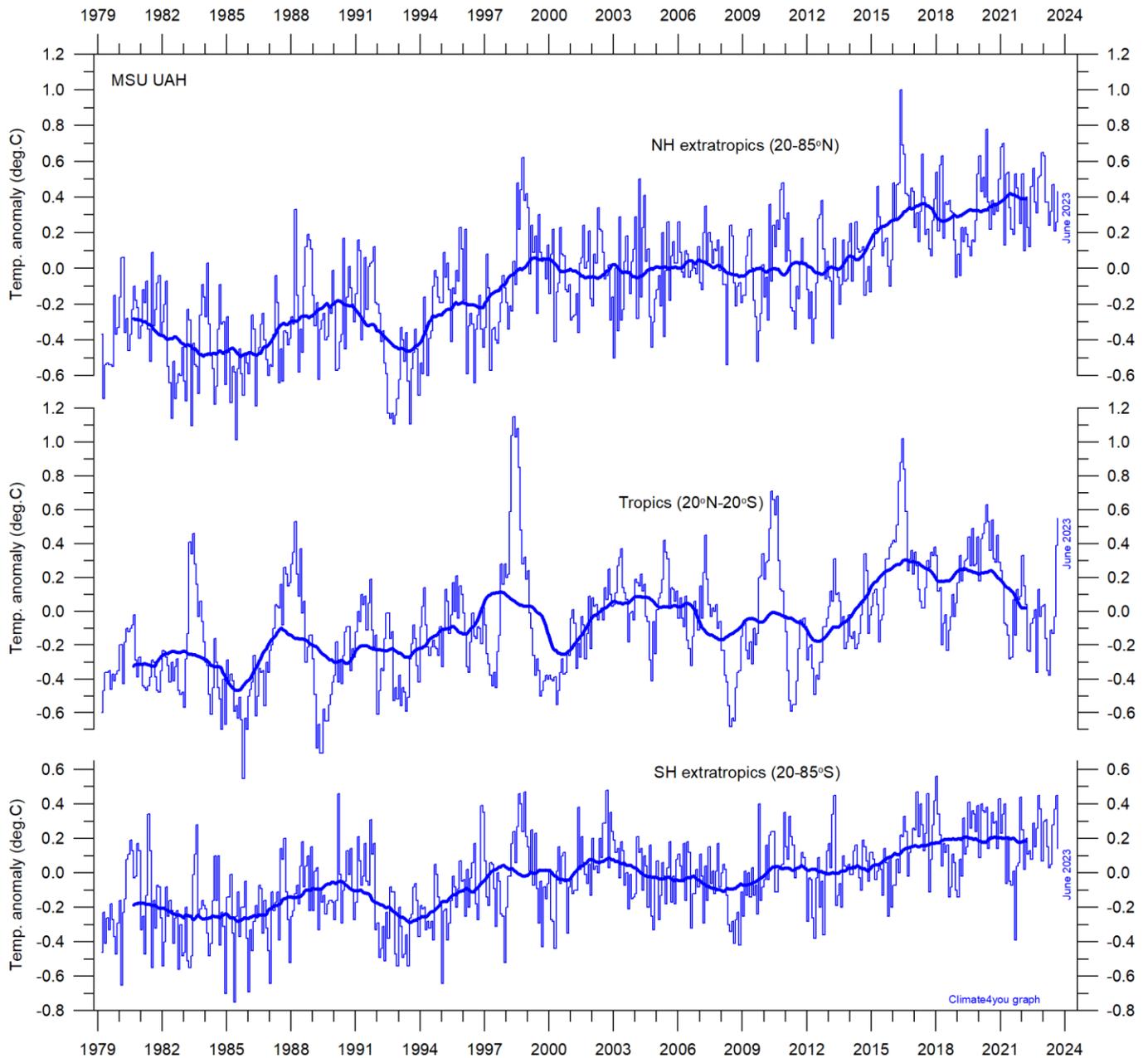
Global monthly average lower troposphere temperature since 1979 for the tropics and the northern and southern extratropics, according to University of Alabama at Huntsville, USA. Thin lines show the monthly temperature. Thick lines represent the simple running 37-month average, nearly corresponding to a running 3-year average. Reference period 1981-2010.

The overall warming since 1980 has dominantly been a northern hemisphere phenomenon, and mainly played out as a marked change between 1994 and 1999. However, this rather rapid temperature change is probably influenced by the Mt. Pinatubo eruption 1992-93 and the subsequent 1997 El Niño episode. The diagram also shows the temperature effects of the strong Equatorial El Niño's in 1997 and 2015-16, as well as the moderate El Niño in 2019. Apparently, these effects were spreading to higher latitudes in both hemispheres with some delay. Just now a new El Niño is beginning in the Pacific Ocean (p.25), as indicated by tropics surface air temperatures.

Arctic and Antarctic lower troposphere temperature, updated to June 2023
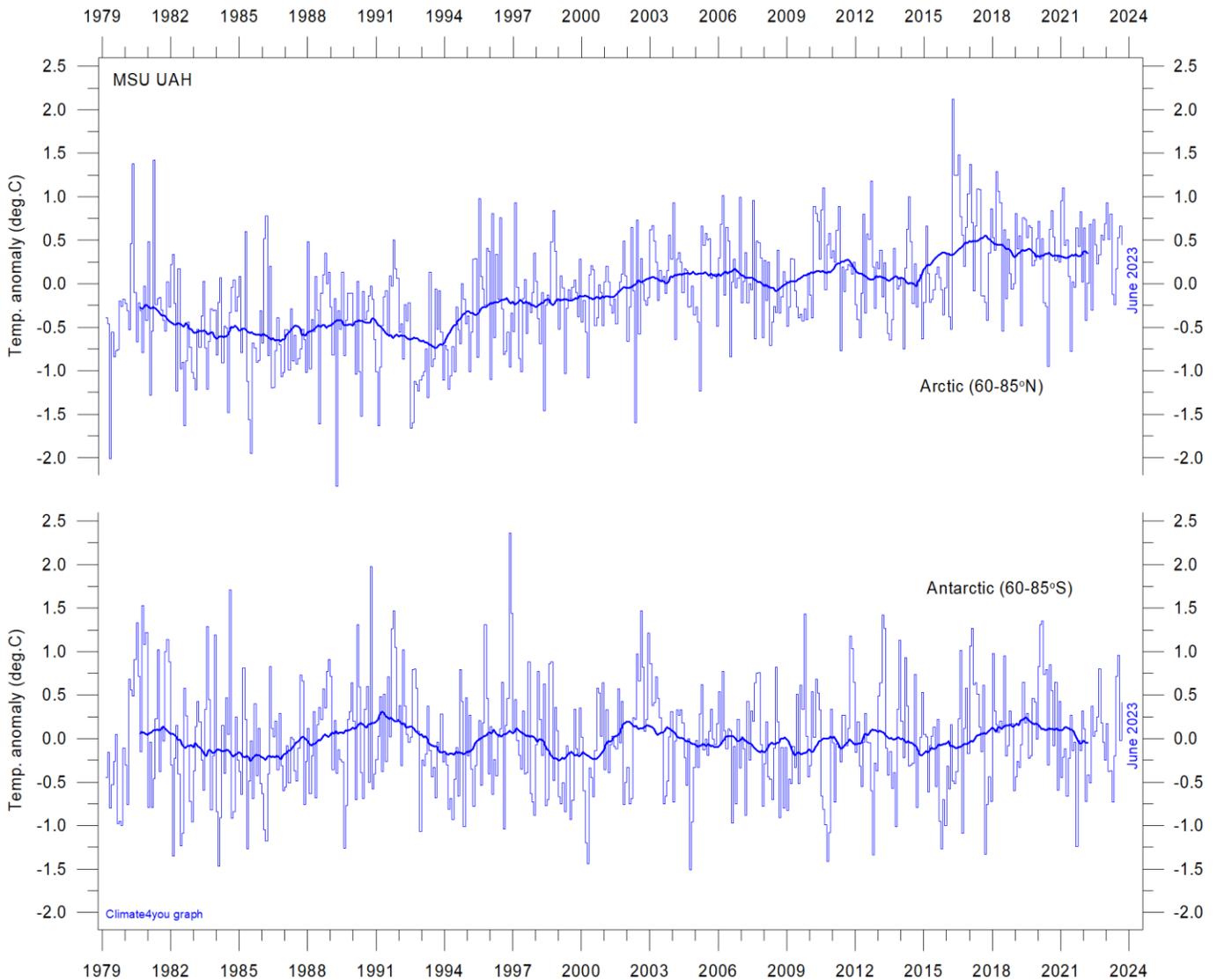
Global monthly average lower troposphere temperature since 1979 for the North Pole and South Pole regions, based on satellite observations ([University of Alabama](#) at Huntsville, USA). Thin lines show the monthly temperature. The thick line is the simple running 37-month average, nearly corresponding to a running 3-year average. Reference period 1991-2020.

In the Arctic region, warming mainly took place 1994-96, and less so subsequently. In 2016, however, temperatures peaked for several months, presumably because of oceanic heat given off to the atmosphere during the 2015-15 El Niño (see also diagram on page 25) and subsequently advected to higher latitudes.

This underscores how Arctic air temperatures may be affected not only by variations in local conditions but also by variations playing out in geographically remote regions.

A slight, but persistent, temperature decrease has characterised the Arctic since the 2016 peak (see also diagrams on page 28-30).

In the Antarctic region, temperatures have basically remained stable since the onset of the satellite record in 1979. In 2016-17 a small temperature peak visible in the monthly record may be interpreted as the subdued effect of the recent El Niño episode.

Arctic and Antarctic surface air temperature, updated to December 2021

Diagram showing area weighted Arctic (70-90ºN) monthly surface air temperature anomalies ([HadCRUT4](#)) since January 2000, in relation to the WMO [normal period](#) 1961-1990. The thin line shows the monthly temperature anomaly, while the thicker line shows the running 37-month (c. 3 year) average.

Diagram showing area weighted Antarctic (70-90ºS) monthly surface air temperature anomalies ([HadCRUT4](#)) since January 2000, in relation to the WMO [normal period](#) 1961-1990. The thin line shows the monthly temperature anomaly, while the thicker line shows the running 37-month (c. 3 year) average.

Diagram showing area weighted Arctic (70-90ºN) monthly surface air temperature anomalies ([HadCRUT4](#)) since January 1957, in relation to the WMO [normal period](#) 1961-1990. The thin line shows the monthly temperature anomaly, while the thicker line shows the running 37-month (c. 3 year) average.

Diagram showing area weighted Antarctic (70-90ºS) monthly surface air temperature anomalies ([HadCRUT4](#)) since January 1957, in relation to the WMO [normal period](#) 1961-1990. The thin line shows the monthly temperature anomaly, while the thicker line shows the running 37-month (c. 3 year) average.

Diagram showing area-weighted Arctic (70-90°N) monthly surface air temperature anomalies ([HadCRUT4](#)) since January 1920, in relation to the WMO [normal period](#) 1961-1990. The thin line shows the monthly temperature anomaly, while the thicker line shows the running 37-month (c. 3 year) average.

Because of the relatively small number of Arctic stations before 1930, month-to-month variations in the early part of the Arctic temperature record 1920-2018 are higher than later (diagram above).

The period from about 1930 saw the establishment of many new Arctic meteorological stations, first in Russia and Siberia, and following the 2nd World War, also in North America, explaining the above difference.

The period since 2005 is warm, about as warm as the period 1930-1940.

As the HadCRUT4 data series has improved high latitude coverage data coverage (compared to the HadCRUT3 series), the individual 5°x5° grid cells have been weighted according to their surface area. This area correction is especially important for polar regions, where longitudes converge rapidly. This approach differs from the approach used by Gillet et al. 2008, which calculated a simple average, with no correction for the substantial latitudinal surface area effect in polar regions.

The area weighted Arctic HadCRUT4 surface air temperature anomalies (p.28-30) correspond rather well to the lower troposphere temperature anomalies recorded by satellites (p.27).

Literature:

Gillett, N.P., Stone, D.A., Stott, P.A., Nozawa, T., Karpechko, A.Y.U., Hegerl, G.C., Wehner, M.F. and Jones, P.D. 2008. Attribution of polar warming to human influence. *Nature Geoscience* 1, 750-754.

Temperature over land versus over oceans, updated to June 2023
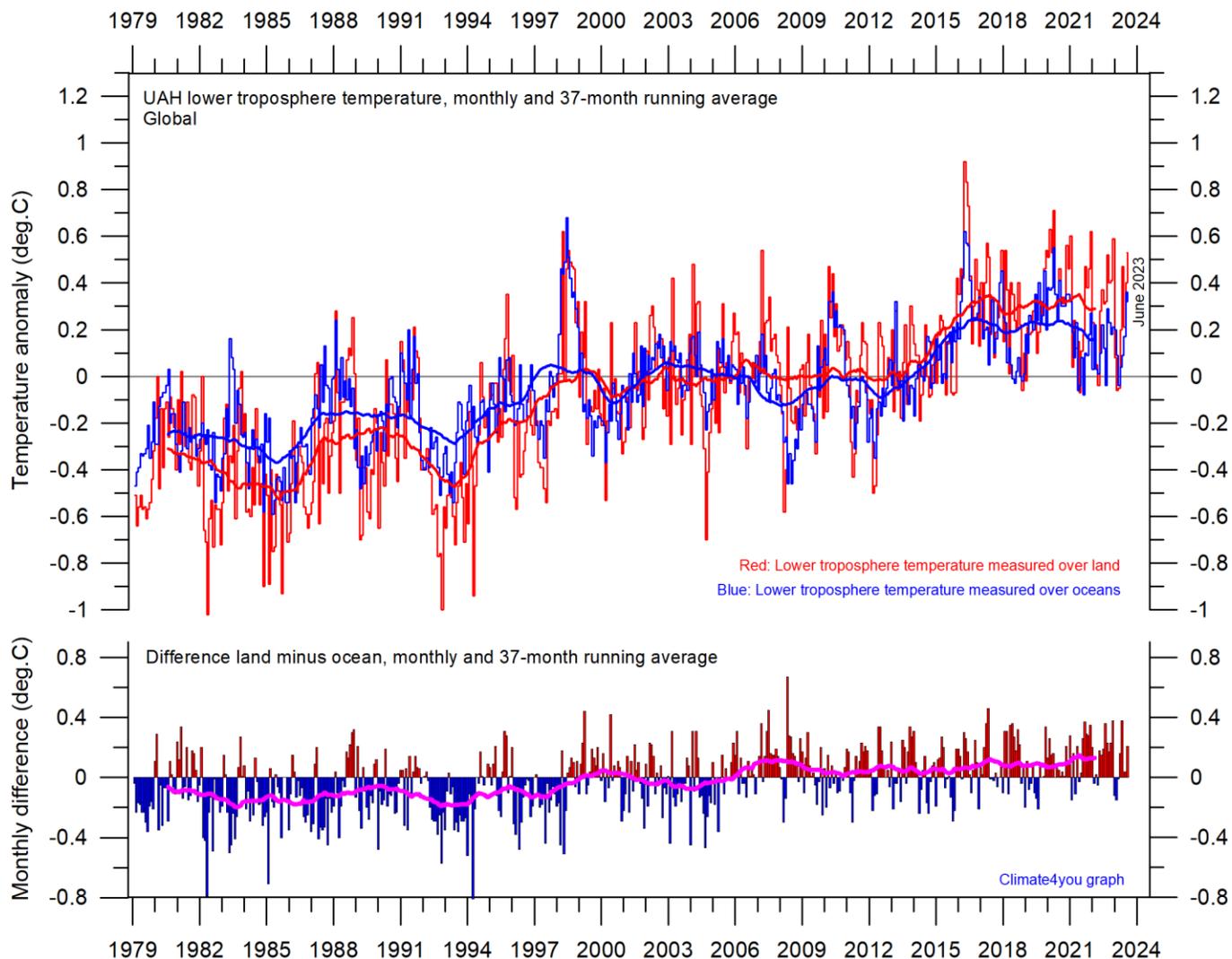
Global monthly average lower troposphere temperature since 1979 measured over land and oceans, respectively, according to University of Alabama at Huntsville, USA. Thick lines are the simple running 37-month average, nearly corresponding to a running 3-year average. Reference period 1991-2020.

Since 1979, the lower troposphere over land has warmed much more than over oceans, suggesting that the overall warming is derived mainly from incoming solar radiation. In addition, there may be supplementary reasons for this divergence, such as, e.g., variations in cloud cover and changes in land use.

Troposphere and stratosphere temperatures from satellites, updated to June 2023
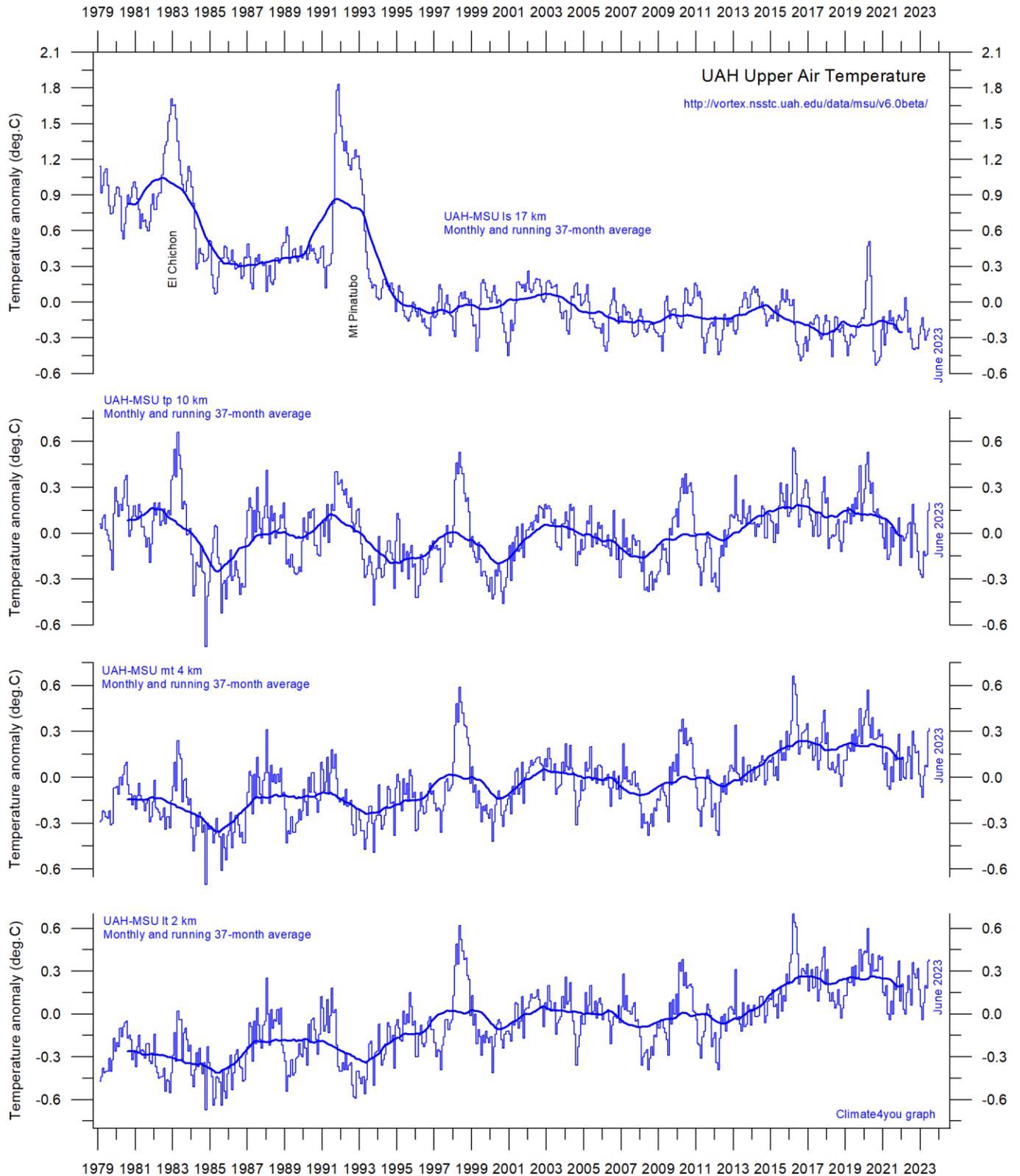
Global monthly average temperature in different according to University of Alabama at Huntsville, USA. The thin lines represent the monthly average, and the thick line the simple running 37-month average, nearly corresponding to a running 3-year average. Reference period 1991-2020.

Arctic and Antarctic sea ice, updated to June 2023
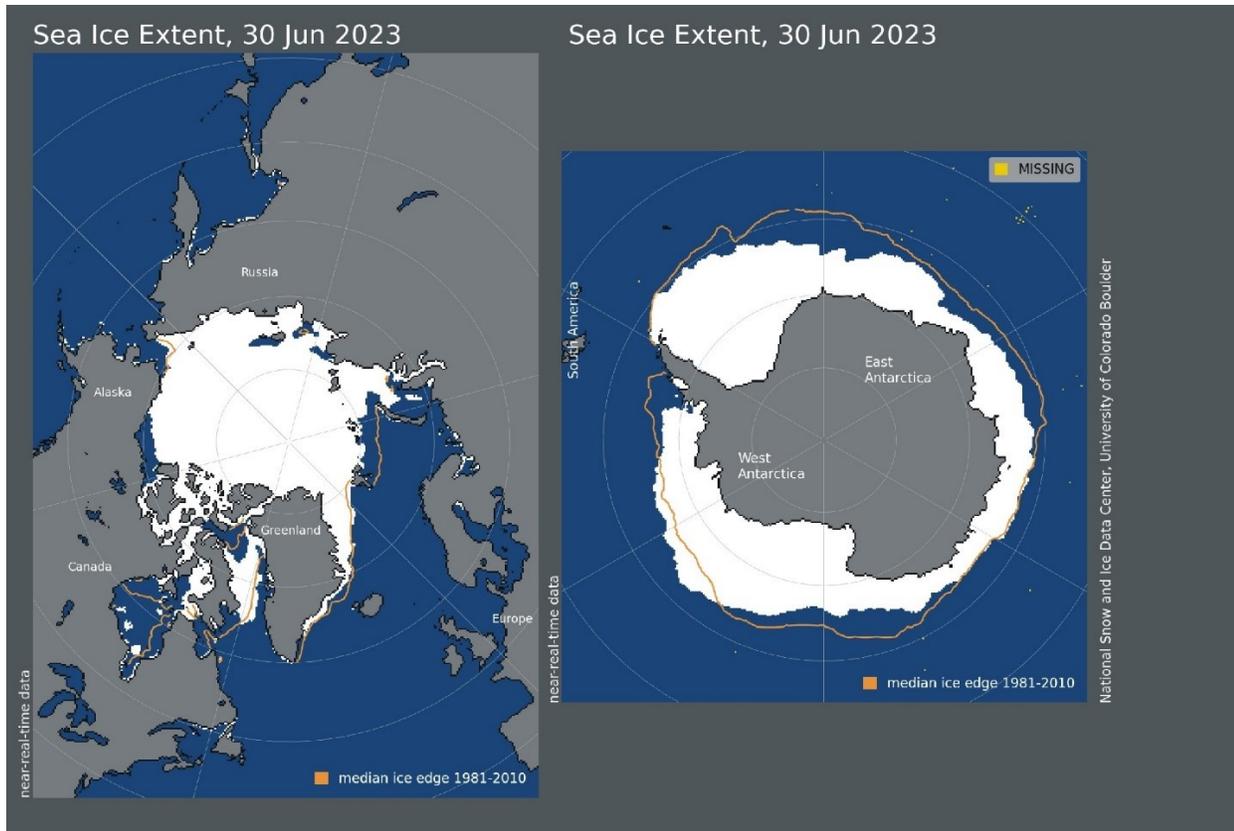
Sea ice extent 30 June 2023. The median limit of sea ice (orange line) is defined as 15% sea ice cover, according to the average of satellite observations 1981-2010 (both years included). Sea ice may therefore well be encountered outside and open water areas inside the limit shown in the diagrams above. Map source: National Snow and Ice Data Center (NSIDC).
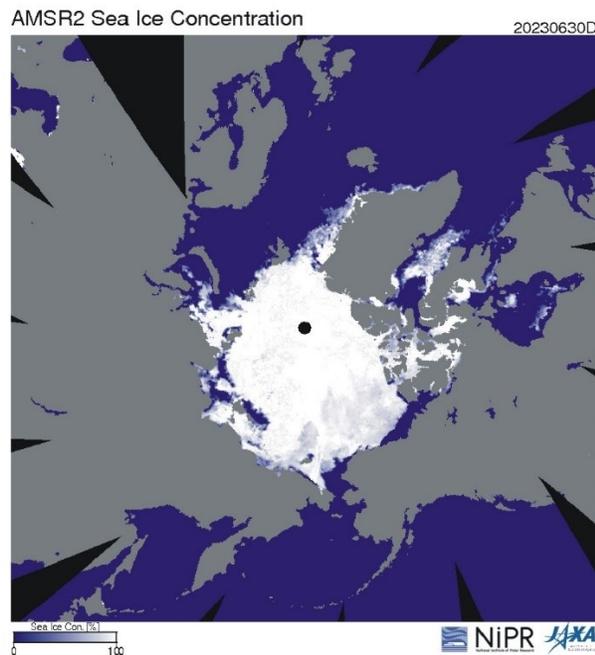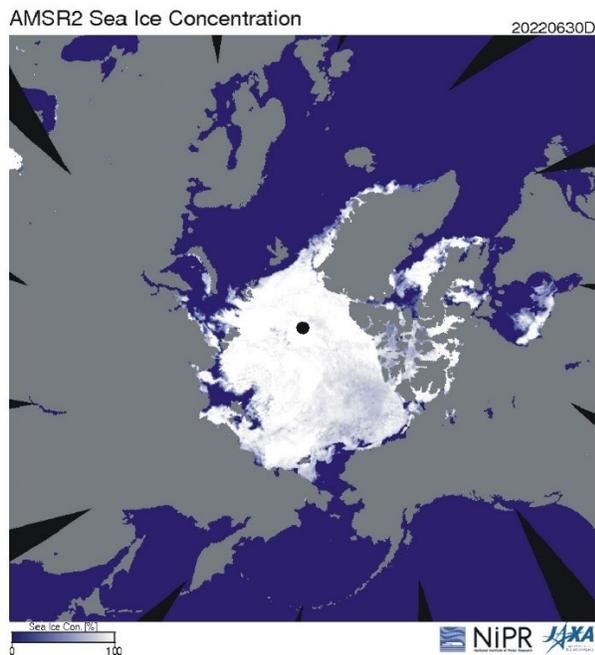
Diagrams showing Arctic sea ice extent and concentration 30 June 2022 (left) and 2023 (right), according to the Japan Aerospace Exploration Agency (JAXA).
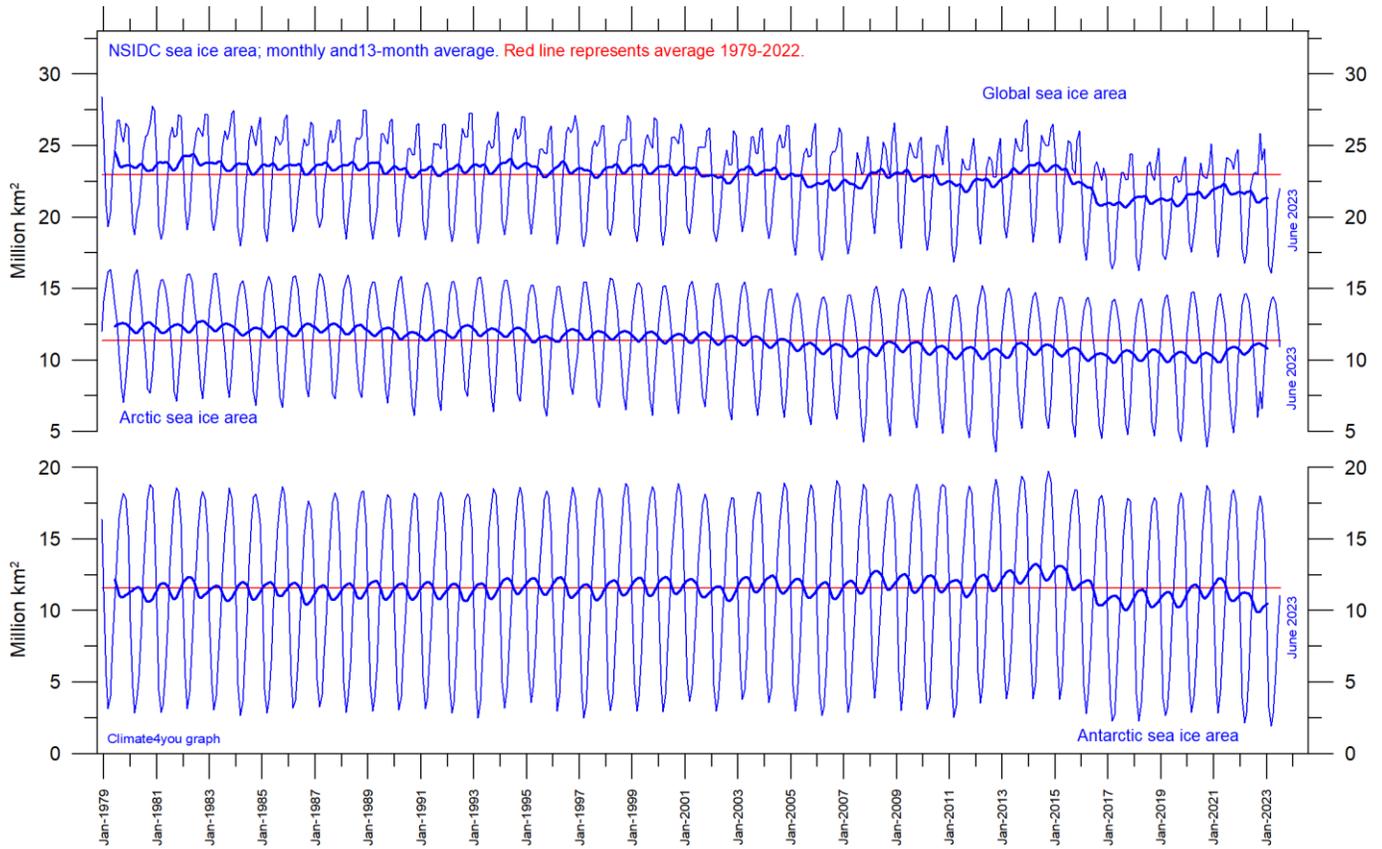
Graphs showing monthly Antarctic, Arctic, and global sea ice extent since November 1978, according to the [National Snow and Ice data Center](#) (NSIDC).
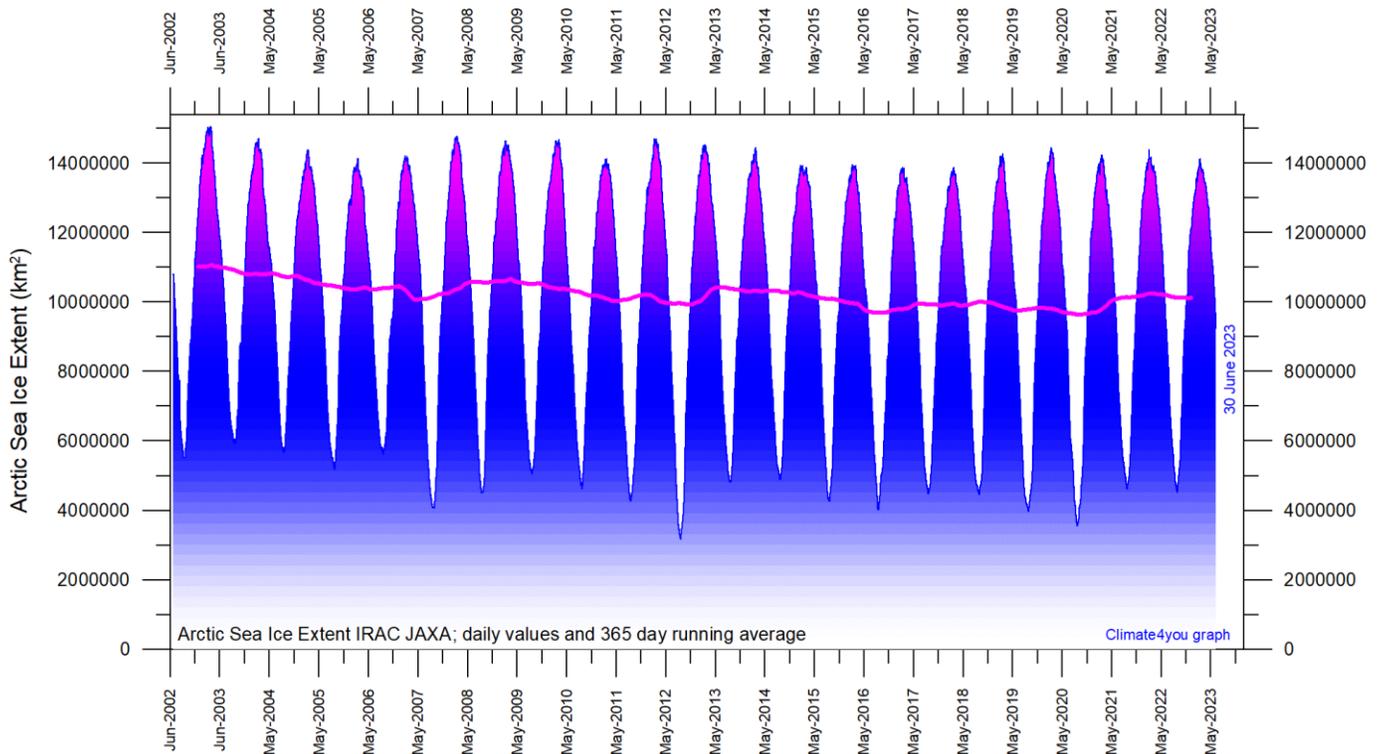
Diagram showing daily Arctic sea ice extent since June 2002, to 30 June 2023, data courtesy of [Japan Aerospace Exploration Agency](#) (JAXA).

Sea Ice Thickness, 30-Jun-2023

Arctic Sea Ice Volume, 30-Jun-2023

Legend:
- 2019
- 2020
- 2021
- 2022
- 2023
- 2004-2013
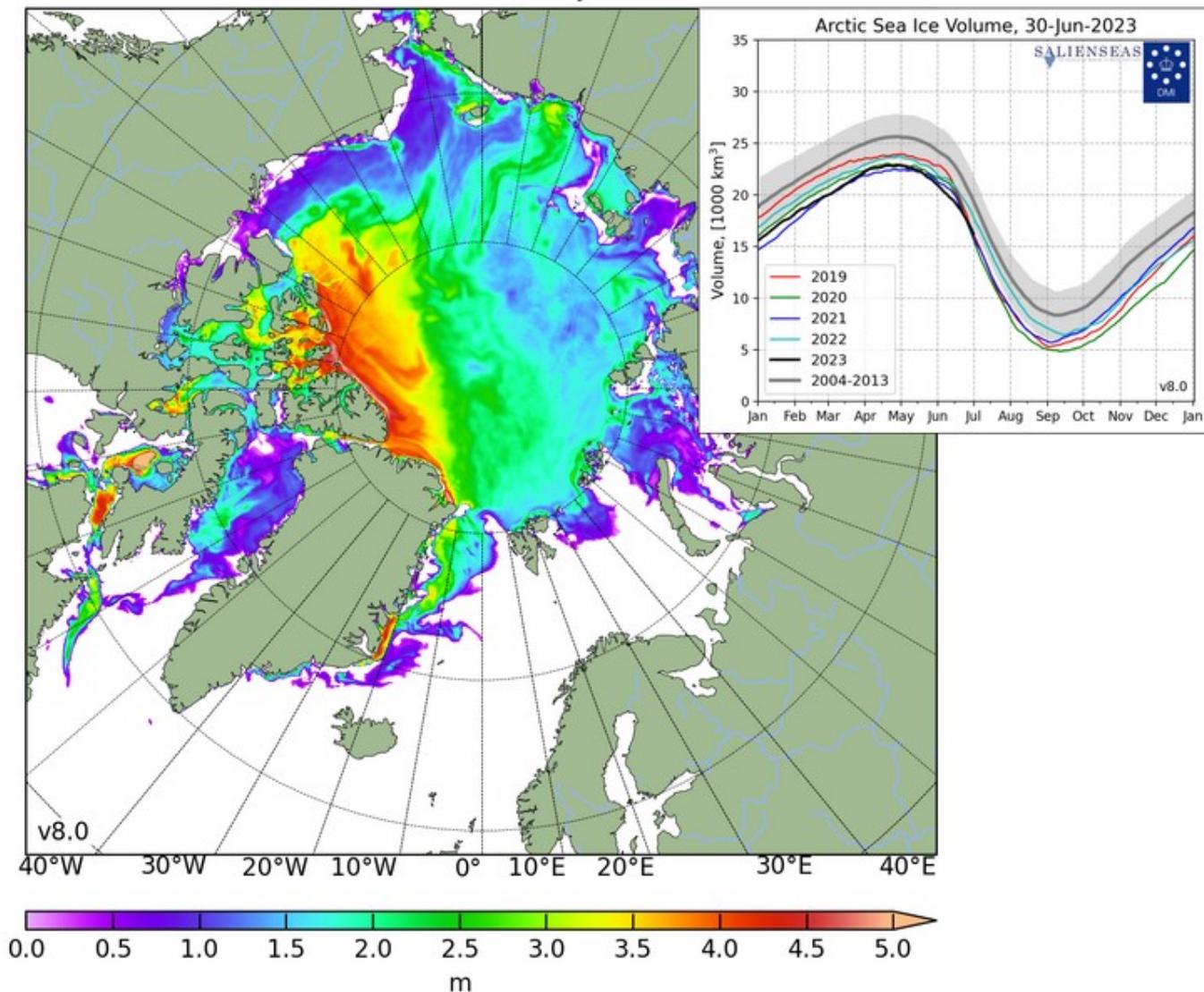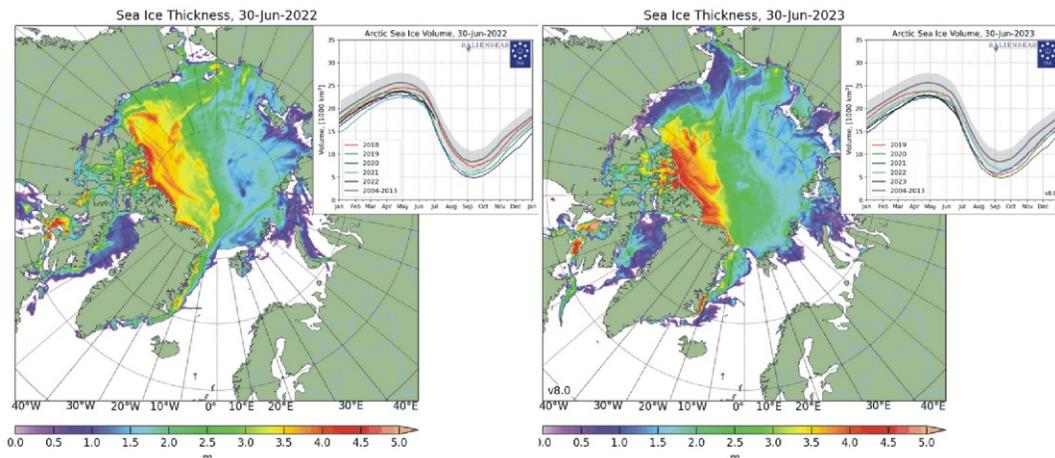
Diagrams showing Arctic sea ice extent and thickness 30 June 2022 (left) and 2023 (right and above) and the seasonal cycles of the calculated total arctic sea ice volume, according to [The Danish Meteorological Institute (DMI)](). The mean sea ice volume and standard deviation for the period 2004-2013 are shown by grey shading. Please note that DMI on 7 December 2021 changed their sea ice calculation model. DMI's description of the model version change can be read here: http://polarportal.dk/en/sea-ice-and-icebergs/sea-ice-thickness-and-volume/
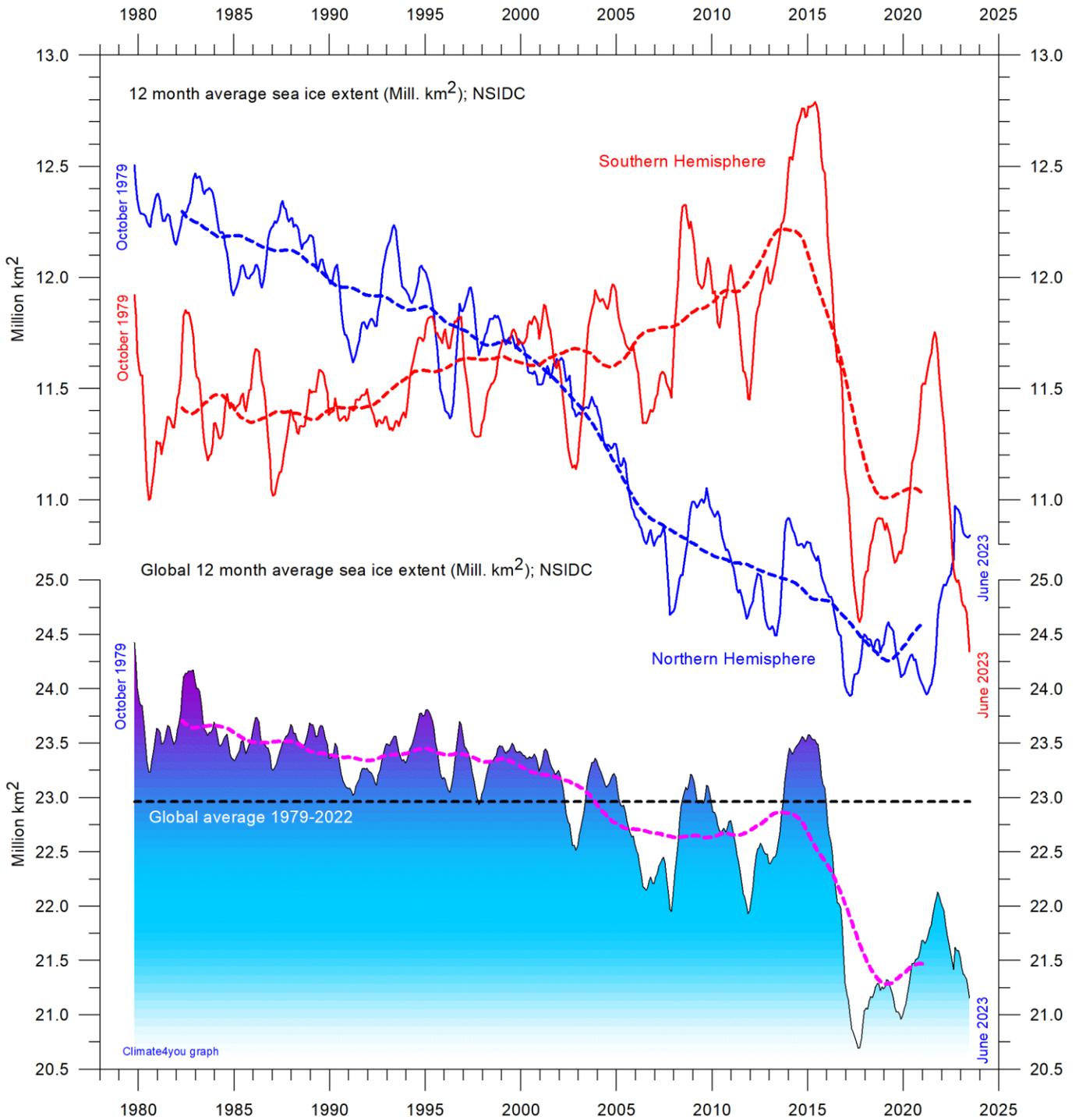
12 month running average sea ice extension, global and in both hemispheres since 1979, the satellite-era. The October 1979 value represents the monthly 12-month average of November 1978 - October 1979, the November 1979 value represents the average of December 1978 - November 1979, etc. The stippled lines represent a 61-month (ca. 5 years) average. Data source: National Snow and Ice Data Center (NSIDC).

Sea level in general

Global (or eustatic) sea-level change is measured relative to an idealised reference level, the geoid, which is a mathematical model of planet Earth's surface (Carter et al. 2014). Global sea-level is a function of the volume of the ocean basins and the volume of water they contain. Changes in global sea-level are caused by – but not limited to - four main mechanisms:

1. Changes in local and regional air pressure and wind, and tidal changes introduced by the Moon.
2. Changes in ocean basin volume by tectonic (geological) forces.
3. Changes in ocean water density caused by variations in currents, water temperature and salinity.
4. Changes in the volume of water caused by changes in the mass balance of terrestrial glaciers.

In addition to these there are other mechanisms influencing sea-level, such as storage of ground water, storage in lakes and rivers, evaporation, etc.

Mechanism 1 is controlling sea-level at many sites on a time scale from months to several years. As an example, many coastal stations show a pronounced annual variation reflecting seasonal changes in air pressures and wind speed. Longer-term climatic changes playing out over decades or centuries will also affect measurements of sea-level changes. Hansen et al. (2011, 2015) provide excellent analyses of sea-level changes caused by recurrent changes of the orbit of the Moon and other phenomena.

Mechanism 2 – with the important exception of earthquakes and tsunamis - typically operates over long (geological) time scales and is not significant on human time scales. It may relate to variations in the seafloor spreading rate, causing volume changes in mid-ocean mountain ridges, and to the slowly changing configuration of land and oceans. Another effect may be the slow rise of basins due to isostatic offloading by deglaciation after an ice age. The floor of the Baltic Sea and the Hudson Bay are

presently rising, causing a slow net transfer of water from these basins into the adjoining oceans. Slow changes of excessively big glaciers (ice sheets) and movements in the mantle will affect the gravity field and thereby the vertical position of the ocean surface. Any increase of the total water mass as well as sediment deposition into oceans increase the load on their bottom, generating sinking by viscoelastic flow in the mantle below. The mantle flow is directed towards the surrounding land areas, which will rise, thereby partly compensating for the initial sea level increase induced by the increased water mass in the ocean.

Mechanism 3 (temperature-driven expansion) only affects the uppermost part of the oceans on human time scales. Usually, temperature-driven changes in density are more important than salinity-driven changes. Seawater is characterised by a relatively small coefficient of expansion, but the effect should however not be overlooked, especially when interpreting satellite altimetry data. Temperature-driven expansion of a column of seawater will not affect the total mass of water within the column considered and will therefore not affect the potential at the top of the water column. Temperature-driven ocean water expansion will therefore not in itself lead to any lateral displacement of water, but only locally lift the ocean surface. Near the coast, where people are living, the depth of water approaches zero, so no measurable temperature-driven expansion will take place here (Mörner 2015). Mechanism 3 is for that reason not important for coastal regions.

Mechanism 4 (changes in glacier mass balance) is an important driver for global sea-level changes along coasts, for human time scales. Volume changes of floating glaciers – ice shelves – has no influence on the global sea-level, just like volume changes of floating sea ice has no influence. Only the mass-balance of grounded or land-based glaciers is important for the global sea-level along coasts.

Summing up: Presumably, mechanism 1 and 4 are the most important for understanding sea-level changes along coasts.

References:

Carter R.M., de Lange W., Hansen, J.M., Humlum O., Idso C., Kear, D., Legates, D., Mörner, N.A., Ollier C., Singer F. & Soon W. 2014. Commentary and Analysis on the Whitehead& Associates 2014 NSW Sea-Level Report. Policy Brief, NIPCC, 24. September 2014, 44 pp. http://climatechangereconsidered.org/wp-content/uploads/2014/09/NIPCC-Report-on-NSW-Coastal-SL-9z-corrected.pdf
Hansen, J.-M., Aagaard, T. and Binderup, M. 2011. Absolute sea levels and isostatic changes of the eastern North Sea to central Baltic region during the last 900 years. Boreas, 10.1111/j.1502-3885.2011.00229.x. ISSN 0300–9483.
Hansen, J.-M., Aagaard, T. and Huijpers, A. 2015. Sea-Level Forcing by Synchronization of 56- and 74-YearOscillations with the Moon's Nodal Tide on the Northwest European Shelf (Eastern North Sea to Central Baltic Sea). Journ. Coastal Research, 16 pp.
Mörner, Nils-Axel 2015. Sea Level Changes as recorded in nature itself. Journal of Engineering Research and Applications, Vol.5, 1, 124-129.

Global sea level from satellite altimetry, updated to October 2022
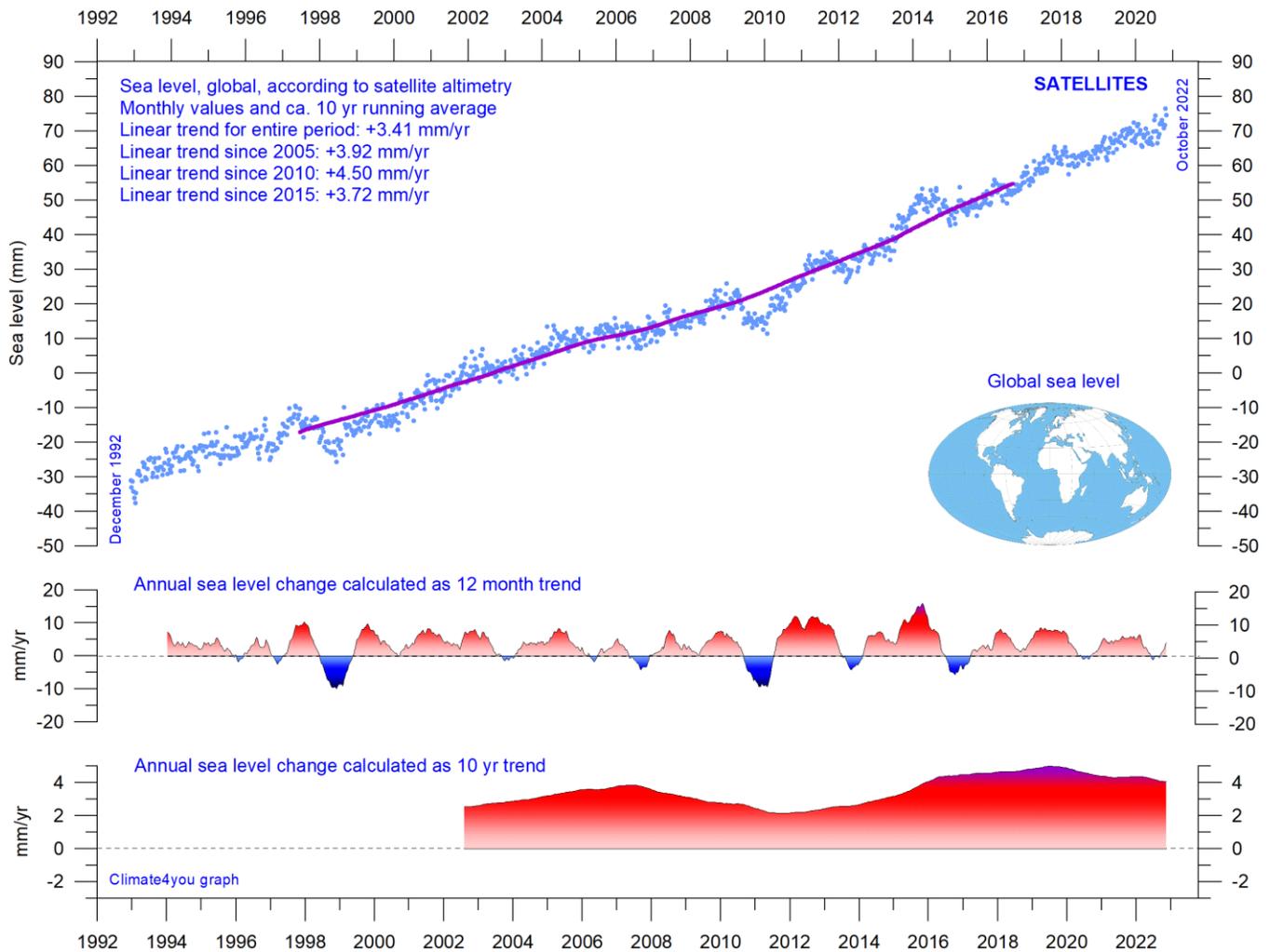
Global sea level since December 1992 according to the Colorado Center for Astrodynamics Research at University of Colorado at Boulder. The blue dots are the individual observations, and the purple line represents the running 121-month (ca. 10 year) average. The two lower panels show the annual sea level change, calculated for 1 and 10-year time windows, respectively. These values are plotted at the end of the interval considered.

Ground truth is a term used in various fields to refer to information provided by direct observation as opposed to information provided by inference, such as, e.g., by satellite observations.

In remote sensing using satellite observations, ground truth data refers to information collected on location. Ground truth allows the satellite data to be related to real features observed on the planet surface. The collection of ground truth data enables calibration of remote-sensing data, and

aids in the interpretation and analysis of what is being sensed or recorded by satellites. Ground truth sites allow the remote sensor operator to correct and improve the interpretation of satellite data.

For satellite observations on sea level ground true data are provided by the classical tide gauges (example diagram on next page), that directly measures the local sea level many places distributed along the coastlines on the surface of the planet.

Global sea level from tide-gauges, updated to December 2020
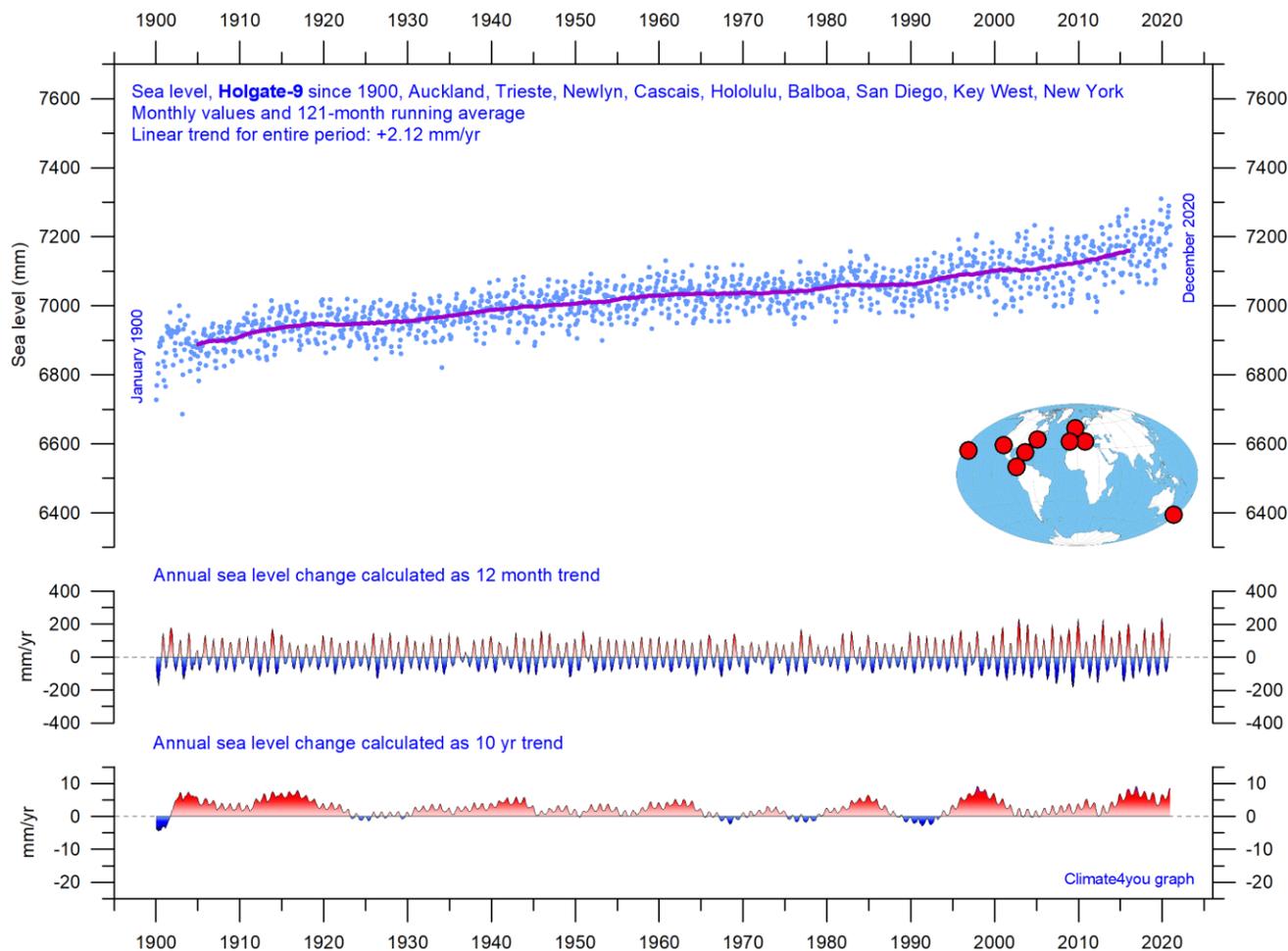
Holgate-9 monthly tide gauge data from PSMSL Data Explorer. Holgate (2007) suggested the nine stations listed in the diagram to capture the variability found in a larger number of stations over the last half century studied previously. For that reason, average values of the Holgate-9 group of tide gauge stations are interesting to follow, even though Auckland (New Zealand) has not reported data since 2000, and Cascais (Portugal) not since 1993. Unfortunately, by this data loss the Holgate-9 series since 2000 is underrepresented with respect to the southern hemisphere and should therefore not be overinterpreted. The blue dots are the individual average monthly observations, and the purple line represents the running 121-month (ca. 10 year) average. The two lower panels show the annual sea level change, calculated for 1 and 10-year windows, respectively. These values are plotted at the end of the interval considered.

Data from tide-gauges all over the world suggest an average global sea-level rise of 1-2 mm/year, while the satellite-derived record (page 37) suggest a rise of about 3.3 mm/year, or more. The noticeable difference (about 1:2) between the two data sets is remarkable but has no generally accepted explanation. It is however known that satellite observations are facing several complications in areas near the coast. Vignudelli et al. (2019) provide an updated overview of the current limitations of classical satellite altimetry in coastal regions.

References:

Holgate, S.J. 2007. On the decadal rates of sea level change during the twentieth century. Geophys. Res. Letters, 34, L01602, doi:10.1029/2006GL028492

Vignudelli et al. 2019. Satellite Altimetry Measurements of Sea Level in the Coastal Zone. *Surveys in Geophysics, Vol.* 40, p. 1319–1349. https://link.springer.com/article/10.1007/s10712-019-09569-1

Northern Hemisphere weekly and seasonal snow cover, updated to June 2023
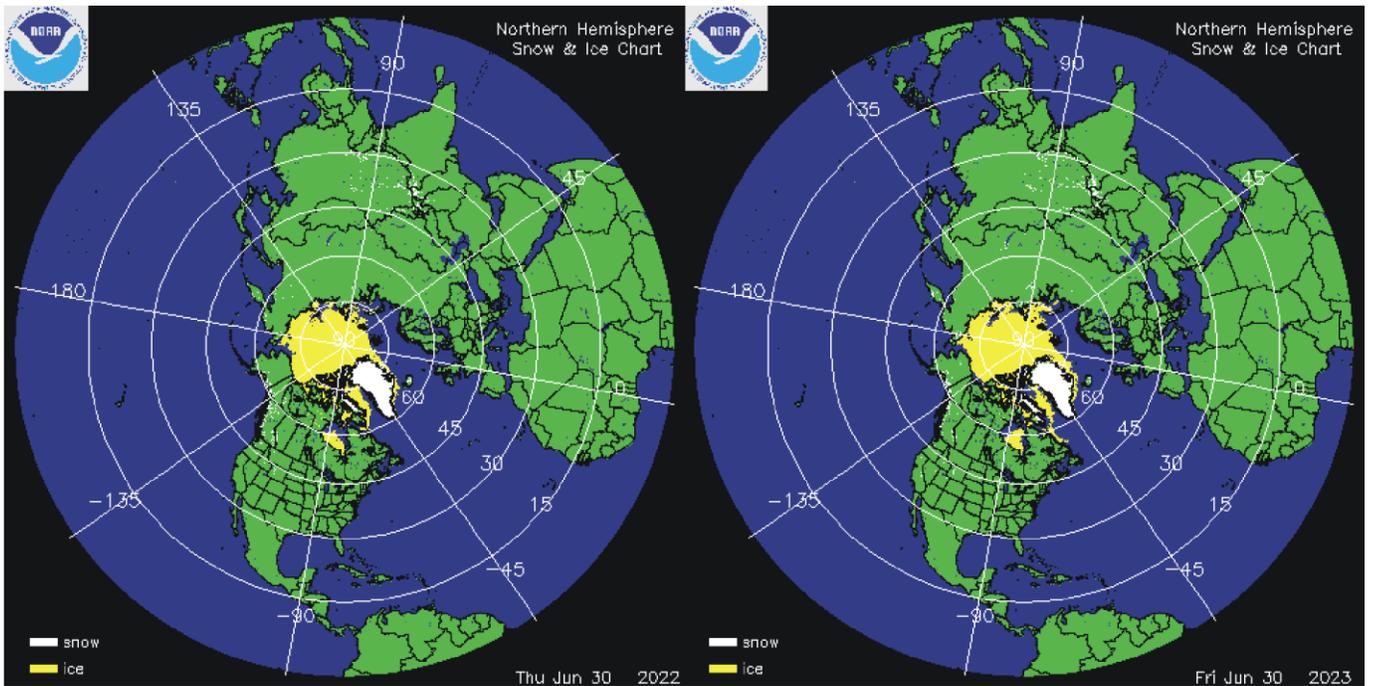
*Northern hemisphere snow cover (white) and sea ice (yellow) 30 June 2022 (left) and 2023 (right). Map source: National Ice Center (NIC).*
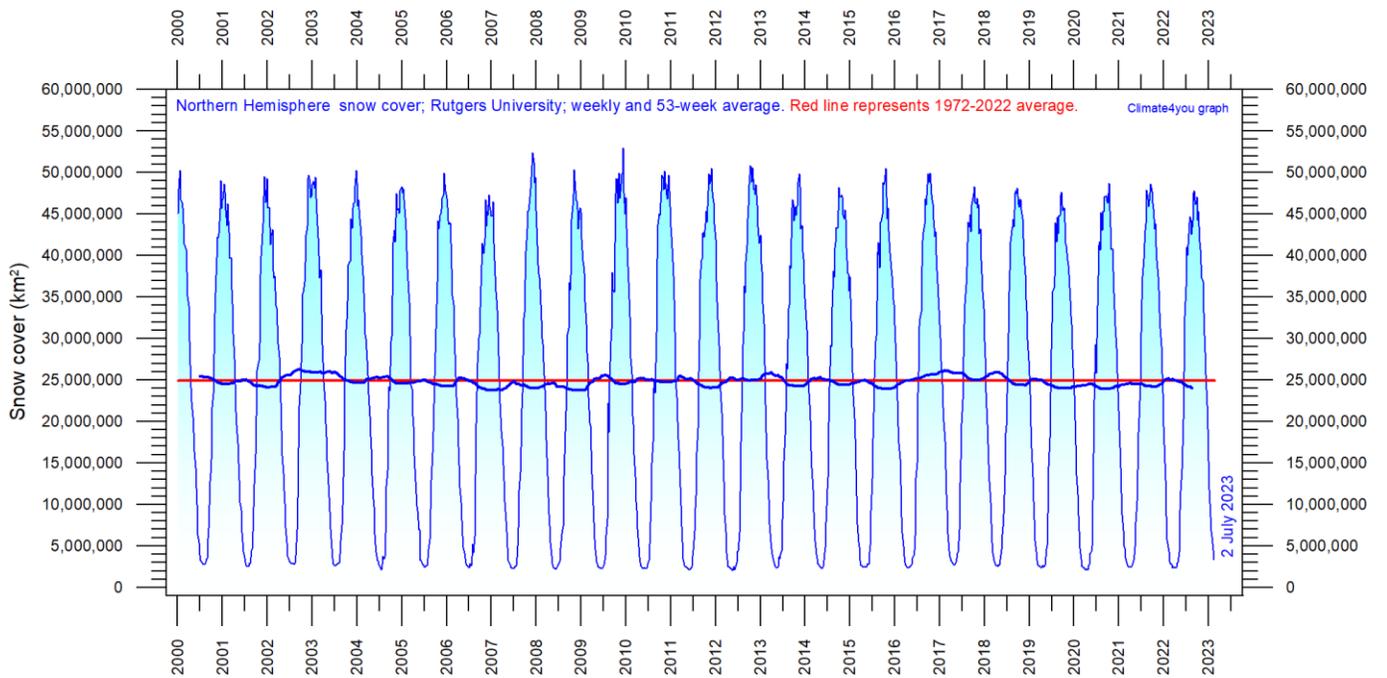
Northern hemisphere weekly snow cover since January 2000 according to Rutgers University Global Snow Laboratory. The thin blue line is the weekly data, and the thick blue line is the running 53-week average (approximately 1 year). The horizontal red line is the 1972-2022 average.
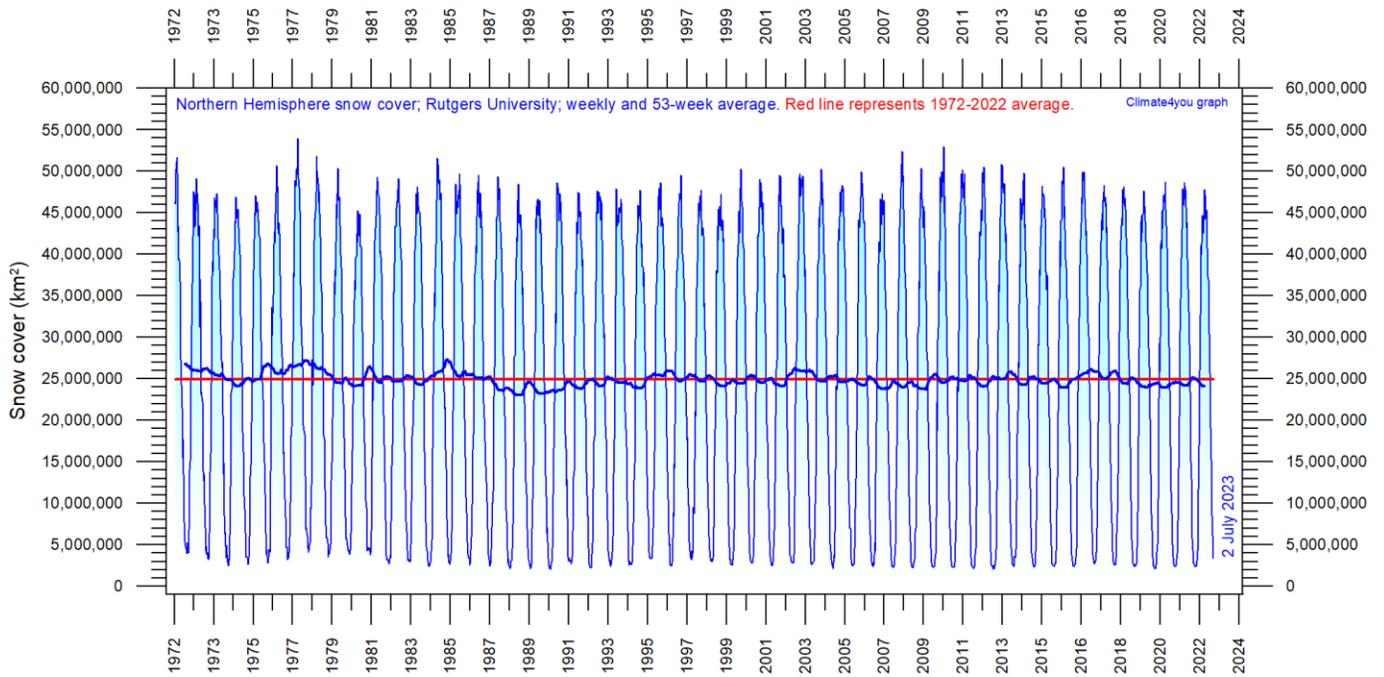
Northern hemisphere weekly snow cover since January 1972 according to Rutgers University Global Snow Laboratory. The thin blue line is the weekly data, and the thick blue line is the running 53-week average (approximately 1 year). The horizontal red line is the 1972-2022 average.
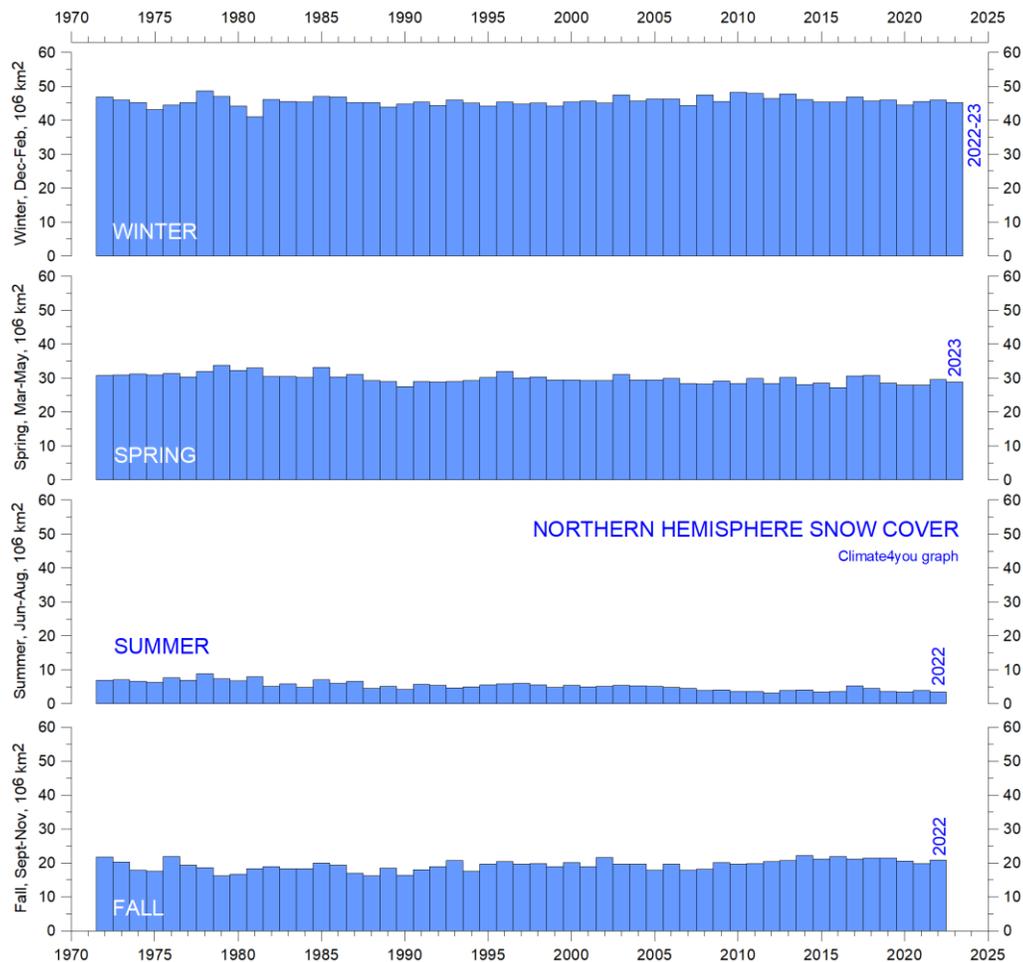
*Northern hemisphere seasonal snow cover since January 1972 according to Rutgers University Global Snow Laboratory.*

Left: Surface mass balance 30 June 2023. Right: Net surface mass balance anomaly since September 1, 2022. Courtesy of Danish Meteorological Institute (DMI).

Atmospheric specific humidity, updated to June 2023
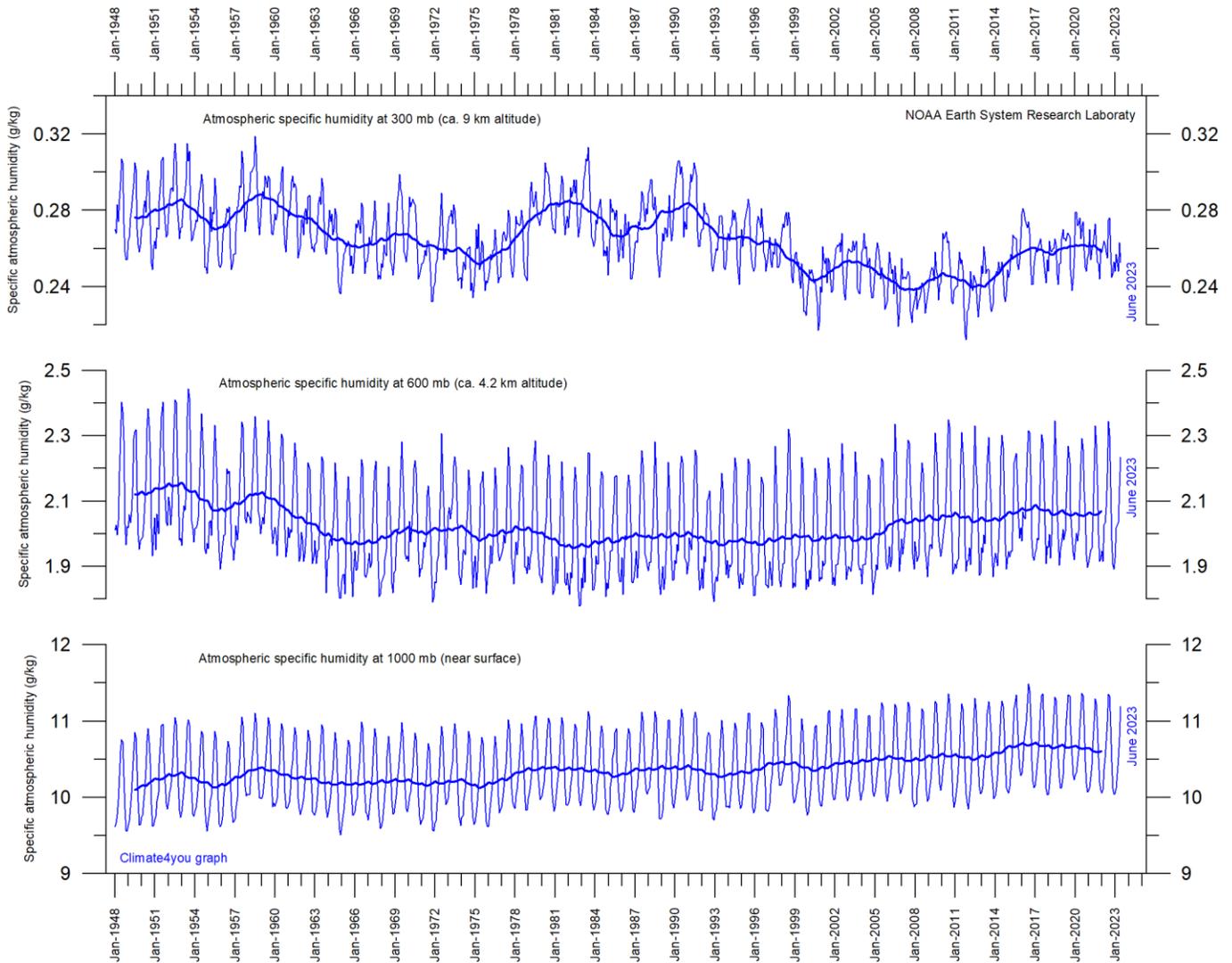
Specific atmospheric humidity (g/kg) at three different altitudes in the lower part of the atmosphere (*the Troposphere*) since January 1948 (*Kalnay et al. 1996*). The thin blue lines show monthly values, while the thick blue lines show the running 37-month average (about 3 years). Data source: *Earth System Research Laboratory (NOAA)*.

Water vapor is the most important greenhouse gas in the Troposphere. The highest concentration is found within a latitudinal range from 50ºN to 60ºS. The two polar regions of the Troposphere are comparatively dry.

The diagram above shows the specific atmospheric humidity to be stable or slightly increasing up to about 4-5 km altitude. At higher levels in the Troposphere (about 9 km), the specific humidity has been decreasing for the duration of the record (since 1948), but with shorter variations superimposed on the falling trend. A Fourier frequency analysis (not shown here) shows these variations to be influenced especially by a periodic variation of about 3.7-year duration.

The persistent decrease in specific humidity at about 9 km altitude is particularly noteworthy, as this altitude roughly corresponds to the level where the theoretical temperature effect of increased atmospheric CO_2 is expected initially to play out.

Atmospheric CO₂, updated to June 2023
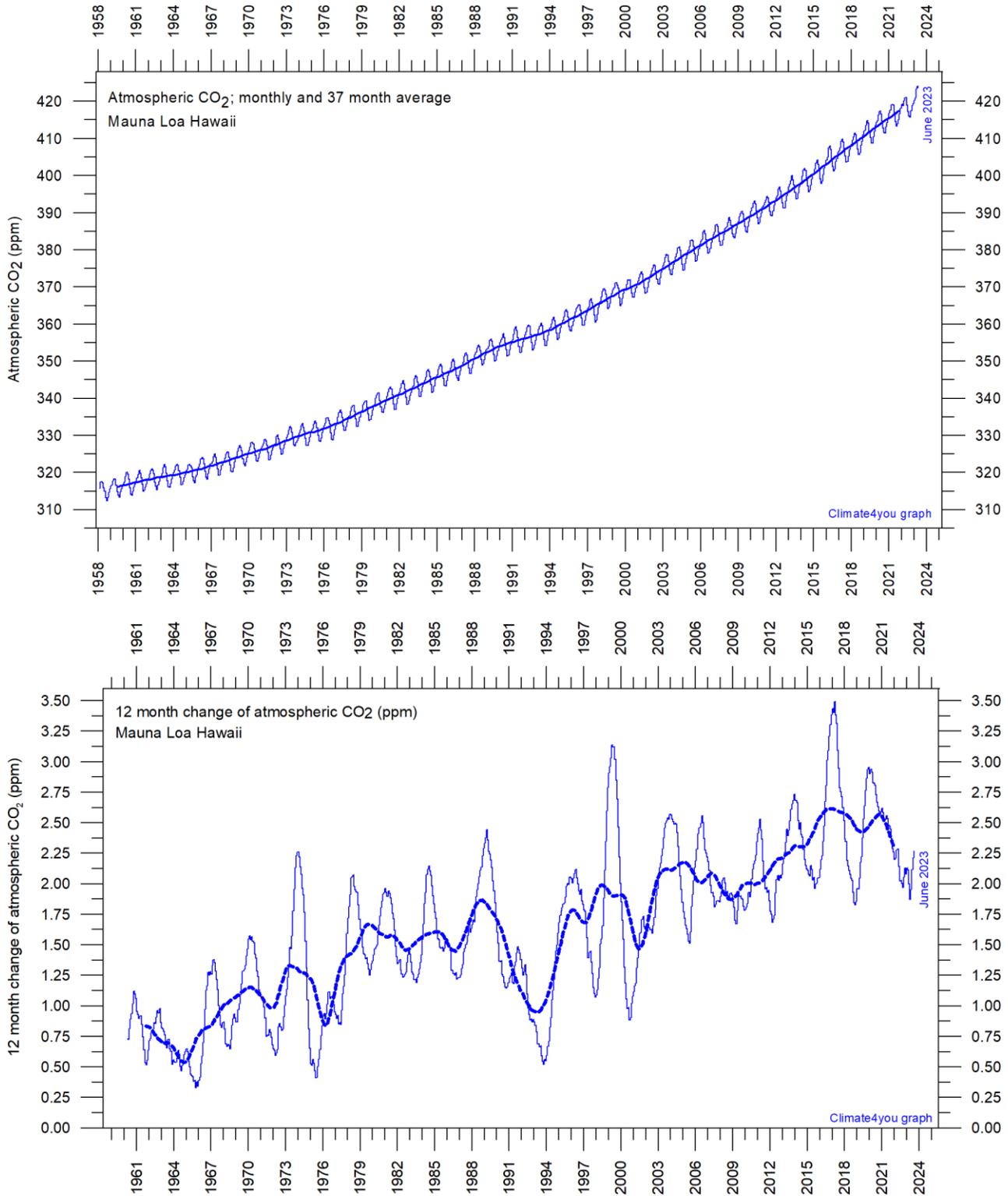
Monthly amount of atmospheric CO₂ (upper diagram) and annual growth rate (lower diagram); average last 12 months minus average preceding 12 months, thin line) of atmospheric CO₂ since 1959, according to data provided by the Mauna Loa Observatory, Hawaii, USA. The thick, stippled line is the simple running 37-observation average, nearly corresponding to a running 3-year average. A Fourier frequency analysis (not shown here) shows the 12-month change of Tropospheric CO2 to be influenced especially by periodic variations of 2.5- and 3.8-years' duration.

Visual association between annual growth rate of atmospheric CO_2 (upper panel) and Oceanic Niño Index (lower panel). See also diagrams on page 40 and 22, respectively.

Changes in the global atmospheric CO_2 is seen to vary roughly in concert with changes in the Oceanic Niño Index. The typical sequence of events is that changes in the global atmospheric CO_2 to a certain degree follows changes in the Oceanic Niño Index, but clearly not in all details. Many processes, natural as well as anthropogenic, controls the amount of atmospheric CO_2, but oceanographic processes are clearly particularly important (see also diagram on next page).

Atmospheric CO_2 and the present coronavirus pandemic

Modern political initiatives usually assume the human influence (mainly the burning of fossil fuels) to represent the core reason for the observed increase in atmospheric CO_2 since 1958 (diagrams on page 44).

The coronavirus pandemic since January 2020 resulted in a marked reduction in the global consumption of fossil fuels. It is therefore enlightening to follow the effect of this reduction on the amount of atmospheric CO_2.

However, there is still no clear effect to be seen of the above reduction in release of CO_2 from fossil fuels. Presumably, the main explanation for this is that the human contribution is too small compared to the numerous natural sources and sinks for atmospheric CO_2 to appear in diagrams showing the amount of atmospheric CO_2 (see, e.g., diagrams on p. 44-46).

The phase relation between atmospheric CO₂ and global temperature, updated to May 2023
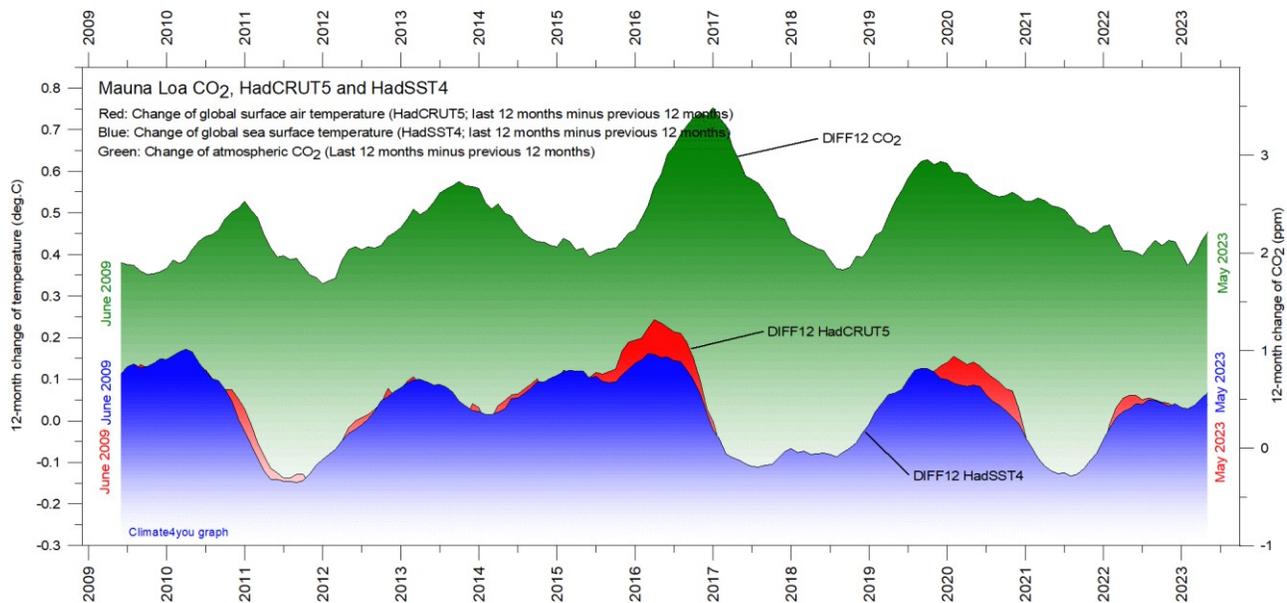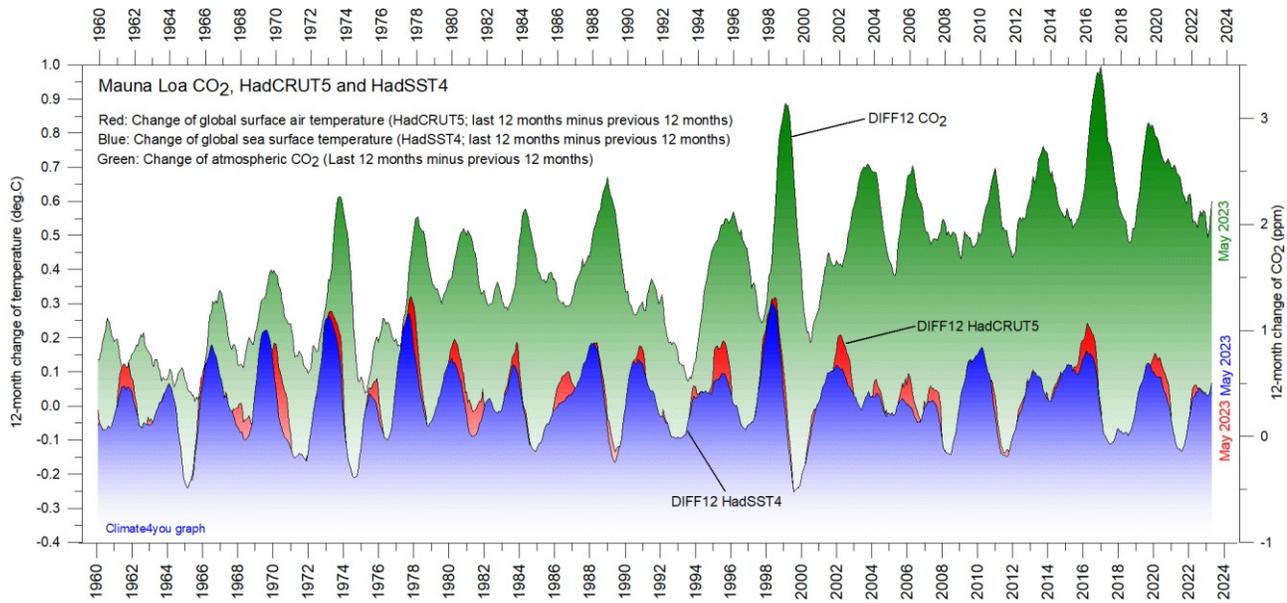
12-month change of global atmospheric CO₂ concentration (Mauna Loa; green), global sea surface temperature (HadSST4; blue) and global surface air temperature (HadCRUT5; red dotted). Entire data series since 1958 in upper figure, and last 15 years in lower figure, to enhance modern dynamics. All graphs are showing monthly values of DIFF12, the difference between the average of the last 12 month and the average for the previous 12 months for each data series.

The typical sequence of events is seen to be that changes in the global atmospheric CO₂ follow changes in global surface air temperature, which again follow changes in global ocean surface temperatures. Thus, changes in global atmospheric CO₂ usually are lagging 9.5–10 months behind changes in global air surface temperature, and 11–12 months behind changes in global sea surface temperature.

Reference: Humlum, O., Stordahl, K. and Solheim, J-E. 2012. The phase relation between atmospheric carbon dioxide and global temperature. Global and Planetary Change, August 30, 2012.
http://www.sciencedirect.com/science/article/pii/S0921818112001658?v=s5

Global air temperature and atmospheric CO₂, updated to June 2023

Atmospheric CO₂ (Mauna Loa)
Global temperature anomaly (UAH MSU)
UAH temperature average 1981-2010
June 2023
Climate4you graph

Atmospheric CO₂ (Mauna Loa)
Global temperature anomaly (RSS MSU)
RSS temperature average 1979-1998
June 2023
Climate4you graph
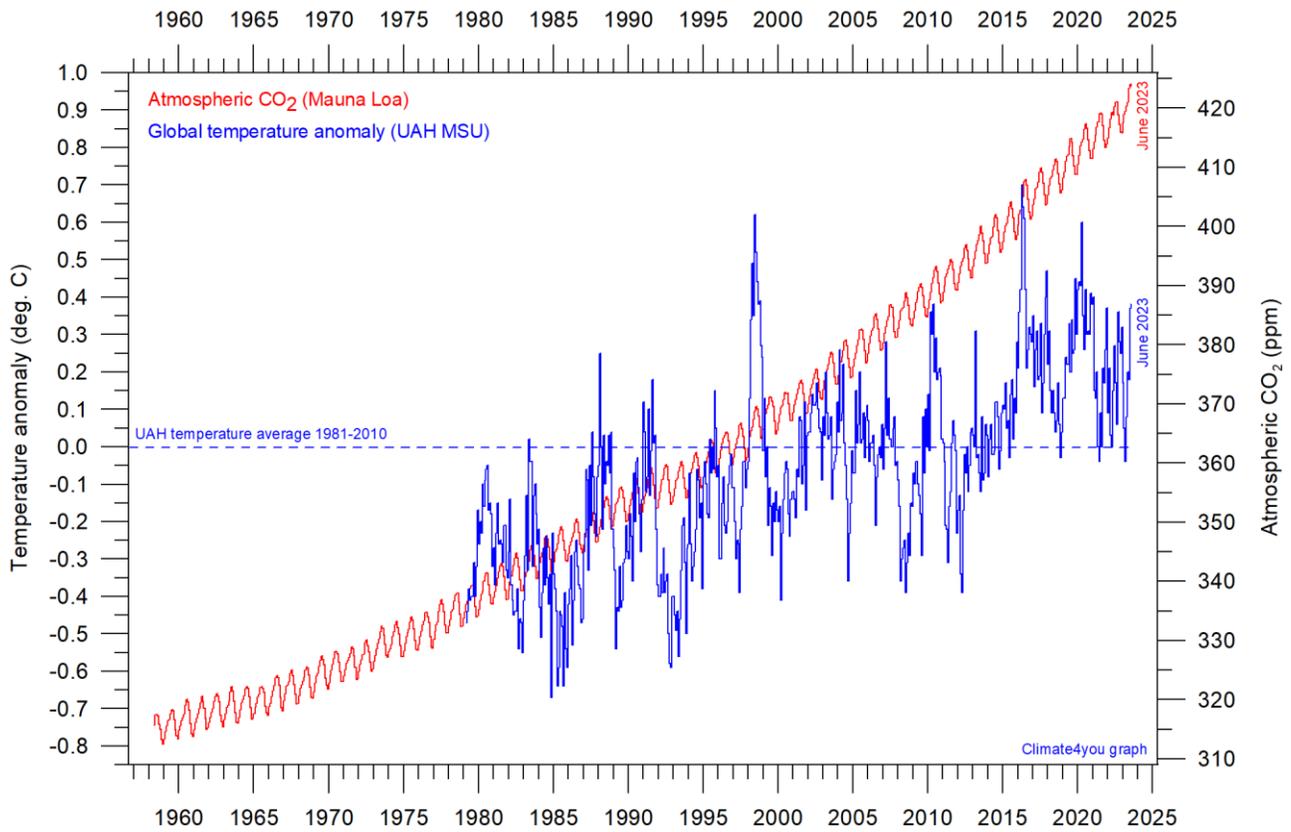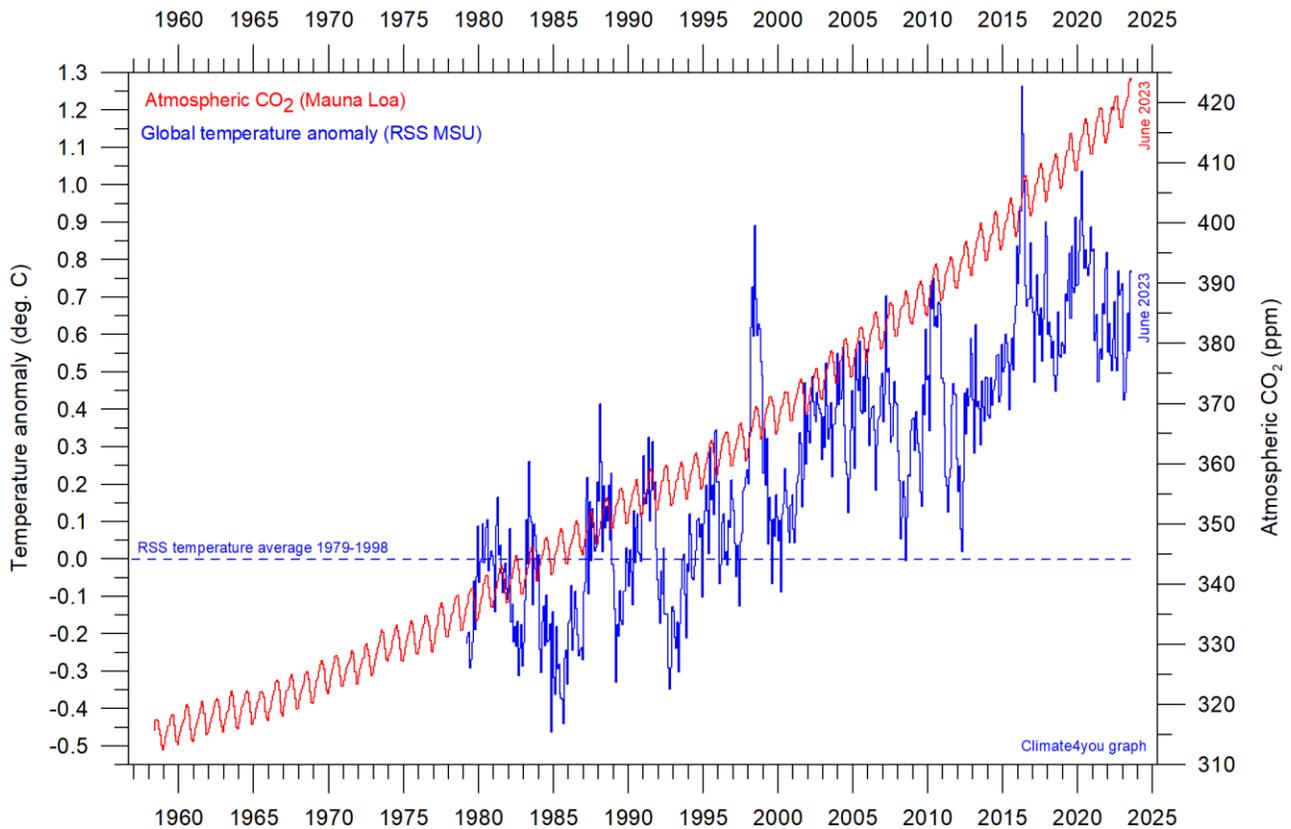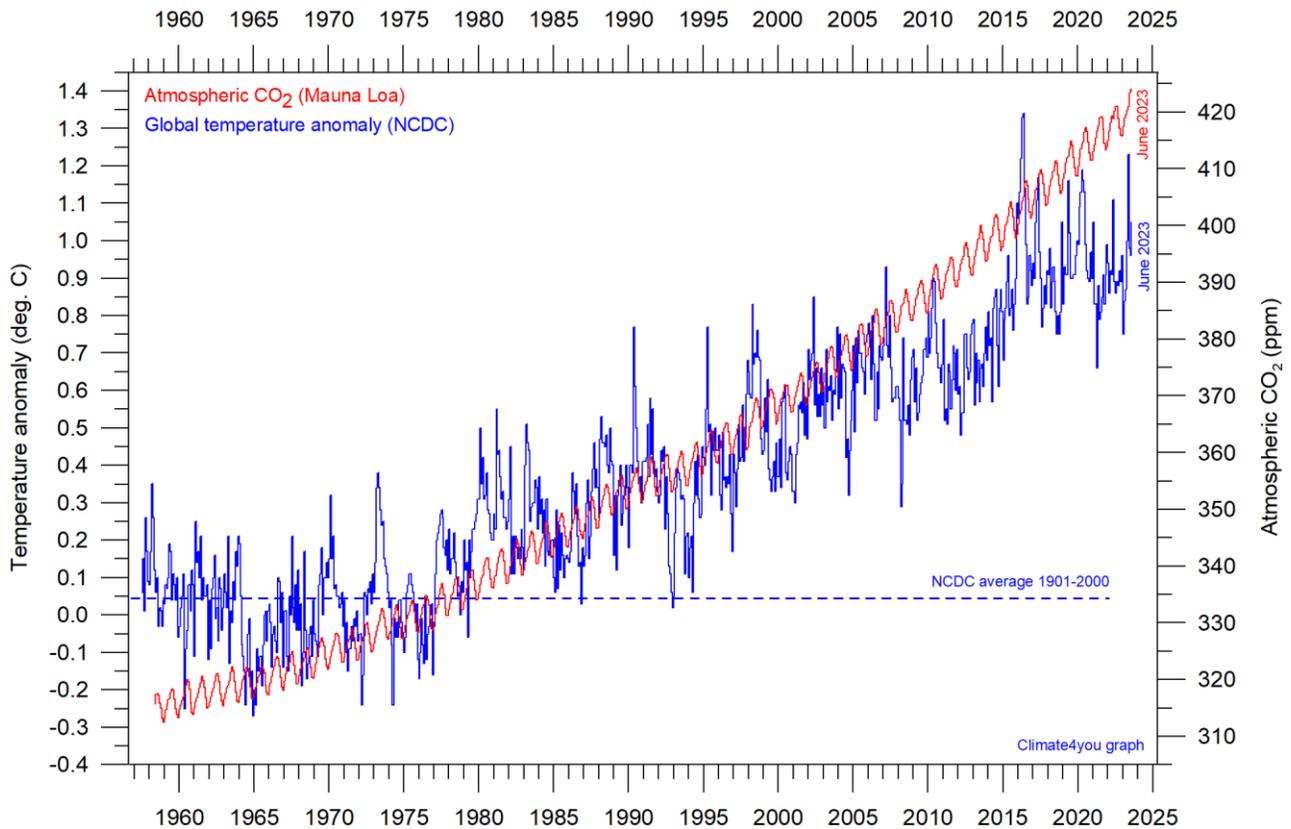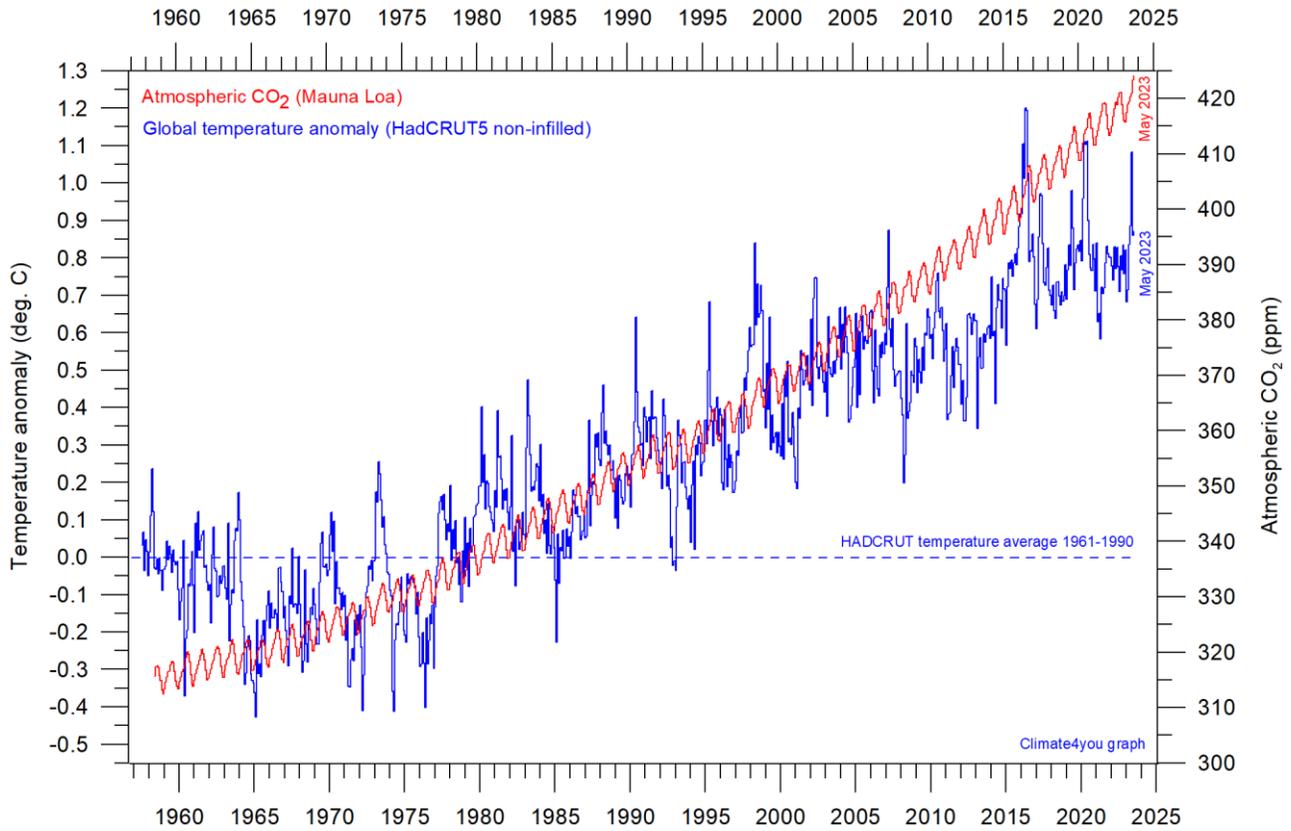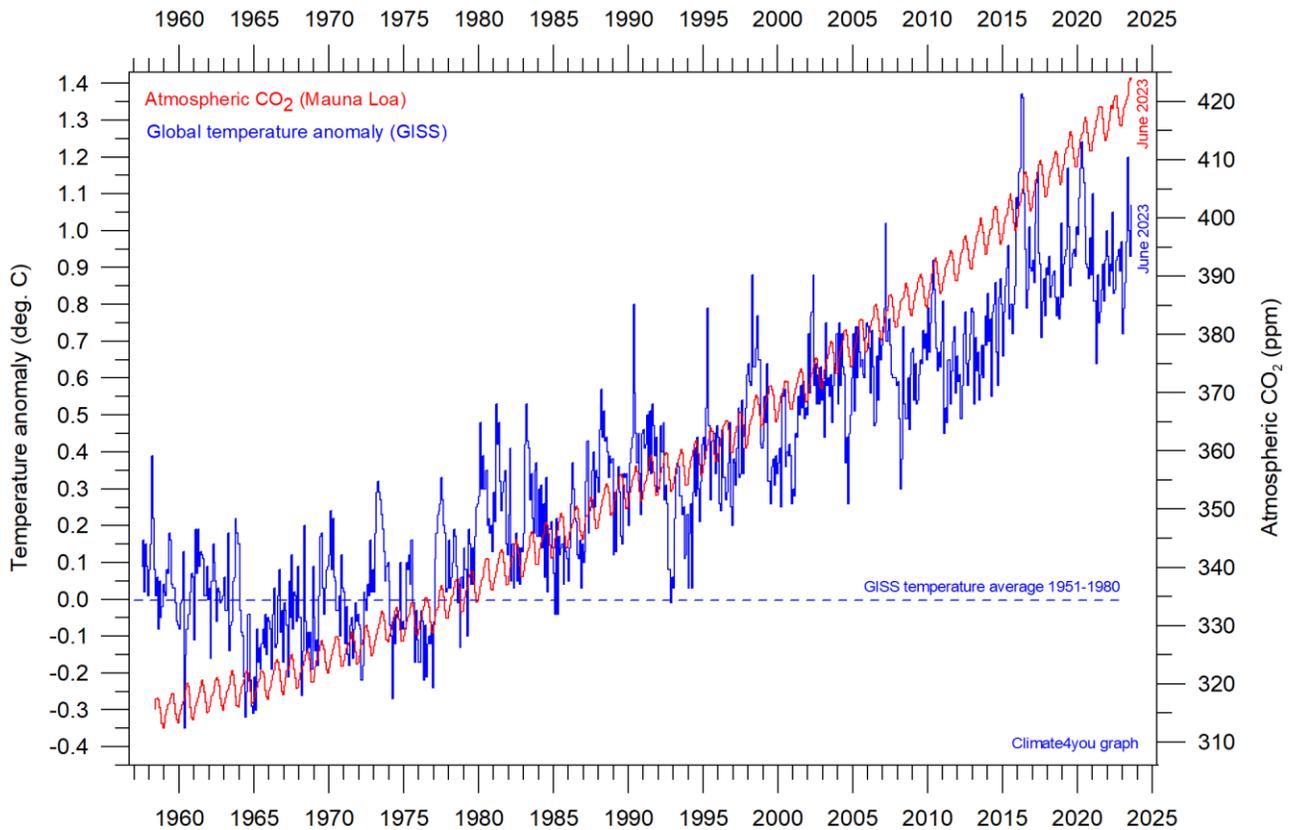
Diagrams showing UAH, RSS, HadCRUT5, NCDC and GISS monthly global air temperature estimates (blue) and the monthly atmospheric CO₂ content (red) according to the [Mauna Loa Observatory](), Hawaii. The Mauna Loa data series begins in March 1958, and 1958 was therefore chosen as starting year for all diagrams above. Reconstructions of past atmospheric CO₂ concentrations (before 1958) are not incorporated in this diagram, as such past CO₂ values are derived by other means (ice cores, stomata, or older measurements using different methodology), and therefore are not directly comparable with direct atmospheric measurements.

Most climate models are programmed to give the greenhouse gas carbon dioxide CO_2 significant influence on the calculated global air temperature. It is therefore relevant to compare different air temperature records with measurements of atmospheric CO_2, as shown in the diagrams above.

Any comparison, however, should not be made on a monthly or annual basis, but for a longer time, as other effects (oceanographic, cloud cover, etc.) may override the potential influence of CO_2 on short time scales such as just a few years.

It is of cause equally inappropriate to present new meteorological record values, whether daily, monthly, or annual, as demonstrating the legitimacy of the hypothesis ascribing high importance of atmospheric CO_2 for global air temperatures. Any such meteorological record value may well be the result of other phenomena. Unfortunately, many media repeatedly fall into this trap.

What exactly defines the critical length of a relevant period length to consider for evaluating the alleged importance of CO_2 remains elusive and still represents a theme for discussions.

Nonetheless, the length of the critical period must be inversely proportional to the temperature sensitivity of CO_2, including feedback effects. Thus, if the net temperature effect of atmospheric CO_2 is strong, the critical period will be short, and vice versa.

However, past climate research history provides some clues as to what has traditionally been considered the relevant length of period over which to compare temperature and atmospheric CO_2.

After about 10 years of concurrent global temperature- and CO_2-increase, IPCC was established in 1988. For obtaining public and political support for the CO_2-hyphotesis the 10-year warming period leading up to 1988 most likely was considered important. Had the global temperature instead been decreasing at that time, politic support for the hypothesis probably would have been difficult to obtain in 1988.

Based on the previous 10 years of concurrent temperature- and CO_2-increase, many climate scientists in 1988 presumably felt that their understanding of climate dynamics was sufficient to conclude about the importance of CO_2 for affecting observed global temperatures.

Thus, it may with confidence be concluded that 10 years in 1988 was considered a period long enough to demonstrate the effect of increasing atmospheric CO_2 on global temperatures. The 10-year period is also basis for the temperature anomality diagrams shown on page 4.

Latest 20-year QC1 global monthly air temperature changes, updated to June 2023
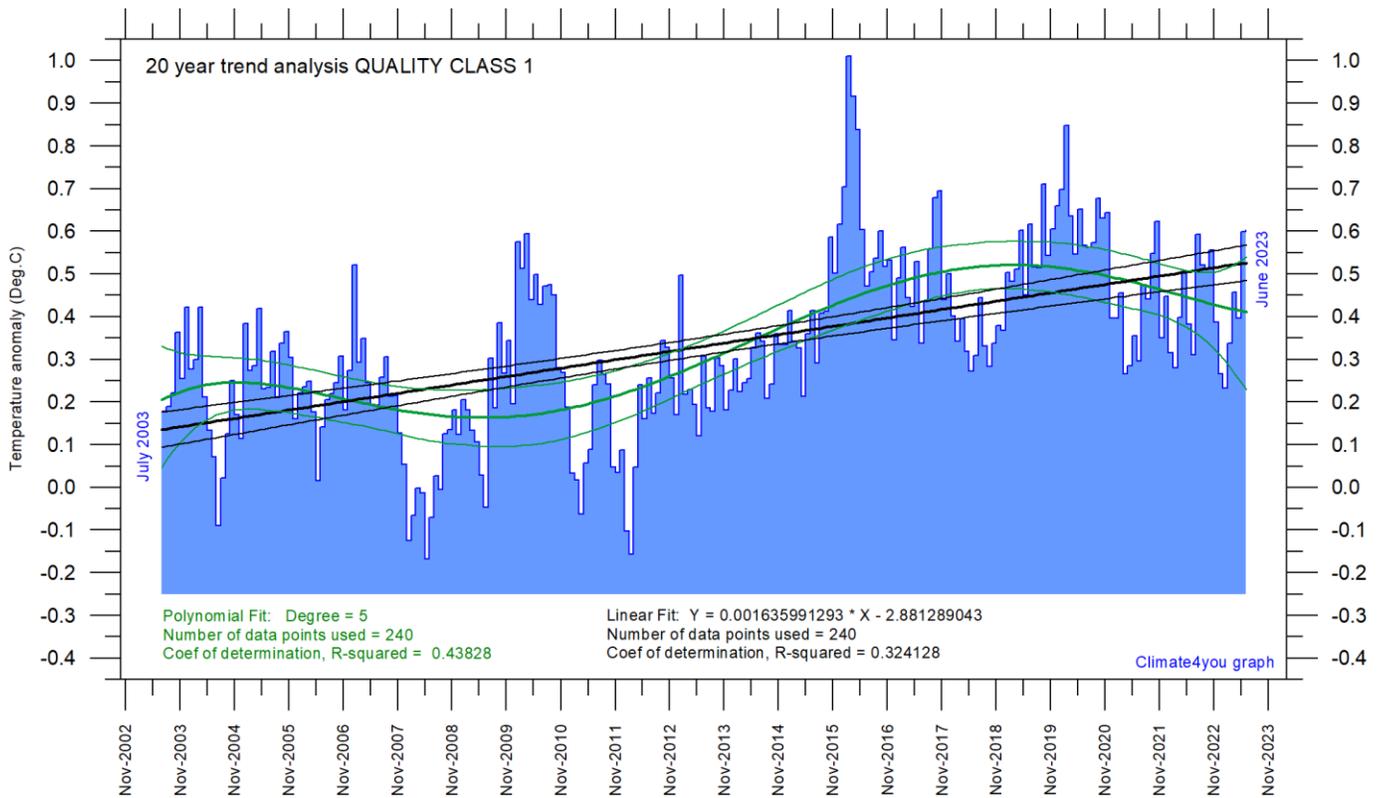
Last 20 years' global monthly average air temperature according to Quality Class 1 (UAH and RSS; see p.6 and 9) global monthly temperature estimates. The thin blue line represents the monthly values. The thick black line is the linear fit, with 95% confidence intervals indicated by the two thin black lines. The thick green line represents a 5-degree polynomial fit, with 95% confidence intervals indicated by the two thin green lines. A few key statistics are given in the lower part of the diagram (please note that the linear trend is the monthly trend).

In the enduring scientific climate debate, the following question is often put forward: Is the surface air temperature still increasing or has it basically remained without significant changes during the last 15-16 years?

The diagram above may be useful in this context and demonstrates the differences between two often used statistical approaches to determine recent temperature trends. Please also note that such fits only attempt to describe the past, and usually have small, if any, predictive power.

In addition, before using any linear trend (or other) analysis of time series a proper statistical model should be chosen, based on statistical justification.

For global temperature time series, there is no *a priori* physical reason why the long-term trend should be linear in time. In fact, climatic time series often have trends for which a straight line is not a good approximation, as is clearly demonstrated by several of the diagrams shown in the present report.

For an commendable description of problems often encountered by analyses of temperature time series analyses, please see Keenan, D.J. 2014: Statistical Analyses of Surface Temperatures in the IPCC Fifth Assessment Report.

See also diagrams on page 12.

Sunspot activity (SIDC) and QC1 average satellite global air temperature, updated to June 2023
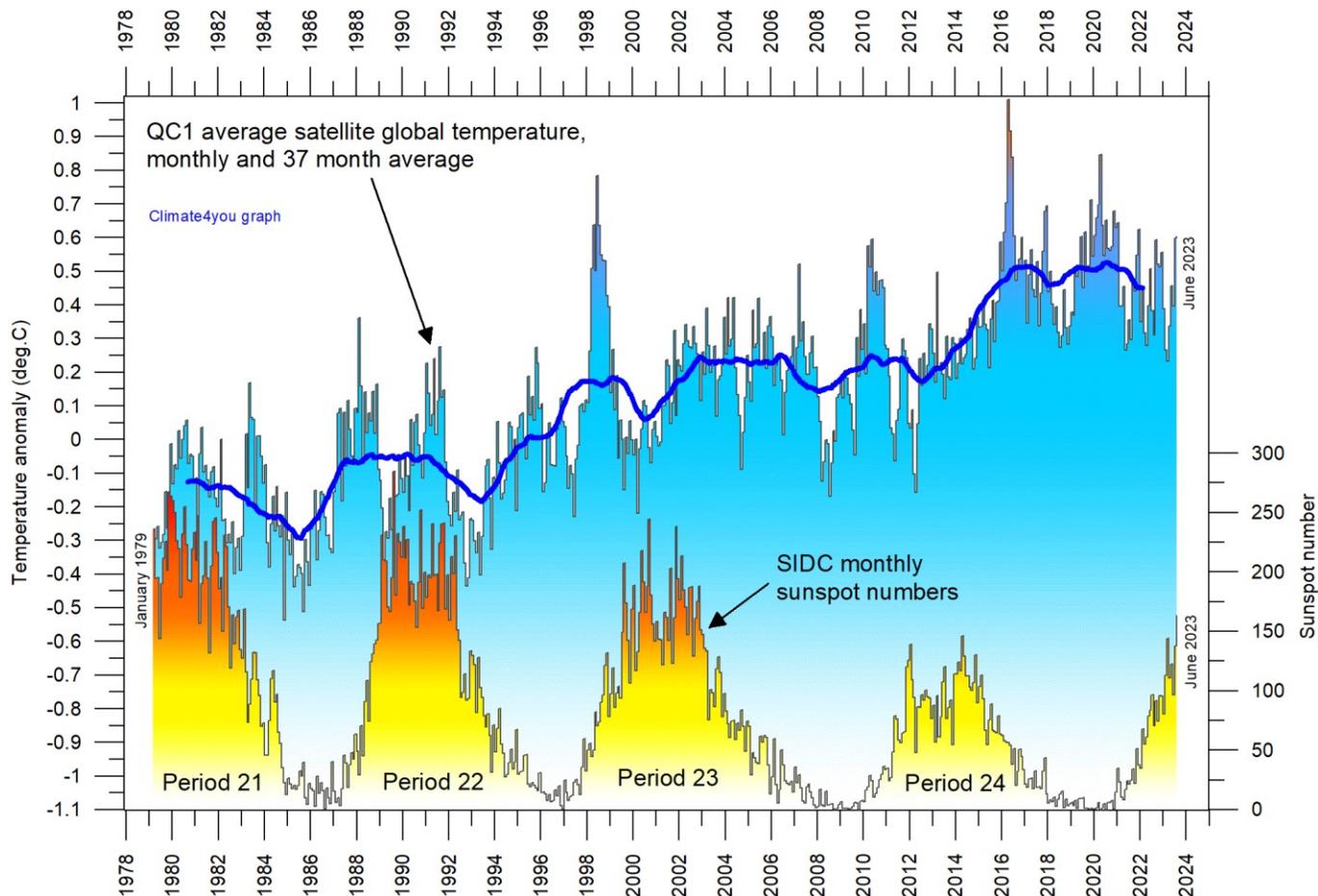

Variation of global monthly air temperature according to Quality Class 1 (UAH and RSS; see p.4) and observed sunspot number as provided by the Solar Influences Data Analysis Center (SIDC), since 1979. The thin lines represent the monthly values, while the thick line is the simple running 37-month average, nearly corresponding to a running 3-year average. The asymmetrical temperature 'bump' around 1998 is influenced by the oceanographic El Niño phenomenon in 1998, as is the case also for 2015-16. Temperatures in year 2019-20 was influenced by a moderate El Niño.

.

Monthly sunspot activity (SIDC) and average neutron counts (Oulu, Finland), updated to June 2023
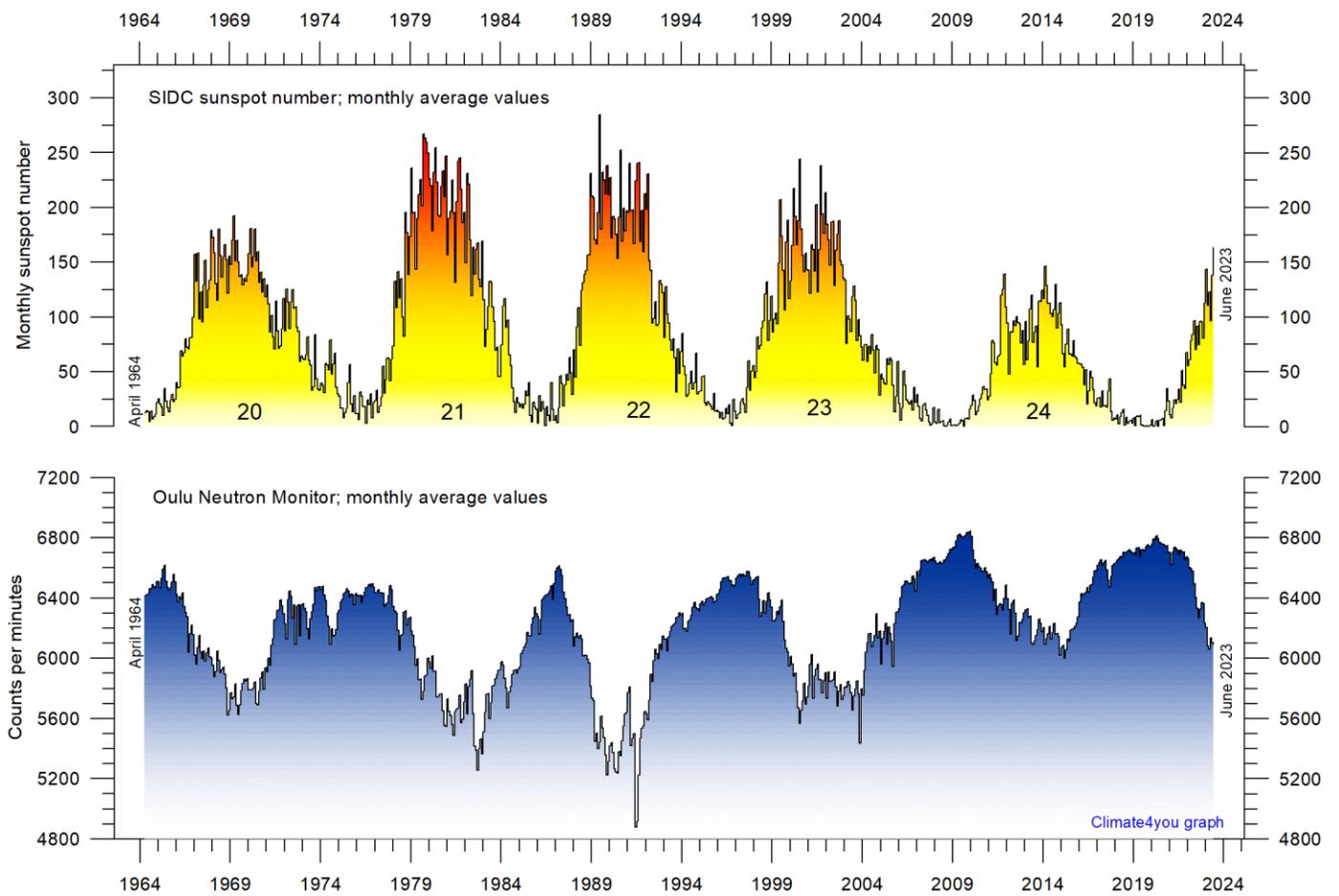
Observed monthly sunspot number (Solar Influences Data Analysis Center (SIDC) since April 1964, and (lower panel) monthly average counts of the Oulu (Finland) neutron monitor, adjusted for barometric pressure and efficiency.

54

Visual association since 1958 between (from bottom to top) Sunspot Number, Oceanic Niño Index (ONI) and annual change rate of atmospheric CO2. and specific humidity at 300 mb (ca. 9 km altitude). Upper two panels: Annual (12 month) change rate of atmospheric CO2 and specific humidity at 300 mb since 1959, calculated as the average amount of atmospheric CO2/humidity during the last 12 months, minus the average for the preceding 12 months (see also diagrams on page 43+44). Niño index panel: Warm (>+0.5ºC) and cold (<0.5ºC) episodes for the Oceanic Niño Index (ONI), defined as 3 month running mean of ERSSTv4 SST anomalies in the Niño 3.4 region (5ºN-5ºS, 120º-170ºW)]. For historical purposes cold and warm episodes are defined when the threshold is met for a minimum of 5 consecutive over-lapping seasons. Anomalies are centred on 30-yr base periods updated every 5 years. Thin vertical stippled lines indicate the visually estimated timing of sunspot minima. The typically sequence following a sunspot minimum appears to be a warm El Niño episode followed by a cold La Niña episode. Effects on change rates of atmospheric CO_2 and atmospheric specific humidity are visually apparent, with ONI variations being followed by changes in first humidity, and then (last) by CO_2.

The above diagram is inspired by the Leamon et al. 2021 publication: *Robert J. Leamon, Scott W. McIntosh, Daniel R. Marsh. Termination of Solar Cycles and Correlated Tropospheric Variability. Earth and Space Science, 2021; 8 (4) DOI: 10.1029/2020EA001223*

Monthly lower troposphere temperature (UAH) and global cloud cover, updated to April 2021
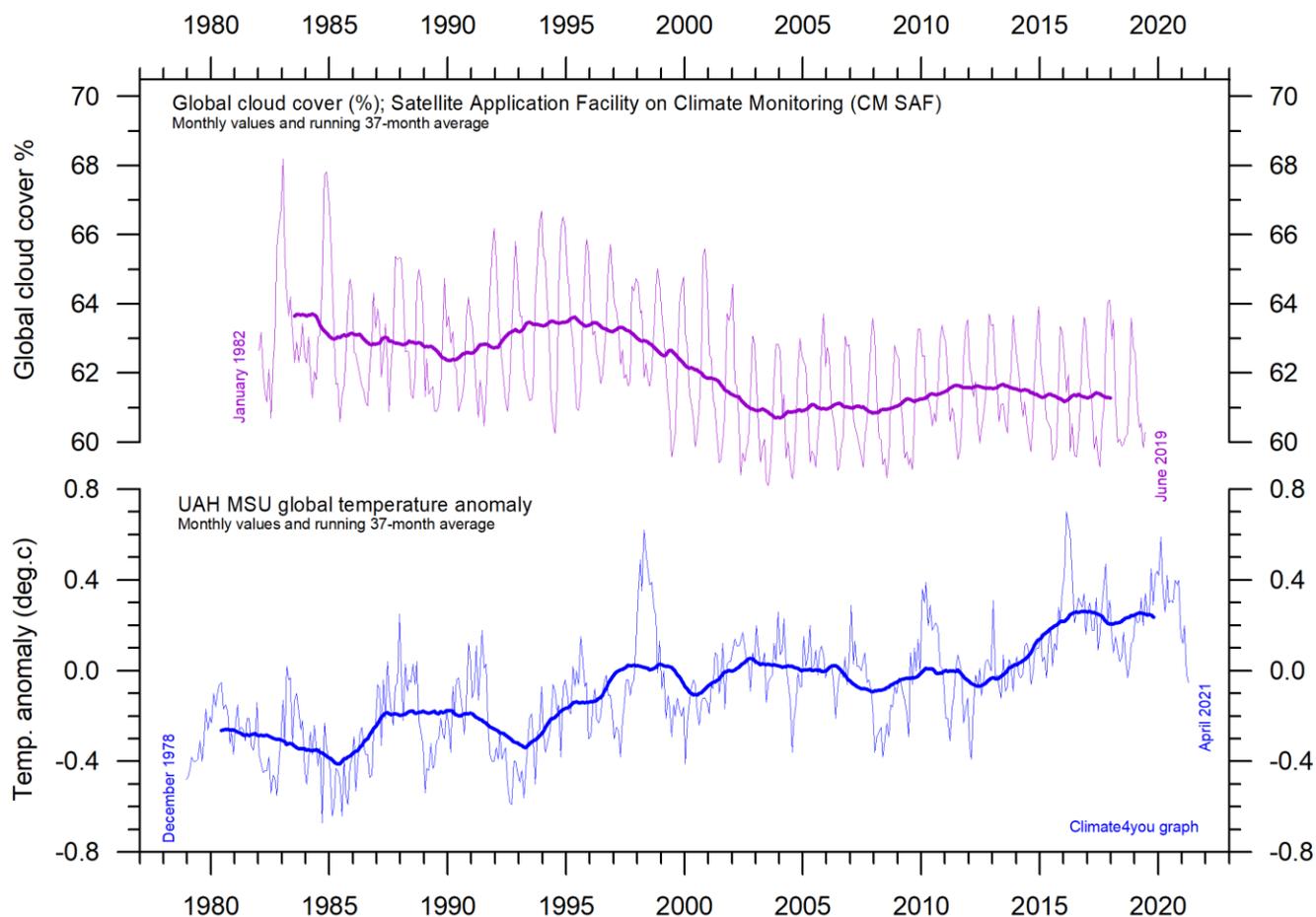
Lower tropospheric air temperature and global cloud cover. Upper panel: Global cloud cover according to Satellite Application Facility on Climate Monitoring. Lower panel: Global monthly average lower troposphere temperature (thin line) since 1979 according to University of Alabama at Huntsville, USA. The thick lines represent the simple running 37-month average. Reference period for UAH is 1991-2020.

Climate and history; one example among many

1808: Danish royal castle Koldinghus destroyed by fire
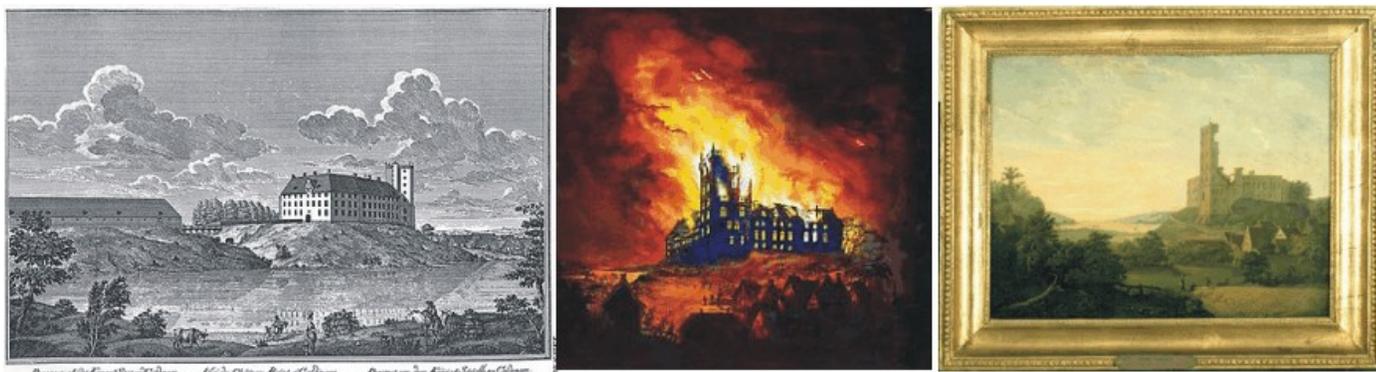
Danish royal castle Koldinghus in Jutland before 1808 (left). Koldinghus on fire the night between 29 and 30 March 1808 (centre). Painting by Hans Harder (1824) showing the ruin of Koldinghus after the fire.

Little Ice Age climatic and political induced disasters were not to end for Denmark by the two lost battles of Copenhagen in 1801 and 1807, respectively, as the unfortunate fate of the royal castle Koldinghus testifies.

Koldinghus is the last of the ancient royal castles in Jutland, western Denmark. The castle was originally founded by king Christoffer I (1252-1259) in 1268, but the oldest remaining part of buildings was built by king Christoffer III (1440–1448). Later king Christian I (1448-1481) and king Christian III (1534-1559) built other parts of the castle. Around 1720, king Frederik IV (1699-1730) contributed with rebuilding around 1720, resulting in a Baroque architecture.

The effects of war between Britain and France were also felt in the town Kolding in southeastern Jutland. Following the second British attack on Denmark and Copenhagen in 1807, Denmark allied herself with France and Spain against Britain and Sweden. About 30,000 French and Spanish soldiers were send to Denmark for support. Part of the plan was that these troops should assist in a campaign to recuperate the Scandian lands (southern Sweden), which was lost to Sweden following the Danish-Swedish war in 1658. When the French and Spanish soldiers arrived, the old castle Koldinghus was opened as quarters for some of these troops. In addition, it became the headquarters for the commander-in-chief of the expeditionary troops, the French marshal Jean-Baptiste Bernadotte.

The winter 1807-1808 was cold compared to modern standards, and temperatures plunged to values below what especially the Spanish troops were used to. Not surprisingly, they attempted to heat the castle correspondingly by firing zealously in the castle's fireplace. The fire risk represented by the soldiers quite rightfully became a worry at

the Danish castle administration, and, eventually, in the night between 29 and 30 March 1808 fire broke out. To fight the raging fire Marshal Bernadotte had his men to form a chain down to the castle lake. The lake, however, was frozen over so that a hole had first to be broken to get liquid water. In the end, it turned out to be impossible to save the castle.

Interior of Koldinghus, February 2022. The fire damaged ruin has now received a new roof and staircases.

Posterity has been inclined to place the blame for the fire entirely on the Spanish soldiers, and it is entirely likely that they, being unused to the Nordic Little Ice Age winter, fired up all too enthusiastically in the castle's fireplace. Another contributing reason, however, might simply be that the maintenance of the castle's chimneys had been neglected. Whatever the real cause, Jutland's last royal castle, which in 1808 still stood in the Baroque form it had attained through Frederik IV's rebuilding in the years around 1720, was lost.

Koldinghus was never rebuild as a royal castle, and quickly became one of the romantic ruins which were widely admired in the 19th century. The planned, combined military effort against Sweden was never initiated, partly because of lack of suitable transports, and partly because the Spanish troops decided to regroup at more southerly latitudes. Instead of attacking Sweden, marshal Jean-Baptiste Bernadotte later (1810) was offered and accepted the position as new Swedish king under the name Karl XIV Johan.

*****

All diagrams in this report, along with any supplementary information, including links to data sources and previous issues of this newsletter, are freely available for download on www.climate4you.com

Yours sincerely,

Ole Humlum (Ole.Humlum@gmail.com)

Arctic Historical Evaluation and Research Organisation, Longyearbyen, Svalbard

20 July 2023.

Planned publication of next newsletter: around 26 August 2023.